# NADH CHANNELING BETWEEN DEHYDROGENASES: ENZYME KINETICS, PROTEIN INTERACTION AND MOLECULAR MODELING STUDIES

By

ZELJKO M. SVEDRUZIC

Bachelor of Science

University of Zagreb,

Zagreb, Croatia,

June, 1998

Submitted to the faculty of the
Graduate College of the
Oklahoma State University
in partial fulfillment of
requirements for
the Degree of
DOCTOR OF PHILOSOPHY
December, 2000

NADH CHANNELING BETWEEN DEHYDROGENASES:

ENZYME KINETICS, PROTEIN INTERACTION AND

MOLECULAR MODELING STUDIES

Thesis Approved:

H. Chris Spivey

Thesis adviser

Robert L Matts

Dean of the Graduate College

# PREFACE

How do molecules make life? What makes life different from chemistry? How did chemistry become life? How do chemical properties of proteins and nucleic acids translate into functional cell physiology? There has been a wide speculation that densely packed molecules in the cell matrix can form specific molecular structures that modulate molecular properties beyond chemical properties of the individual components. Many of such complexes have been reported in the past, many more are formed by extremely weak interaction and remain unknown. The weak complexes have been difficult to study due to their delicate nature. The research in this thesis presents experimental approaches developed to analyze the properties of the weak molecular complexes. This study shows that weak molecular complexes between NAD(H) dehydogenase are possible and that NAD(H) dehydrogenase complexes are active in NADH channeling with a specific ping pong mechanism.

I want to acknowledge my deep gratitude to my thesis advisor Dr. H. Olin Spivey, for his enormous patience, mentorship and overall support. I want to express my deep gratitude to Eric Lehoux PhD2B, for his enormous friendship and thoughtful scientific and all other discussions. Eric it was a great pleasure to work with you. I am deeply grateful to undergraduate students that helped in this research: C. Eldon Wagner, Frank A. Hays,

David Kidd and many others. Many thanks to fellow graduate students Dr. Aron Fenton, Dr. Yang Xudong, Bradly Scroggins and many others. Many thanks to Drs. James Blair, Ms. Judy Hall, Drs. Chang-An Yu, Linda Yu, Robert Matts, Andrew Mort, and John Cushman who generously provided some of the equipment used in these experiments. Many thanks to Dr Steve White for generous help with the SGI workstations. My deep appreciation to Professor Chang-An Yu for his willingness to participate in my thesis committee and for his reference letter. I want to thank all members of my thesis committee, Drs. Robert Matts, Richard Essenberg, and Mario Rivera. I am sorry for writing 200 page long thesis. Many thanks to professional and very kind staff at the Department of Biochemistry and Molecular Biology at OSU. I apologize for missing many others who helped make this research go. Moje duboko postovanje prema mojim roditeljima Bosiljki i Miji Svedruzic, kao i mojoj sestri Drazenki Svedruzic. Mnogo vas volim, bez vas ne bih uspjeo ostvariti svoje ciljeve. The research presented in this thesis was generously supported by NSF and Oklahoma State University.

TABLE OF CONTENTS

LIST OF TABLES

LIST OF FIGURES

Figure Page

## NOMENCLATURE

| | |
|---|---|
| AcCoA | acetyl-CoA |
| AUC | analytical ultracentrifugation |
| ATP | adenosine triphosphate |
| by | beaker's yeast |
| CoA | coenzyme A |
| Da | Dalton equivalent to g/mol |
| DHAP | dihydroxyacetone phosphate |
| Ea | enzyme acceptor in enzyme buffering tests |
| Ed | enzyme donor in enzyme buffering tests |
| EDTA | ethylenediamine tetracetic acid |
| GAPDH | glyceraldehyde-3-phosphate dehydrogenase (E.C. 1.2.1.12) |
| αGDH | alpha glycerol-phosphate dehydrogenase (E.C. 1.1.1.8) |
| G-6-P | glucose-6-phosphate |
| G-6-PDH | glucose-6-phosphate dehydrogenase (E.C. 1.1.1.49) |
| βHAD | beta hydroxyacetyl CoA dehydrogenase (E.C. 1.1.1.37) |
| f | free, usually as a subscript (sometimes superscript) to indicate free (non channeled) reaction |

| | |
|---|---|
| h | human |
| hl | horse liver |
| k | kilo or a kinetic rate constant eg $k_{ij}$ depending on the context |
| Kd | equilibrium dissociation constant |
| Ki | inhibition constant in steady state enzyme kinetic measurements |
| Km | Michaellis-Menten constant in steady state enzyme kinetic measurements |
| LADH | horse liver alcohol dehydrogenase (E.C. 1.1.1.1) |
| LDH | lactate dehydrogenase (E.C. 1.1.1.27) |
| m | mitochondrial |
| MDH | malate dehydrogenase (E.C 1.1.35) |
| 2-ME | 2 mercapthoethanol |
| MOPS | (3-[N-Morpholino]propanesulfonic acid) |
| NADH | β -nicotinamide adenine dinucleotide reduced H form |
| NAD | β -nicotinamide adenine dinucleotide |
| PAGE | polyacrylamide gel electrophoresis |
| PEG | polyethylene glycol |
| PGK | phosphoglycerol kinase (E.C. 2.7.2.3) |
| ph | porcine heart |
| pm | porcine muscle |
| R | ratio of $v_{exp}$ and $v_{cal}$ in enzyme buffering experiments (eqn. 2.2) |
| rm | rabbit muscle |
| SDS | sodium dodecylsulfate |

| | |
|---|---|
| TRIS | 2-Amino-2-(hydroxymetyl)aminomethane |
| $v_{cal}$ | calculated rate for free reaction in enzyme buffering tests in case if there is no channeling (eqn. 2.1) |
| $V_{ch}$, $v_{ch}$ | steady state maximal velocity (V), and reaction rate (v) for channeled reaction in the enzyme buffering tests |
| $V_{cl}$, $v_{cl}$ | steady state maximal velocity (V), and reaction rate (v) for classical, free diffusion reaction in the enzyme buffering tests |
| $V_{exp}$, $v_{exp}$ | steady state maximal velocity (V), and reaction rate (v), measured in enzyme buffering experiments |
| Vmax | maximal velocity in steady state kinetics measurements |

# CHAPTER 1 Introduction: Why Substrate Channeling

## 1.1 Substrate Channeling, Supramolecular Organization and Metabolic Regulation

Cellular metabolism is a vast array of highly synchronized and correlated chemical reactions. The regulation mechanisms within such a complex chemical mixture are numerous and extensively studied. One of the little understood control mechanisms is substrate channeling. Substrate channeling is a process that happens when active sites of two enzymes come in proximity (or direct contact) so that the common substrate can be exchanged between the two sites with limited or no diffusion to the surrounding media. Substrate channeling is an expression of supramolecular organization although channeling can occur with only transiently formed enzyme complexes. Supramolecular complexes are a well known phenomenon in cell biochemistry. Pyruvate dehydrogenase, alpha-keto-glutarate dehydrogenase, fatty acid synthetase, RNA polymerase, ribosomes, and inner mitochondrial membrane respiratory complexes are some examples of supramolecular aggregates acting as a coherent biological unit. The biological properties of these complexes are normally greater than the sum of the individual component properties, and in some cases the individual components are even inactive when isolated from the complex. The molecular aggregates just mentioned are formed by strong interactions between the components, so that the complex is stable enough to be isolated and studied by established biochemical procedures. In this thesis I would like to draw intention to supramolecular complexes formed by *weak protein interactions*. Considerable experimental evidence has suggested that the cell matrix *in vivo* contains delicate protein aggregations that do not survive standard purification procedures (Srere,

1987; Srere & Mathews, 1990). The functional nature of weak and strong complexes can be the same, but the two differ in their ability to "survive" routine purification procedures. Identifying and studying weak complexes is a challenging task and, therefore, has been neglected by many biochemists. Consequently the existence of weak complexes is often overlooked, poorly understood, or even rejected (Ovadi, 1991).

Speculations about the importance of weak protein complexes started in 1960s (e.g. (Srere, 1967)) and has gained substantial experimental support and acceptance since then. The basis of the idea is that cellular proteins participating in the same or related metabolic pathways tend to form specific complexes (Srere, 1987). These interactions within the complex can bring specific biological properties to the participating components - properties not found in the individual complexes. Substrate channeling is one of the properties specific for enzyme complexes: it takes at least two proteins to channel. In addition to interactions between enzymes, interactions of enzymes with membrane and cytoskeletal components are also prevalent (Clegg, 1992). A comprehensive review of reported interactions between proteins participating in metabolic pathways is given by Srere (Srere, 1987). The review summarizes experimental evidence that indicates the presence of protein interactions within a number of diverse metabolic pathways. The widespread presence of this phenomenon suggests that interactions between metabolically related proteins could be a general property of cellular processes. The older and conventional view is that soluble enzymes and metabolites are randomly distributed in their organelles. In this view, metabolic regulation is necessarily achieved by very different mechanisms and has very different properties (Spivey & Merz, 1989; Welch & Easterby, 1994). Additional studies are

needed to clarify the situation. Due to the complexity of the problem, the study of supramolecular organization requires careful experimental controls, modifications of existing techniques or even development of new techniques. Experiments described in this thesis are one example. Currently available evidence supports some degree of supramolecular organization though random diffusion mechanism can not be completely excluded. Due to the complexity of the problem, very often experimental conclusions are highly dependent on proper control and techniques. A careful analysis of crude cell extracts is a good first point to look for evidence about the specific protein aggregates present in vivo. Analysis of *E coli* crude cell extract by size exclusion chromatography shows that a complete set of glycolytic enzymes tend to elute as a single complex (Mowbray & Moses, 1976). Similar complexes have been observed between the Krebs cycle enzymes in mitochondrial matrix extracts (Robinson *et al.*, 1987). An interesting example of weak protein interactions among the Krebs cycle enzymes was illustrated in experiments with yeast cell phenotypes normally able to grow on acetate (Kispal *et al.*, 1989; Kispal *et al.*, 1988). Deletion of the mitochondrial citrate synthase gene in yeast cells produces a phenotype unable to grow on acetate by disrupting the Krebs cycle. Introduction of the native citrate synthase restores the acetate competent phenotype, but this acetate+ phenotype can also be restored by introduction of catalyticaly inactive citrate synthase. This is a chemical paradox in which metabolic chemistry can be regained by introduction of chemically inactive enzyme. Furthermore deletion of isocitrate dehydrogenase (NAD) also produces an acetate incompetent phenotype [Minard *et al.*, 1998]. However in contrast to citrate synthase, deletion of isocitrate dehydrogenase (NAD) does not remove its chemistry from that cellular compartment.

NADP-isocitrate dehydrogenase present in the same compartment is capable of carrying out the NAD-isocitrate dehydrogenase chemistry but is involved in a different metabolic pathway. The acetate- phenotype experiments do not make sense if one assumes that the enzymes in yeast mitochondria are randomly distributed and non-interacting molecules in a soluble phase. Instead it seems necessary to conclude that protein-protein interactions are a required factor for active metabolism in these instances (Ovadi & Srere, 1996). In this view, the inactive citrate synthase was able to restore metabolism since its surface interactions restored the required metabolic assembly. The metabolic assembly with enzymatically inactive citrate synthase was not optimally functional, but was enough to keep the cells alive. On the other hand, NADP-isocitrate dehydrogenase was not able to compensate for missing NAD-isocitrate dehydrogenase since it belongs to a different metabolic assembly. In addition, evidence for channeling *in vivo* between Krebs cycle enzymes was shown by $^{13}C$ NMR (Sumegi *et al.*, 1992). These authors showed that an asymmetrically $^{13}C$ labeled precursor can enter the Krebs cycle and emerge as an asymmetric product (alanine) in spite of passing through two symmetrical intermediates (succinate and fumurate). After careful study of alternative causes, the most reasonable conclusion is that succinate and fumarate are directly transferred (channeled) between the enzymes generating and utilizing both of these substrates. Metabolic studies of cells with permeabilized membranes is another way to detect the presence of weak metabolic complexes acting in vivo. Working with permeabilized hepatocytes Cheung and the coworkers have shown that enzymes of the urea cycle will not utilize metabolites that are not generated by the enzymes within the cycle (Cheung *et al.*, 1989; Watford, 1989). The urea cycle enzymes act as a closed unit, similar to a supramolecular complex with

metabolite channeling between participating enzymes. The nature of delicate supramolecular structures is easy to understand if one considers characteristics of cytoplasm *in vivo*. Cytoplasmic protein concentrations are in the range of 200 to 400 mg/ml (Clegg, 1992; Goodsell, 1991; Srere, 1981; Zimmerman & Minton, 1993), and enzyme concentrations in mitochondrial matrix are considered to have extremely high values 560 mg/ml (Srere, 1967; Srere, 1972; Srere, 1981). Therefore, cellular protein concentrations are close to those in protein crystals characterized by X ray crystallography. Assuming an average molecular weight of 100,000, the proteins in mitochondrial matrix would need to be virtually in hard contact with each other - a condition closer to a gel than a solution (Srere, 1981; Zimmerman & Minton, 1993). Theoretical and experimental analysis of concentrated protein solutions indicate that dense packing can provide tens of kcal/mol of free energy in support of protein interaction (Berg, 1990; Zimmerman & Minton, 1993). Specific protein-protein interaction affinities can be considerably increased in concentrated protein solutions by excluded volume effects (Berg, 1990). Application of this theory to the more complex biological media (macromolecules of different size and shape) was first developed by Minton (e.g. see review (Berg, 1990; Zimmerman & Minton, 1993). However Berg (Berg, 1990), made important extensions of this theory by considering the contributions of solvent to the excluded volume effects. These effects are the consequence of the fact that macromolecules at high concentrations occupy a significant fraction of the solution volume in contrast to small molecules at the same molar concentration. Thus macromolecules exclude a significant fraction of the solution volume from placement of other macromolecules in the solution. This loss of positional freedom is a decrease in

entropy of the solution mixture, which in physiological media can be very large. This decrease in entropy of the solution is equivalent to an unfavorable increase in Gibbs free energy ($\Delta G = \Delta H - T\Delta S$), which the system will try to minimize. Several processes can reduce this $\Delta G$, e.g., precipitation of the macromolecules, transitions to more compact macromolecular conformations (Lerman, 1973) or in some cases association of macromolecules. In addition to excluded volume effects, weak interactions of macromolecules to surfaces (e.g., membranes or cytoskeletal surfaces) (Zimmerman & Minton, 1993), and cage effects (Cann, 1996; Fried & Crothers, 1981) can provide large enhancements in association affinities of macromolecules. However, during protein purification, all of these phenomena are greatly reduced by dilution and loss of cell structures.

Numerous unsuccessful attempts to manipulate *in vivo* metabolism by changing the enzyme expression level or kcat/Km properties are good illustrations of the inadequate concept of the cell matrix as unorganized soup of metabolic processes (Fraenkel, 1986; Fraenkel, 1992; Stephanopoulos & Vallino, 1991). If metabolism is an unorganized soup of chemical reactions limited only by enzyme ability to process its substrate, changing the enzyme expression level or kcat/Km properties should produce predictable alterations in cell metabolism. The enzymes selected for such manipulations are presumed in current biochemical textbooks as flux controlling enzymes (Chao & Liao, 1993; Heinisch & Zimmermann, 1985; Schaaff *et al.*, 1989). Several attempts were made to manipulate glycolytic flux by manipulating the expression level of phosphofructokinase (PFK), which is assumed to be the main "faucet" for the glycolytic flux (Davies & Brindle, 1992). Experiments have shown that glycolytic pathway *in vivo*

was unaffected by an increase in phosphofructokinase catalytic power (Chao & Liao, 1993; Heinisch & Zimmermann, 1985; Schaaff et al., 1989). Similar lack of change in metabolic flux was observed after manipulation of phosphofructokinase allosteric properties (Heinisch & Zimmermann, 1985). Such observations are not limited to PFK. The lack of connection between enzyme catalytic power and its share in metabolic flux can be observed with other glycolytic enzymes (Fraenkel, 1986; Schaaff et al., 1989). The combination of these experiments indicate that glycolysis can not be described as an unorganized soup of enzymatic reactions. Several authors have suggested that glycolytic enzymes act as supramolecular complex: a glycosome (Kurganov *et al.*, 1985; Srivastava & Bernhard, 1986; Srivastava & Bernhard, 1987). Glycolytic enzymes of blood parasite *Trypanosma bruceii* form glycosome that is stable enough to be isolated (Blattner *et al.*, 1998). Srivastava and Bernard (Srivastava & Bernhard, 1987) have indicated that glycolytic enzymes in the cytosol of other cells are present in stoichiometric ratios. The metabolite concentration is close to the concentration of respective binding sites. The glycosome in other organisms can be a supramolecular aggregate formed by weak interactions. Apart form glycolysis the attempts to alter metabolism by manipulation of enzyme expression level or kcat/Km properties were unsuccessful in other metabolic pathways (Bailey, 1991; Bailey *et al.*, 1990; Liao *et al.*, 1994; Liao *et al.*, 1996). Successful manipulation with the metabolic flux was reported in tryptophan synthesis (Patnaik & Liao, 1994). In that case the metabolic flux increase was achieved by increase in the complete set of enzymes responsible for the synthesis.

Supramolecular organization is an impressive manifestation of the structural organization in nature. Supramolecular organization can be viewed as a specific

dimension in the organization of matter that transforms chemistry into biology. Supramolecular organization may also have been important in the creation of living organisms. It can be viewed as the bridge that transformed catalytic RNA and polypeptides to the most primitive cells - a bridge that converted "simple" chemical processes in organized biological processes.

## 1.2 Physiological Relevance of Substrate Channeling

For cell physiology, substrate channeling is a unique and powerful metabolic control mechanism. Substrate channeling contribution to cellular metabolism is impressive and not clearly intuitive. The next few paragraphs will describe potential metabolic features based on substrate channeling.

**(1). Localization of the effective metabolite concentration, i.e., micro-compartmentation**. Enzyme activity is dependent upon substrate concentration. If the metabolism is a random soup of metabolites, the effective metabolite concentration will be distributed through the whole cell. That requires high quantities of each metabolite and makes a significant drain on the cell resources. Every change in cellular metabolism is slowed because of the need to readjust metabolite concentration throughout the cell. In case of substrate channeling the effective substrate concentration is local due to the limited diffusion. With the localization the optimal enzyme activity and the corresponding metabolic function, can be sustained with a minute substrate quantity and limited drain on the cell resources. The localization also allows for quick changes in cell metabolism with short adaptation time for cellular physiological responses. Many experiments have shown that cellular metabolite concentrations are closely matched with the concentration of their enzyme

binding sites indicating that many of the metabolites are enzyme bound *in vivo* (Srivastava & Bernhard, 1987) . Comparable concentrations of the metabolites and their enzyme binding sites, and substrate channeling can be the two main mechanisms that assure metabolite localization. Physiological relevance of the localized metabolite concentration can be illustrated by mMDH reaction. The reaction produces oxaloacetate (OAA) and NADH from malate and NAD. The reaction equilibrium heavily favors malate and NAD reactants. Only a few micromolar OAA would be achieved at equilibrium even with the high [malate] and [NAD] present in vivo. This raises a dilemma for the MDH, citrate synthase, and complex I reactions – [NADH]x[OAA] product is too high for the MDH reaction and [OAA] and [NADH] too low for the citrate synthase and complex I reactions, respectively (Ovadi *et al.*, 1994). Fixing one of these two problems exacerbates the other. These dilemmas can be circumvented, however, by invoking channeling of NADH to complex I and channeling of OAA to citrate synthase – both of which have been experimentally demonstrated in vitro (Ushiroyama et al. 1992; Datta et al. 1985). In addition the presence of a specific weak interaction has been demonstrated between mMDH and Fumarase (Beeckmans & Kanarek, 1981).

**(2) Simultaneous Presence of Competing Reactions.** The second advantage of substrate channeling is the cell's ability to have competing reactions happening simultaneously. If metabolic pathway 1 makes metabolite A go to B, in case of localized metabolites there would be no problem for metabolic pathway 2 to make A to go to C or B to go to A independently of the reaction 1. Simultaneous presence of competing reactions is difficult or impossible without metabolite

localization. Cell's ability to run competing reactions independently would put cell homeostasis rather than chemistry in charge of cell metabolism. It has been suggested that different isozymes have developed under the evolutionary pressure to fit in specific supramolecular complexes (Ureta, 1991).

**(3) Protection of the unstable metabolites**. The third advantage of micro-compartmentation is protection of unstable metabolic intermediates. Cellular concentrations of phosphoribosylamine and its respective enzymes PRPP-AT (phosphoribosylpyrophosphate aminotransferase) and GAR-syn (glycinamide ribonucleotide synthetase) suggest that the cellular phosphoribosylamine diffusion rate between the two enzymes is about 1 $s^{-1}$ (Rudolph & Stubbe, 1995). Phosphoribosylamine decomposes to ribose 5-phosphate with rate of 0.14 $s^{-1}$, suggesting that in the case of free diffusion most of the substrate will be decomposed before it passes between the two enzymes. Channeling of phosphoribosylamine was found between PRPP-AT and GAR-syn (Rudolph & Stubbe, 1995), indicating that *in vivo* channeling can protect unstable intermediate. Channeling of phosphoribosylamine between PRPP-AT and GAR-syn is shown to be mediated by weak protein interaction.

**(4) Metabolic Regulation by Regulation of the Weak Protein Interaction.** In number of cases where channeling or presence of weak supramolecular interaction has been observed, the protein interaction was regulated by a specific metabolite (Beeckmans & Kanarek, 1981; Beeckmans *et al.*, 1989; Fahien & Kmiotek, 1979; Fahien *et al.*, 1979; Fahien *et al.*, 1988; Fahien *et al.*, 1989; Fahien & Teller, 1992; Fukushima *et al.*, 1989). These observations suggest that the cellular metabolite

concentration can control metabolism by controlling supramolecular assembly. The regulatory metabolite does not even need to be substrate for the enzymes.forming the complex (Beeckmans et al., 1989; Fahien et al., 1988). Small molecule effects on supramolecular organization and its metabolic features brings interesting idea for a new approach in drug design. Drugs are normally designed to act as inhibitors in the enzyme active site. Disadvantage of that approach is that many enzymes share similar chemistry so the drugs are toxic due to poor specificity. An alternative approach in drug design could be to prepare drug cocktails that target both enzyme inhibition and its supramolecular organization. Two targets in specified metabolic path increase chance for treatment specificity and also allows for lower concentration for each of the drugs in the cocktail.

Substrate channeling can be the reason why most of the metabolic enzymes are oligomers. Different subunits can interface with donor (for substrate) and acceptor (for product) enzymes. After 10 years of research on supramolecular organization between the enzymes of amino acid catabolism, Fahien and collaborators proposed that difference in response to metabolic acidosis between hepatocytes and cells of kidney medulla is due to the differences in supramolecular organization of these cells (Fahien & Kmiotek, 1979; Fahien et al., 1979; Fahien et al., 1988; Fahien et al., 1989; Fahien & Teller, 1992).

## 1.3 Supramolecular Organization Between NAD(H) Dehydrogenases

The research in this thesis investigates supramolecular organization between NAD(H) dependent dehydrogenases. NAD(H) metabolism has unique position in cell physiology and represents very interesting object of study. NAD(H) metabolism has

ubiquitous importance in cellular homeostasis. The cellular [NAD]/[NADH] ratio regulates aerobic and anaerobic glycolysis, and cellular energy production. Apart from glycolysis, the [NAD]/[NADH] ratio regulates a great number of catabolic pathways. NAD(H) metabolism is clearly separated in two highly unequilibrated compartments: cytosolic and mitochondrial (Devlin, 1996; Newsholme & Leech, 1985). The [NAD]/[NADH] ratio in the cytosol is 700 favoring catabolic reaction. The opposite situation is observed in the mitochondrial matrix where [NAD]/[NADH] is 0.1 favoring respiratory oxidation. Two highly unequlibriated compartments are physically separated by the mitochondrial membrane but strongly connected chemically by several transmembrane reactions. Since the proper physiological function in each compartment is highly sensitive to [NAD]/[NADH] ratios, it is interesting to see how two different [NAD]/[NADH] ratios are preserved while maintaining communication. NADP(H) metabolism can be viewed as the third compartment of the NAD(H) related metabolism. Cytosolic [NADP]/[NADPH] $\approx$ 0.1. Cytosolic [NADP]/[NADPH] regulates numerous anabolic reactions (Devlin, 1996; Newsholme & Leech, 1985). NADP(H) and NAD(H) metabolism are separated by enzyme specificity, but also communicate through some shared metabolites (e.g. cytosolic citrate synthase and malic enzyme which exist as NAD and NADP enzymes). Again it is interesting to see how two highly different redox states are maintained in parallel with close communications between them. In summary NAD(H) metabolism is connected with multiple cellular processes and is a key factor in regulating the cell physiology. Multiple interconnected yet unequilibrated compartments indicate that the NAD(H) metabolism is a rich source of metabolic regulation mechanism including supramolecular organization. Several *in vivo* studies have suggested that

NAD(H) metabolism within each of the three main compartments is separated in subcompartments although there are no obvious physical barriers (Cronholm, 1985a; Cronholm, 1985b; Cronholm, 1987; Cronholm & Curstedt, 1984; Cronholm *et al.*, 1974; Grivell *et al.*, 1995).

The possible existence of substrate channeling between NAD(H) dehydrogenases *in vitro* was first reported 50 years ago (Cori *et al.*, 1950; Nygaard & Rutter, 1956). The phenomena has been object of various *in vivo* (Cronholm, 1985a; Cronholm, 1985b; Cronholm, 1987; Cronholm & Curstedt, 1984; Cronholm et al., 1974) and *in vitro* (Srivastava & Bernhard, 1987; Ushiroyama *et al.*, 1992) studies. These studies have given conflicting conclusions. (Rognstad, 1991; Srivastava *et al.*, 1989; Wu *et al.*, 1991; Wu *et al.*, 1992). The goal of the research presented in this thesis was to reexamine channeling and interaction between the NAD(H) dehydrogenases. Four interactive approaches have been used: experimental and theoretical enzyme kinetics, protein association, and molecular modeling studies. The work presented confirms channeling between the NAD(H) dehydrogenases, and indicates subtle nature of the phenomena. Chapter 2 presents evidence of channeling between NAD(H) dehydrogenases by use of the enzyme buffering test. Chapter 3 shows that channeling between NAD(H) dehydrogenase can happen in vitro even without detectable equilibrium interaction between the channeling components in the absence of the catalytic reaction (absence of cosubstrate of Ea). Furthermore, chapter 3 shows that an extensive association between two NAD(H) dehydrogenases can be observed in some cases with specific conditions. Chapter 4 describes an attempt to model a channeling complex by use of molecular structures. Chapter 5 integrates conclusions from the previous three chapters and

provides a channeling mechanism consistent with the experimental data. This mechanism solves an enigma for the substrate channeling system and several others. Specifically, kinetic data with numerous enzymes show saturation with respect to their protein substrates with $K_m$'s in the low μM range, yet no detectable association of the enzyme with its protein substrate can be detected in the absence of the catalytic reaction (absence of the cosubstrate). The proposed mechanism is the first to explain the failure of the widely accepted misconception that channeling has to be accompanied with strong equilibrium interaction (Arias *et al.*, 1998; Keizer & Smolen, 1992; Wu et al., 1992). As such the proposed mechanism represents a turning point in addressing the problems (surprises?) of substrate channeling (Rudolph & Stubbe, 1995) and sets a milestone for future endeavors.

## 1.4 References


Arias, W. M., Pettersson, H. & Pettersson, G. (1998). Mechanism of NADH transfer among dehydrogenases. *Biochim Biophys Acta* **1385**, 149-56.

Bailey, J. E. (1991). Toward a science of metabolic engineering. *Science* **252**, 1668-75.

Bailey, J. E., Birnbaum, S., Galazzo, J. L., Khosla, C. & Shanks, J. V. (1990). Strategies and challenges in metabolic engineering. *Ann N Y Acad Sci* **589**, 1-15.

Beeckmans, S. & Kanarek, L. (1981). Demonstration of Physical Interactions between Consecutive Enzymes of the Citric Acid Cycle and of the Aspartate-Malate Shuttle. A Study Involving Fumarase, Malate Dehydrogenase, Citrate Synthase and Aspartate Aminotransferase. *Eur. J. Biochem.* **117**, 527-535.

Beeckmans, S., Van Driessche, E. & Kanarek, L. (1989). The Visualization by Affinity Electrophoresis of a Specific Association between the Consecutive Citric Acid Cycle Enzymes Fumarase and Malate Dehydrogenase. *Eur. J. Biochem.* **183**, 449-454.

Berg, O. G. (1990). Influence of Macromolecular Crowding on thermodinamic activity: Solubility and Dimerization Constants for Spherical and Dumbbell-Shaped Molecules in a Hard-Sphere Mixture. *Biopolymers* **30**, 1027-1037.

Blattner, J., Helfert, S., Michels, P. & Clayton, C. (1998). Compartmentation of phosphoglycerate kinase in Trypanosoma brucei plays a critical role in parasite energy metabolism. *Proc Natl Acad Sci U S A* **95**, 11596-600.

Cann, J. R. (1996). Theory and practice of gel electrophoresis of interacting macromolecules. *Anal Biochem* **237**, 1-16.

Chao, Y. P. & Liao, J. C. (1993). Alteration of growth yield by overexpression of phosphoenolpyruvate carboxylase and phosphoenolpyruvate carboxykinase in Escherichia coli. *Appl Environ Microbiol* **59**, 4261-5.

Cheung, C. W., Cohen, N. S. & Raijman, L. (1989). Channeling of urea cycle intermediates in situ in permeabilized hepatocytes. *J Biol Chem* **264**, 4038-44.

Clegg, S. J. (1992). Cellular Infrastructure and Metabolic Organization. In *From Metabolite, to Metabolism, to Metabolon* (Stadtman, E. R. & Chock, P. B., eds.), Vol. 33, pp. 3-15. Academic Press, New York.

Cori, C. F., Velick, S. F. & Cori, G. T. (1950). The Combination of Diphosphopyridine Nucleotide with Glyceraldehyde Phosphate Dehydrogenase. *Biochim. Biophys. Acta* **4**, 160-169.

Cronholm, T. (1985a). Hydrogen transfer between ethanol molecules during oxidoreduction in vivo. *Biochem J* **229**, 315-22.

Cronholm, T. (1985b). Incorporation of the 1-pro-R and 1-pro-S hydrogen atoms of ethanol in the reduction of acids in the liver of intact rats and in isolated hepatocytes. *Biochem J* **229**, 323-31.

Cronholm, T. (1987). Effect of ethanol on the redox state of the coenzyme bound to alcohol dehydrogenase studied in isolated hepatocytes. *Biochem J* **248**, 567-72.

Cronholm, T. & Curstedt, T. (1984). Heterogeneity of the sn-glycerol 3-phosphate pool in isolated hepatocytes, demonstrated by the use of deuterated glycerols and ethanol. *Biochem J* **224**, 731-9.

Cronholm, T., Matern, H., Matern, S. & Sjovall, J. (1974). Transfer of deuterium from (1-2H2) ethanol to Krebs cycle and related acids of rat liver in vivo. *Eur J Biochem* **48**, 71-80.

Davies, S. E. & Brindle, K. M. (1992). Effects of overexpression of phosphofructokinase on glycolysis in the yeast Saccharomyces cerevisiae. *Biochemistry* **31**, 4729-35.

Devlin, T. M., Ed. (1996). Biochemistry with Clinical Correlations. 4th edit: Wiley.

Fahien, L. A. & Kmiotek, E. (1979). Precipitation of complexes between glutamate dehydrogenase and mitochondrial enzymes. *J Biol Chem* **254**, 5983-90.

Fahien, L. A., Kmiotek, E. & Smith, L. (1979). Glutamate dehydrogenase--malate dehydrogenase complex. *Arch Biochem Biophys* **192**, 33-46.

Fahien, L. A., Kmiotek, E. H., MacDonald, M. J., Fibich, B. & Mandic, M. (1988). Regulation of malate dehydrogenase activity by glutamate, citrate, alpha-ketoglutarate, and multienzyme interaction. *J Biol Chem* **263**, 10687-97.

Fahien, L. A., MacDonald, M. J., Teller, J. K., Fibich, B. & Fahien, C. M. (1989). Kinetic advantages of hetero-enzyme complexes with glutamate dehydrogenase and the alpha-ketoglutarate dehydrogenase complex. *J Biol Chem* **264**, 12303-12.

Fahien, L. A. & Teller, J. K. (1992). Glutamate-malate metabolism in liver mitochondria. A model constructed on the basis of mitochondrial levels of enzymes, specificity, dissociation constants, and stoichiometry of hetero-enzyme complexes. *J Biol Chem* **267**, 10411-22.

Fraenkel, D. G. (1986). Mutants in glucose metabolism. *Annu Rev Biochem* **55**, 317-37.

Fraenkel, D. G. (1992). Genetics and intermediary metabolism. *Annu Rev Genet* **26**, 159-77.

Fried, M. & Crothers, D. M. (1981). Equilibria and kinetics of lac repressor-operator interactions by polyacrylamide gel electrophoresis. *Nucleic Acids Res* **9**, 6505-25.

Fukushima, T., Decker, R. V., Anderson, W. M. & Spivey, H. O. (1989). Substrate channeling of NADH and binding of dehydrogenases to complex I. *J Biol Chem* **264**, 16483-8.

Goodsell, D. S. (1991). Inside a living cell. *Trends Biochem Sci* **16**, 203-6.

Grivell, A. R., Korpelainen, E. I., Williams, C. J. & Berry, M. N. (1995). Substrate-dependent utilization of the glycerol 3-phosphate or malate/aspartate redox shuttles by Ehrlich ascites cells. *Biochem J* **310**, 665-671.

Heinisch, J. & Zimmermann, F. K. (1985). Is the phosphofructokinase-reaction obligatory for glucose fermentation by Saccharomyces cerevisiae? *Yeast* **1**, 173-5.

Keizer, J. & Smolen, P. (1992). Mechanisms of metabolite transfer between enzymes: diffusional versus direct transfer. *Curr Top Cell Regul* **33**, 391-405.

Kispal, G., Evans, C. T., Malloy, C. & Srere, P. A. (1989). Metabolic studies on citrate synthase mutants of yeast. A change in phenotype following transformation with an inactive enzyme. *J Biol Chem* **264**, 11204-10.

Kispal, G., Rosenkrantz, M., Guarente, L. & Srere, P. A. (1988). Metabolic changes in Saccharomyces cerevisiae strains lacking citrate synthases. *J Biol Chem* **263**, 11145-9.

Kurganov, B. I., Sugrobova, N. P. & Mil'man, L. S. (1985). Supramolecular organization of glycolytic enzymes. *J Theor Biol* **116**, 509-26.

Lerman, L. S. (1973). Physico-Chemical Properties of the Nucleic Acids. In *Physico-Chemical Properties of the Nucleic Acids* (Duchesne, J., ed.). Academic Press, New York.

Liao, J. C., Chao, Y. P. & Patnaik, R. (1994). Alteration of the biochemical valves in the central metabolism of Escherichia coli. *Ann N Y Acad Sci* **745**, 21-34.

Liao, J. C., Hou, S.-Y. & Chao, Y.-P. (1996). Pathway Analysis, Engineering, and Physiological Considerations for Redirecting Central Metabolism. *Biotechnology and Bioengineering* **52**, 129-140.

Minard, K. I., G. T. Jennings, T. M. Loftus, D. Xuan, and L. McAlister-Henn. 1998. Sources of NADPH and expression of mammalian $NADP^+$-specific isocitrate dehydrogenases in *saccharomyces cereviaiae. J. Biol. Chem.* **273**, 31486-93.

Mowbray, J. & Moses, V. (1976). The tentative identification in Escherichia coli of a multienzyme complex with glycolytic activity. *Eur J Biochem* **66**, 25-36.

Newsholme, E. & Leech. (1985). *Biochemistry for Medical Students*. 2nd edit, Wiley.

Nygaard, A. P. & Rutter, W. J. (1956). Interaction of Pyridine-Nucleotide Linked Enzymes. *Acta Chem. Scand.* **10**, 37-48.

Ovadi, J. (1991). Physiological Significance of Metabolite Channelling. *J. Theor. Biol.* **152**(1), 1-22.

Ovadi, J., Huang, Y. & Spivey, H. O. (1994) Binding of malate dehydrogenase and NADH channelling to complex I. *J. Molec. Recog.* **7**, 265-272.

Ovadi, J. & Srere, P. A. (1996). Metabolic consequences of enzyme interactions. *Cell Biochem Funct* **14**, 249-58.

Patnaik, R. & Liao, J. C. (1994). Engineering of Escherichia coli central metabolism for aromatic metabolite production with near theoretical yield. *Appl Environ Microbiol* **60**, 3903-3908.

Robinson, J. B., Jr., Inman, L., Sumegi, B. & Srere, P. A. (1987). Further characterization of the Krebs tricarboxylic acid cycle metabolon. *J Biol Chem* **262**, 1786-90.

Rognstad, R. (1991). Evidence against tight channelling of NADH in hepatocytes. *Arch Biochem Biophys* **286**, 555-61.

Rudolph, J. & Stubbe, J. (1995). Investigation of the mechanism of phosphoribosylamine transfer from glutamine phosphoribosylpyrophosphate amidotransferase to glycinamide ribonucleotide synthetase. *Biochemistry* **34**, 2241-50.

Schaaff, I., Heinisch, J. & Zimmermann, F. K. (1989). Overproduction of glycolytic enzymes in yeast. *Yeast* **5**, 285-90.

Spivey, H. O. & Merz, J. M. (1989). Metabolic Compartmentation. *BioEssays* **10**, 127-130.

Srere, P. A. (1967). Enzyme Concentrations in Tissues. *Science* **158**, 936-937.

Srere, P. A. (1972). Is There an Organization of Krebs Cycle Enzymes in the Mitochondrial Matrix? In *Energy Metabolism and the Regulation of Metabolic Processes in Mitochondria* (Mehlman, M. A. & Hanson, R. W., eds.), pp. 79-91. Academic Press, New York.

Srere, P. A. (1981). Protein Crystals as a Model for Mitochondrial Matrix Proteins. *Trends in Biochem. Sci.* **6**, 4-6.

Srere, P. A. (1987). Complexes of sequential metabolic enzymes. *Annu Rev Biochem* **56**, 89-124.

Srere, P. A. & Mathews, C. K. (1990). Purification of multienzyme complexes. *Methods Enzymol* **182**, 539-51.

Srivastava, D. K. & Bernhard, S. A. (1986). Enzyme-Enzyme Interactions and the Regulation of Metabolic Reaction Pathways. *Curr. Tops. Cell. Regul.* **28**, 1-68.

Srivastava, D. K. & Bernhard, S. A. (1987). Biophysical Chemistry of Metabolic Reaction Sequences in Concentrated Enzyme Solution and in the Cell. *Ann. Rev. Biophys. Biophys. Chem.* **16**, 175-204.

Srivastava, D. K., Smolen, P., Betts, G. F., Fukushima, T., Spivey, H. O. & Bernhard, S. A. (1989). The Direct Transfer of NADH between α-Glycerol Phosphate Dehydrogenase and Lactate Dehydrogenase. Fact or Misinterpretation? *Proc. Natl. Acad. Sci., USA* **86**, 6464-6468.

Stephanopoulos, G. & Vallino, J. J. (1991). Network rigidity and metabolic engineering in metabolite overproduction. *Science* **252**, 1675-81.

Sumegi, B., McCammon, M. T., Sherry, A. D., Keys, D. A., McAlister-Henn, L. & Srere, P. A. (1992). Metabolism of [3-13C]pyruvate in TCA cycle mutants of yeast. *Biochemistry* **31**, 8720-5.

Ureta, T. (1991). The role of isoenzymes in metablite channeling. *J. Theor. Biol.* **152**, 8319-8327.

Ushiroyama, T., Fukushima, T., Styre, J. D. & Spivey, H. O. (1992). Substrate Channeling of NADH in Mitochondrial Redox Processes. In *From Metabolite, to Metabolism, to Metabolon* (Stadtman, E. R. & Chock, P. B., eds.), Curr. Top. Cell. Regul., Vol. 33, pp. 291-307. Academic Press, New York.

Watford, M. (1989). Channeling in the urea cycle: a metabolon spanning two compartments. *Trends Biochem Sci* **14**, 313-4.

Welch, G. R. & Easterby, J. S. (1994). Metabolic channeling versus free diffusion: transition-time analysis. *Trends Biochem Sci* **19**, 193-7.

Wu, X., Gutfreund, H., Lakatos, S. & Chock, P. B. (1991). Substrate Channeling in Glycolysis: A Phantom Phenomenon. *Proc. Natl. Acad. Sci. USA* **88**, 497-501.

Wu, X. M., Gutfreund, H. & Chock, P. B. (1992). Kinetic method for differentiating mechanisms for ligand exchange reactions: application to test for substrate channeling in glycolysis. *Biochemistry* **31**, 2123-8.

Zimmerman, S. B. & Minton, A. P. (1993). Macromoleculare Crowding: Biochemical, Biophysical, and Physiological Consequences. *Annual Review of Biophysic and Biomolecular Structure* **22**, 27-65.

# CHAPTER 2 Enzyme Kinetic Measurements

## 2.1 Introduction

The possibility of channeling between NAD(H) dehydrogenases was first reported nearly 50 years ago (Cori *et al.*, 1950; Mahler & Elowe, 1954; Nygaard & Rutter, 1956). Thirty years later Srivastva and Bernard (Srivastava & Bernhard, 1984) used the enzyme buffering method to characterize NADH channeling between a large number of dehydrogenase enzyme pairs and elucidate the chiral specificity of this transfer of NADH. This channeling happens between enzymes from very different phylogenic origins. Channeling has only been observed between dehydrogenases of opposite chiral specificity - type A dehydrogenase will channel with type B, but no channeling has been observed between A and A or between B and B type dehydrogenases (Srivastava & Bernhard, 1985). The two chiral types of NAD(H) dehydrogenases, the A and the B type, are defined on the basis of which of the two C4 nicotinamide hydrogen is transferred in the enzymatic reduction (You, 1982; You, 1985). Limited molecular modeling studies suggested that A-B type selectivity is due to the complementary conformations of the bound NAD(H), and the conservation of the complementary charges surrounding the NAD(H) binding site (Srivastava *et al.*, 1985). A few years after Srivastava and Bernhard's work, channeling was reported between the NAD(H) dehydrogenases of the mitochondrial matrix and complex I (Fukushima *et al.*, 1989; Ushiroyama *et al.*, 1992). Numerous attempts were made to test for channeling by fast kinetics of NADH transfer between dehydrogenases. (Arias *et al.*, 1998; Arias & Pettersson, 1997; Srivastava *et al.*, 1989; Wu *et al.*, 1991). However all these studies were made in the absence of the catalytic reaction, which, as shown in this thesis, precludes the formation of the bi-enzyme complex essential for NADH channeling.

Therefore these fast kinetic studies provide no test of NADH channeling. Currently then, the only experimental method providing evidence for NADH channeling is the "enzyme buffering method", described in this chapter. NADH channeling presents two special problems making it impractical to utilize the other common methods for testing for substrate channeling (Spivey & Ovadi, 1999). Firstly, it is a case where the precursor (NAD) is regenerated in the enzymatic reaction following the NADH channeled step. Since the reactant and the product in the coupled reactions are the same, isotopic tests of channeling become very insensitive. Secondly, this channeling occurs without detectable complex formation between the enzymes in the absence of the catalytic reaction. This prevents use of several tests that work with stable enzyme complexes (op. cit.). Although the enzyme buffering method has been criticized, we find all of these criticisms demonstrably defective (Svedruzic & Spivey, 2000). In fact, the enzyme buffering method can be unusually rigorous in favorable cases. This rigorousness derives in large part from the excellent control experiments provided by pairing each enzyme in question with one of the same chiral specificity (A with A or B with B). No NADH channeling has ever been documented between such enzyme pairs. These control experiments, therefore, provide a rigorous measure of the accuracy of the enzyme buffering experiments performed with enzymes of opposite chiral specificity since the latter experiments are done with essentially identical enzyme and substrate conditions. Results from four published control experiments reveal an accuracy of about 10% in the channeling criterion R defined below.

Substrate channeling is an important phenomena, and uncertainties about its existence and even its properties require study. The apparent discrepancies between enzyme buffering, fast kinetics, and protein association measurements are discussed later in this thesis. In this section I describe the properties of the enzyme buffering

experiments, and the properties of the channeling reaction monitored in the enzyme buffering experiments. These observations will be used in combination with the results from protein association, and molecular modeling sections to develop a kinetic mechanism for NADH channeling which is presented in section five of this thesis.

### 2.1.1 Enzyme Buffering Method

NADH channeling between two dehydrogenases, the donor enzyme (Ed) and the acceptor enzyme (Ea), was studied by the enzyme buffering method (Fig. 2.1). These experiments are performed by mixing Ea with a large excess of Ed and NADH. Specifically Ea is used at normal enzyme assay concentrations (a few nM) while Ed is in excess of [NADH], i.e., at 100 μM or more. With these conditions, the majority of NADH present in the solution (>97%) is bound to the Ed leaving free NADH ten to twenty fold below its Km with Ea. The reaction is initiated by adding substrate specific for Ea, and the experimental initial steady-state rate $v_{exp}$ measured at a series of varying [Ed]. The measured reaction rate $v_{exp}$ is compared to the calculated velocity $v_{cal}$, which is defined as the Ea velocity expected if there is no channeling and the only form of NADH available to the Ea is the free NADH (NADH not bound to Ed). The $v_{cal}$ is calculated from the Michaelis-Menten equation,

$$v_{cal} = \frac{V^f_{NADH}[NADH]_f}{K^f_{NADH} + [NADH]_f} \tag{2.1}$$

where $V^f_{NADH}$ and $K^f_{NADH}$ are the Michaelis-Menten parameters for the reaction of Ea with free NADH (Fig. 2.1 A). The $[NADH]_f$, is the concentration of free NADH in equilibrium with the Ed-NADH in the given enzyme buffering measurement. The concentration of Ea is far too small to affect the equilibrium between Ed and NADH. Also the half-life for dissociation of Ed-NADH is just a few msec, whereas the rate of the

**Figure 2.1 (A-B). The NADH Dehydrogenase Activity Measurements in the Standard Assay (A), and the Enzyme Buffering Experiments (B).**

**(A)** The figure illustrates standard assays for NAD(H) dehydrogenases, which in all cases discussed in this thesis (except GAPDH family) follow ordered Bi-Bi mechanism where NADH binds first. The measured reaction velocity ($v_f$) can be expressed by the standard Michaelis-Menten equation giving $K_{NADHf}$ and $V_{NADHf}$ values. These are the same $K_{NADHf}$ and $V_{NADHf}$ values used in combination with $[NADH]_f$ to calculate $v_{cal}$ as indicated in the equation 2.1. **(B)** This figure illustrates the enzyme buffering experiment. The big rectangle illustrates the assay ingredients before the start of the reaction. Nanomolar concentrations of Ea are incubated with NADH and an excess of NAD(H) binding sites of Ed (*E*nzyme *d*onor). The small rectangle (the right part of the big rectangle) shows dynamic equilibrium between two NADH forms present: $NADH_f$ and Ed-NADH. The reaction shown is started by adding B, the oxidized substrate of Ea (black triangle) although in practice Ea is normally the last reagent added. The measured reaction velocity $v_{exp}$, (v *exp*erimental) consist of two reactions: the channeled reaction ($v_{ch}$), and the non-channeled reaction ($v_{cl}$, for v *cl*assical). The Ea substrate in the channeling reaction is Ed-NADH complex. The Ea substrate in the non-channeled reaction is $NADH_f$ encountered through classical, free diffusion path. In case of no channeling, the vexp is to within experimental error identical to $v_{cal}$ (eqn. 2.1) and consist of $v_{cl}$ only.

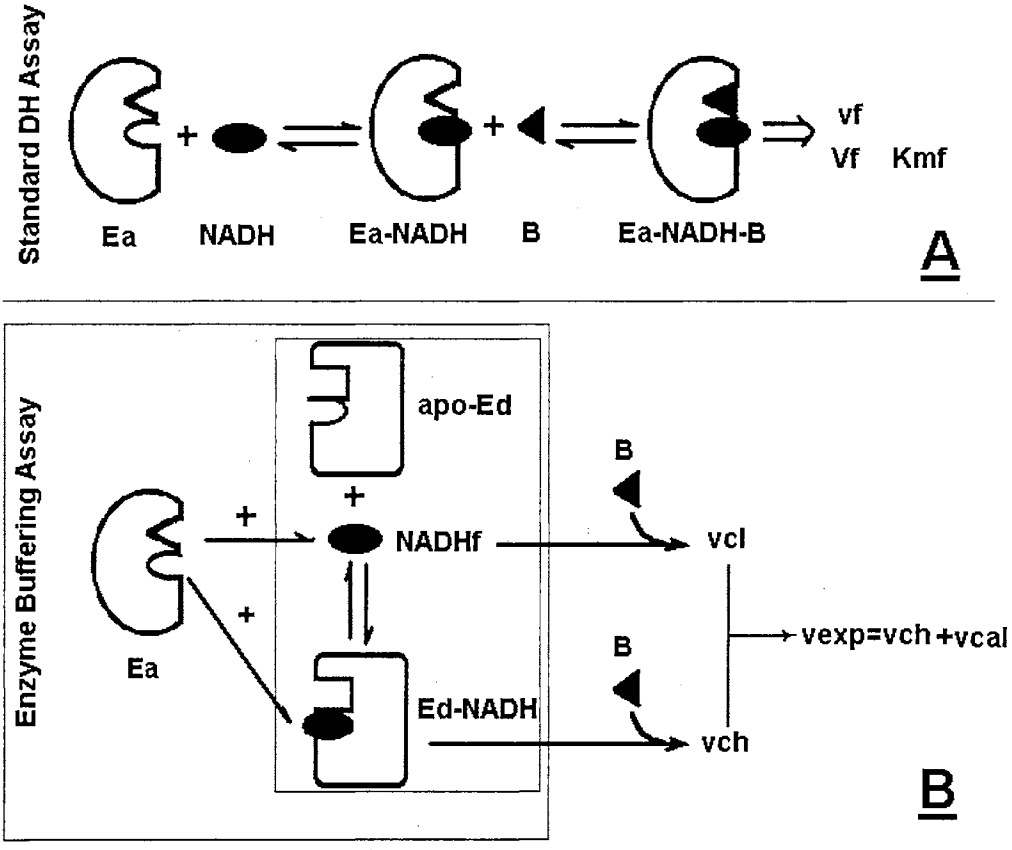
Standard DH Assay
Ea
NADH
Ea-NADH
B
Ea-NADH-B
vf
Vf
Kmf
A
Enzyme Buffering Assay
apo-Ed
NADHf
Ea
Ed-NADH
B
vcl
B
vch
vexp=vch+vcal
B

initial velocity part of the Ea reaction is about 30 sec. Therefore, $[NADH]_f$ stays in equilibrium with Ed throughout the reaction of Ea that is followed.

Fig. 2.1 B shows that the $v_{exp}$ measured in the enzyme buffering test is a composite of the two reactions: $v_{ch}$, the flux through the channeled path, and $v_{cl}$, the flux through the classical, free diffusion path. In the case of no channeling $v_{cl}$ will equal $v_{cal}$ of Eqn (2.1). Thus the criterion of substrate channeling is the ratio,

$$R = \frac{v_{\exp}}{v_{cal}} \tag{2.2}$$

All enzymes studied followed Eqn (2.1) in the absence of Ed. However, it is important to realize that this is not a requirement for application of the enzyme buffering method. The Michaelis-Menten equation of (2.1) is just a convenient way to represent the experimental velocity as a function of free NADH. One could even use a completely empirical equation to represent this or more complex functions, e.g., allosteric response, without any effect on the experimental R value. The point is that the enzyme buffering test does not require any knowledge of the kinetic mechanisms involved – a feature that adds to its rigorous nature.

If R is significantly greater than 1, the most reasonable explanation is that Ea can utilize both bound and free NADH, since the bound form is, by far, the predominant form present. Other mechanisms for obtaining R > 1 ("anomalous kinetics") have been considered and found deficient (Svedruzic & Spivey, 2001). However, R cannot possibly be greater than 1 unless $[NADH]_f << K_{NADH}$, a situation that the critics have consistently overlooked (Chock & Gutfreund, 1988; Srivastava et al., 1989). Thus for a

successful enzyme buffering test, it is essential that the [Ed] be high enough to guarantee this condition. With well designed enzyme buffering tests, even though the total [NADH] is about 50 μM, $[NADH]_f$ is only a few tenths of a μM, i.e., about 0.1 of the $K_{NADH}$. Thus $v_{cal}$ can only be about 0.1 of $V_{NADH}$ under these circumstances. $[NADH]_f$ is "buffered" at this concentration by the excess of Ed, hence the name "enzyme buffering test" (it is the NADH that is buffered).

The experimental measurements needed for the enzyme buffering test are: 1) the enzyme kinetic constants of Ea ($K_{NADHf}$ and $V_{NADHf}$) for free NADH (measurements in the absence of Ed), 2) determination of [NADH]f for each [Ed] used in the enzyme buffering experiments, and 3) the enzyme buffering experiments, which are simply repeats of step 1) except in the presence of varying concentrations of Ed. The kinetic constants $K_{NADHf}$ and $V_{NADHf}$ are quite accurately determined in step 1) because NADH oxidation is normally the favored direction of these dehydrogenases. Therefore, long initial velocity rates are obtained.

The second step of the enzyme buffering test, determination of the $[NADH]_f$ in equilibrium with each [Ed] has most often been done by measuring the dissociation constant of Ed-NADH by fluorescence titration methods (Srivastava & Bernhard, 1985). However, this is subject to uncertainty unless independently verified by control experiments using enzyme buffering measurements between enzymes of the same chiral specificity. This uncertainty results from the fact that the fluorescence titrations necessarily must use lower concentrations of Ed than needed for the enzyme buffering tests. At these higher [Ed], there is too little dissociation of Ed-NADH to allow the measurement of its Kd. However, many of these dehydrogenases undergo some

concentration dependent dissociation (e.g., homotetramer to dimer), which might introduce changes in the Kd with changes in [Ed]. Non-channeling control experiments can test for such changes in Kd. For the few such control experiments presented by Srivastava and Bernhard (op cit.) they do demonstrate the accuracy of the Kd measured by fluorescence experiments. (This fact is ignored by the critics.) Consequently, we have preferred to measure the $[NADH]_f$ in equilibrium with Ed by control experiments in all cases. In some cases two independent non channeling experiments were used to estimate $[NADH]_f$. One can calculate a Kd from these data. This Kd as well as the $K_{NADHf}$ and $V_{NADHf}$ of the enzyme buffering test can be related to values in the literature for further confirmation.

The enzyme buffering measurements are normally performed with two strategies: a) varying [Ed] at constant [NADH]total and b) varying [Ed] with constant ratio of NADH/Ed. The latter gives $v_{exp}$ vs. [Ed-NADH] curves that are very close to the rectangular hyperbolic Michaelis-Menten function, in spite of the inhibition from the apo-Ed. Thus these data provide a quick visual interpretation of the results. The apparent Vm found from such curves via double reciprocal plots or nonlinear least squares fit to the Michaelis-Menten equation are, however, significantly below the true Vm due to the inhibition by the apo-Ed. The method of varying [Ed] at constant [NADH] total invariably gives higher channeling ratios R and a measure of the apo-Ed inhibition. These data with constant [NADH] total cannot be interpreted graphically, but data from both methods can be analyzed by nonlinear least squares analysis and a kinetic model equation.

It should be emphasized, however, that the enzyme buffering tests do not require such analysis. The R criterion, of Eqn (2.2), a purely experimental number, is all that is needed for the test of channeling. The use of kinetic models is pursued for other objectives, specifically to try to understand the molecular mechanism of the NADH channeling.

### 2.1.2. Non-Channeling (Control) Enzyme Buffering Experiments: Experiments with Ea and Ed of the same Chiral Type

No channeling has been reported in the enzyme buffering experiments between dehydrogenases of the same chiral specificity (Srivastava & Bernhard, 1985). The two chiral types of NAD(H) dehydrogenases, A type and the B type, are defined on the basis of which of the two C4 nicotinamide hydrogens gets transferred in the enzymatic reduction (You, 1982; You, 1985). In this work, we use non-channeling experiments to estimate $[NADH]_f$ in the enzyme buffering experiments. In this way, every channeling experiment can be directly related to one or several non-channeling experiments. In the non-channeling experiments (Fig. 2.1), Ea can only use the free from of NADH, hence the measured Ea reaction rate ($v_{exp}$) is a direct function of $[NADH]_f$ (Eqn 2.3). The measured $v_{exp}$ in the non-channeling experiment is related to $[NADH]_f$ as indicated by the expression:

$$[NADH]_f = \frac{K^f_{NADH} \cdot v_{exp}}{(V^f_{NADH} - v_{exp})} \qquad (2.3)$$

The relation is an algebraic rearrangement of the Michaelis-Menten equation for the Ea reaction. The $K^f_{NADH}$ and $V^f_{NADH}$ refer to the kinetic parameters of the free Ea reaction (Fig. 2.1 A). The calculated $[NADH]_f$ value is used in the Eqn. 2.1 for $v_{cal}$, which is subsequently used in Eqn. 2.2 in evaluation of an actual channeling experiment. As

additional control the calculated $[NADH]_f$ can be used to calculate the apparent Kd for the Ed-NADH complex. The apparent Kd value can be compared with literature reported values to make connection between our experiments and the experiments in the past. The apparent Kd for the Ed-NADH complex can be calculated using relation:

$$\text{appKd} = \frac{[NADH]_f([Ed_t - [NADH]_b)}{([NADH]_t - [NADH]_f)} \tag{2.4}$$

taking into account that:

$$[NADH]_b = [Ed]_b = [NADH]_t - [NADH]_f$$

$$[Ed]_t = [Ed]_f + [Ed]_b$$

where subscripts t refer to the total concentration of the component present at the beginning of the measurement, f refer to the free component, and b refers to bound component in complex. If the Kd is independently measured, e.g, by fluorescence titrations, the non-channeling experiments can also quantify all other errors in the enzyme buffering tests (both systematic and random errors) since the components and concentrations are virtually identical in the control and channeling cases. Results from four such control experiments (Svedruzic & Spivey, 2001) demonstrate that R values from Eqn (2.2) are within 10% of the expected 1.00. In sharp contrast to these control experiments, R values between 4 and 20 have been reported for some A-B pairs – 40 to 200-fold larger than the experimental errors. The critics ignore these control experiments.

### 2.1.3 Ea Michaelis-Menten Parameters for Oxidized Substrate B in the Enzyme Buffering Experiments

Although the enzyme buffering criterion R is very rigorous when significantly greater than 1, the maximum R value is limited by the relative magnitude of enzyme

kinetic constants and Kd for Ed-NADH in ways unrelated to channeling. Thus as will be demonstrated in chapter 5, R can often be ≈ 1 even when > 90% of the reaction flux is passing through the channeling path. The enzyme buffering criterion R is very insensitive to channeling in these cases. Therefore, other potentially useful criteria were sought. One such criterion is the apparent $K_b$ for the cosubstrate B. For a sequential ordered Bi Bi mechanism, this apparent $K_b$ is given by

$$\text{app}K_b = \left(\frac{[\text{NADH}]_f + K_{ia}}{[\text{NADH}]_f + K_a}\right) \cdot K_b \qquad (2.5)$$

where $K_{ia}$ is the inhibition constant for NADH, and for ordered Bi Bi mechanism it is equal to Kd Ea-NADH. The $K_a$ and $K_b$ are the true Michaelis-Menten constants of substrates A and B in the absence of channeling (e.g., in the absence of Ed). $K_a$ and $K_b$ can be measured in standard enzyme assays. $K_{ia}$ is the Kd of Ea-NADH and can be measured by any method that measures the Kd. The equation for apparent $K_b$ of Ea will be different from Eqn (2.6) for dehydrogenases with different steady-state mechanisms, but several of our Ea enzymes, e.g., LDH, follow the ordered mechanism for the free NADH path, and we will limit our use of this criterion to those enzymes as Ea. Thus if the apparent $K_b$ in the enzyme buffering experiments is significantly different from that predicted by Eqn (2.5), this will be strong evidence of anomalous kinetics and due quite likely to NADH channeling. If this apparent $K_b$ is close to that predicted by Eqn (2.5), anomalous kinetics cannot be excluded since this might happen by fortuitous values of the kinetic constants that give very similar apparent $K_b$, Thus, we might expect false negatives, but not false positives for anomalous kinetics by this test.

## 2.2. Materials and Methods

### 2.2.1 Materials

*Materials.* All chemicals unless otherwise indicated were purchased from Sigma Chemical Co, (St. Louis MO). DHAP was Li salt, pyruvate was sodium salt. Both NAD and NADH were of the highest purity commercially available (more than 99%). BSA was RIA grade, fraction V powder. Acetoacethyl-CoA was prepared from Diketal and CoALi (Lynen *et al.*, 1958). Blue Sephadex was purchased from Pharmacia, (Pharmacia Biotech). Dye Mātrex™ red A gel was purchased from Sigma.

*Buffers and Solutions.* Unless otherwise indicated: Tris/HCl pH=7.5 buffer refers to: 50 mM Tris/HCl pH=7.5, 2 mM EDTA, 10 mM 2-ME. In all measurements with LADH, 2-ME was replaced with 5 mM glutathione. The buffer pH was adjusted at room temperature. Stock solutions of 150 mM Li DHAP were prepared in deionized $H_2O$ and kept frozen for three months at -20 °C. Stock solutions of 2.0 M Na pyruvate with 0.02% $NaN_3$ were kept at 4 °C for six months. Stock solutions of 300 mM of 3-phosphoglycerate were kept frozen for three months at -20 °C. Stock, 10 mM acetoacetyl-CoA solutions were used within five months. NADH stock solutions were prepared in 120 mM $Na_2CO_3$ buffer in a light isolated container and used within two weeks of preparation. NAD was prepared fresh before each measurement, and used within 8 hours from preparation. ATP was prepared as 100 mM stock solution, stored at –20 °C, and used within 3 months of preparation. The concentration and the stability of each substrate were measured enzymatically.

### 2.2.2 Methods

*Enzyme kinetics*. Each kinetic measurement was repeated two to three times. If the results were not reproducible within 15%, the measurements were tested for specific problems and repeated until this precision was achieved. The 15% measurement precision is indicated on all graphs with ± 7.5% error bars. In all calculations an enzyme unit is defined as 1μmol of NADH oxidized per minute at 25°C. An absorbtivity of 6.22 $10^3$ $M^{-1}$ $cm^{-1}$ was used for NADH. In some enzyme buffering tests, the rates were calculated using the absorptivity of protein bound NADH. All assay mixtures had 1 mg/ml BSA to prevent denaturation of assayed protein due to absorption to the cuvette surface. Before each assay the initial NADH absorbance was recorded, and disappearance of the first 20% of total absorbance was followed as linear reaction to calculate the initial rate calculation. For all GAPDH activity measurements, the reaction mixture had 3 mM 3-phosphoglycerate, 1 mM ATP, 2 mM $MgCl_2$ and 10 U/ml of 3-phospoglycerate kinase (PGK). For specific activity measurements (unless otherwise indicated in the text) NADH was 100 μM. The assay buffer was Tris/HCl pH = 7.5. In contrast to other GAPDH, byGAPDH is strongly activated by NAD produced during the assay. The reaction rate was made linear by using byGAPDH from the stock that contained 100 μM NAD. Unless otherwise indicated all LDH assay mixtures were prepared with 630 μM pyruvate, and 100 μM NADH in Tris/HCl pH = 7.5. The αGDH was assayed in the same Tris buffer with 300 μM of dihydroxyacetone phosphate, and 100 μM NADH. The βHAD was assayed in Tris/HCl pH=7.5 and 100 μM of acetoactylCoA and 100 μM NADH. LADH assays were in Tris/HCl pH = 7.5 except that 2-meraptoethanol was

replaced with 5 mM glutathione. The assay mixture also had 400 μM benzaldehyde and NADH was 100 μM unless otherwise indicated.

*Proteins*

Baker's yeast (*Saccharomyces cerevisiae*) GAPDH was prepared in our lab (Byers, 1982). The enzyme was stored as an ammonium sulfate suspension and used within a week of its elution from the Blue Sephadex column. The specific activity measured in the NADH oxidation direction was between 95-110 U/mg. Rabbit muscle GAPDH was purchased from Sigma, and further purified by NAD affinity elution from the Blue Sephadex column. Before loading on the Blue Sephadex column, the protein was dialyzed in 50 mM Tris/HCl pH = 7.5, 10 mM 2-ME. The same buffer was used in all subsequent chromatography steps. The dialyzed protein was loaded on the column, and the column was washed with several bed volumes. After the wash the protein was eluted with 10 mM NAD. The protein elutes in a very broad peak with a recovery of 50-60%. The eluted protein was concentrated by slowly adding $(NH_4)_2SO_4$ to 100 % saturation in ice, and subsequent centrifugation. The purified enzyme was stored as a suspension in 90% ammonium sulfate and used in the enzyme buffering experiments within a month of purification. The specific activity was 75-90 U/mg before the blue Sephadex treatment, and 100-120 U/mg for blue Sephadex treated protein. Both, blue Sephadex treated and untreated rmGAPDH appear as homogenous bands on SDS-PAGE. Rabbit muscle αGDH was purchased from Sigma. Most of the measurements were done on the commercial enzyme without any purification. For some measurements the commercial enzyme was further purified on a dye affinity Red A agarose column by NADH affinity elution. The protein was first dialyzed in 50 mM Tris/HCl buffer with

100 mM NaCl. The protein bound to the matrix was washed with several bed volumes with the Tris/HCl buffers. The protein was eluted with 10 mM NADH in the same buffer. The recovery was about 50%. The protein is concentrated by adding $(NH_4)_2SO_4$ to 100 % saturation, and subsequent centrifugation. The specific activity before the Red A column was 190 to 230 U/mg, and after the column 210-240 U/mg. Before chromatography on the red A column, SDS-PAGE of the enzyme shows a few contaminating bands, but after the column the protein appears as a single band. Rabbit muscle LDH, porcine muscle LDH and porcine heart LDH were purchased from Sigma as $(NH_4)_2SO_4$ suspension and used without further purification. All three proteins on SDS-PAGE analysis appear as a single band. LADH was purchased as $(NH_4)_2SO_4$ suspension from Boeringer Meinheim and used without further purification. BsGAPDH was purchased form Sigma as lyophilized powder. The $(NH_4)_2SO_4$ suspension of bsGAPDH S mutant was a generous gift of professor Branlant and collaborators (Clermont *et al.*, 1993).

*Enzyme buffering experiments*. To remove tightly bound nucleotides all enzymes used as Ed were treated with charcoal directly before the enzyme buffering measurements. One milligram of charcoal was added per milligram of protein, the solution was vortexed and left in ice for 10 min before charcoal was removed by spinning in a microcentrifuge at the maximal speed for 10-15 minutes. The success of the procedure was followed by measuring changes in the absorbance ratio 280/260 nm. After two charcoal treatments the 280/260 ratio did not change with further treatment. NADH and NAD assay measurements have shown that once when charcoal treatment gives stable 280/260 nm absorbance ratio, more than 90% of enzyme sites are in the apo form.

The enzyme buffering reaction mixture was 150 μL prepared in a microcuvette. The Ed was put in the cuvette first, and left for a few minutes to thermally equilibrate in the cuvette holder. During that time the solution absorbance was followed to test the Ed stability. If Ed is unstable, enzyme denaturation can be seen as an increase in the solution turbidity and hence absorbance. Denatuartion is especially rapid with rmGAPDH. To avoid denaturation of rmGAPDH, it had to be dialyzed and used within a 5 to 6 hour period. After stability of Ed was confirmed, NADH, and the oxidized substrate of Ea were added. Before and after adding of NADH the solution absorbance was recorded. This is a necessary precaution since the absorptivity of enzyme bound NADH is significantly changed from that of free NADH by some dehydrogenases. The absorptivity of NADH bound to rmGAPDH was measured to be 5.2 $10^3$ $M^{-1}$ $cm^{-1}$, and the absorptivity of NADH bound to αGDH was measured to be 4.7 $10^3$ $M^{-1}$ $cm^{-1}$. These altered absorptivities were considered when the reaction rates were calculated. Finally before starting the reaction by addition of Ea, it is necessary to test for NADH oxidation by the high concentrations of Ed. These NADH oxidations can either come from trace amounts of Ed enzyme contaminating Ea or from NADH oxidase activities within Ed. In some cases the "NADH oxidases" can oxidize NADH even in the absence of added cosubstrates. These oxidases can either be due to contaminants within Ed or in some cases are intrinsic to Ed. For the Ed used in this study, measured Ea background activity was negligible (less than 5-10% of measured activity in the presence of Ea) with the exception of byGAPDH. The byGAPDH was very difficult to purify from trace contamination of MDH activity and we never realiably measured channeling between these two enzymes. After these control measurements were completed, the channeling

reaction was started by addition of Ea. The measured rate was estimated from the first 20% of the reaction on the basis of total NADH absorbance measured before the start of the reaction.

*Curve Fitting and Numerical Analysis*. All curve fitting was done with Microcal Origin program. All Km curves were fitted by nonlinear least squares approach to a hyperbolic function and equal weights assigned to all points.

*Measurements* All measurements were performed on Shimadzu 160uv spectrophotometer. Unless otherwise indicated the cuvette holder temperature was maintained at 25 ± 0.2 °C. Protein concentrations were determined by absorbance at 280 nm, using the following absorptivities ($M^{-1}$ $cm^{-1}$): rmαGDH $4.78x10^4$ ; phLDH $1.7x10^5$; rmLDH $1.75x10^5$; rmGAPDH $1.16x10^5$; and byGAPDH $1.3x10^5$.

## 2.3 Results

### 2.3.1 Enzyme Buffering Measurements

The results form the majority of our enzyme buffering channeling experiments are summarized in the Table 2.1. The selected enzymes have various metabolic and phylogenic origins. A R value ($v_{exp}/v_{cal}$) higher than 1 indicates channeling. R values equal to 1, or lower than 1, could be indication of no channeling or a specific case of channeling where R value is not an adequate criteria for channeling detection (see chapter 5). For some enzyme pairs the R value indicated in the Table 2.1 is given as a range of values. The variations in the R value are due to the different experimental conditions as indicated further in this section. In cases where R is a single number, the given value is an average of a set of identical experiments.

Very strong evidence of channeling (R ≈35) was observed with the phLDH (Ed)-byGAPDH (Ea) pair (Table 2.1). As described in chapter 5, the high R values for byGAPDH are almost certainly due to the unusually high Km of byGAPDH for NADH, which allows the channeling criterion R of Eqn (2.2) to be especially high (since the [NADH]f is especially low relative to this high Km). The next highest R values are found with byGAPDH as donor enzyme. The reason is currently not so clear for this relatively high R, but is also likely to be due to the favorable kinetic and dissociation constants. In keeping with other literature (Srivastava & Bernhard, 1985), channeling

**Table 2.1 Summary of enzyme buffering experiments with NAD(H) dehydrogenases.**

The table summarizes results of channeling experiments with various Ea : Ed combinations used in our experiments. All measurements were performed in 50 mM Tris/HCl, pH=7.5, 2 mM EDTA, 10 mM 2-ME. In the measurements with ADH, 2-ME was replaced with 5mM glutathione. The initial velocity rates were measured at 25 °C, by following NADH absorbance at 340 nm. The R values were calculated using equations 2.1 and 2.2. The R values given as a single value are average of the several identical measurements. When the R values are given as a range, they represent results from measurements with variable conditions as indicated in the rest of the text. Abbreviations used: ltLDH, lobster tail muscle LDH; tmLDH, trout muscle LDH; ecMDH, *E coli* MDH; tfMDH, *Thermus flavus*; aKV, α keto valeric acid. All other abbreviations are as used in the rest of the text.

Table 2.1

| Ed (type) | Ea (type) | Ea-Vf U/mg | Ea-$Kf_{NADH}$ μM | Kd,Ed-NADH μM | R |
|---|---|---|---|---|---|
| rmGAPDH(B) | phLDH(A) | 130 ± 20 | 7.8 ± 0.9 | 0.8 ± 0.15 | 1.3 - 2 |
| | pmLDH(A) | 440 ± 30 | 8.2 ± 1.2 | 0.8 ± 0.15 | 1.1-1.6 |
| | tmLDH(A) | 335 ± 35 | 4.1 ± 0.4 | 0.8 ± 0.15 | 1.34 |
| | bsLDH(A) | 90 ± 8 | 20 ± 1.5 | 0.8 ± 0.15 | 1.84 |
| | ltLDH(A) | 450 ± 40 | 11 ± 0.75 | 0.8 ± 0.15 | 1 |
| | phLDH-aKV(A) | 5.5 ± 0.4 | 8 ± 0.6 | 0.8 ± 0.15 | 1.3 |
| | phcMDH(A) | 430 ± 30 | 9 ± 0.55 | 0.8 ± 0.15 | 1.2-1.6 |
| | hlADH(A) | 40.5 ± 4 | 7 ± 0.6 | 0.8 ± 0.15 | 1.0-1.4 |
| byGAPDH(B) | phLDH(A) | 130 ± 20 | 7.8 ± 0.9 | 3.3 ± 0.8 | 6.6-10.6 |
| | pmLDH(A) | 440 ± 30 | 8.2 ± 1.2 | 3.3 ± 0.8 | 6.2-7.8 |
| | hlADH(A) | 40.5 ± 4 | 7 ± 0.6 | 3.3 ± 0.8 | 4.5-8 |
| | phcMDH | 430 ± 30 | 9 ± 0.55 | 3.3 ± 0.8 | 5.6-9.6 |
| | bsLDH(A) | 90 ± 8 | 20 ± 1.5 | 3.3 ± 0.8 | 6 |
| bsGAPDH(B) | phLDH(A) | 130 ± 20 | 7.8 ±0.9 | 0.3 ± 0.02 | 1.28 |
| | bsLDH(A) | 90 ± 8 | 20 ± 1.5 | 0.3 ± 0.02 | 0.95 |
| chicken mGAPDH(B) | phLDH(A) | 130 ± 20 | 7.8 ± 0.9 | 1.01 ± 0.9 | 2.75 |
| bsGAPDH. Smut(B) | phLDH(A) | 130 ± 20 | 7.8 ± 0.9 | 0.6 ± 0.05 | 1.3 |
| | bsLDH(A) | 90 ± 8 | 20 ± 1.5 | 0.60 ± 0.05 | 1.25 |
| rm αGDH(B) | phLDH(A) | 130 ± 20 | 7.8 ± 0.9 | 0.96 ± 0.094 | 3.0-4.0 |
| | rmLDH(A) | 140 ± 20 | 4.4 ± 0.4 | 0.96 ± 0.094 | 3-3.5 |
| | phcMDH(A) | 430 ± 30 | 9 ± 0.55 | 0.96 ± 0.094 | 2.0-3.5 |
| | phmMDH(A) | 440 ± 30 | 13 ± 0.9 | 0.96 ± 0.094 | 2.0-3.1 |
| | ecMDH | 2500 ± 300 | 13 ± 0.87 | 0.96 ± 0.094 | 1.8 |
| | tfMDH(A) | 81 ± 8.0 | 3.2 ± 0.2 | 0.96 ± 0.094 | 0.8 |
| phLDH(A) | rmGAPDH(B) | 105 ± 15 | 3.7 ± 0.3 | 1.1 ± 0.15 | 1.2 |
| | byGAPDH(B) | 110 ± 20 | 43 ± 8 | 1.1 ± 0.15 | 30-40 |
| | bsGAPDH(B) | 94 ± 8 | 3.4 | 1.1 ± 0.15 | 2.4 |
| | rm αGDH(B) | 230 ± 30 | 2.5-3.3 | 1.1 ± 0.15 | 2.7-3.5 |
| rmLDH(A) | rmGAPDH(B) | 105 ± 15 | 3.7 ± 0.3 | 3.2±0.6 | 1.15 |
| ph cMDH(A) | rmGAPDH(B) | 105 ± 15 | 3.7 ± 0.3 | 7.1±0.89 | 0.92 |

from byGAPDH is not discriminating concerning the phylogenic origin of acceptor enzyme.

Smaller R values were observed with rmαGDH as B type enzyme and various A type enzymes. The R values remain the same in both Ed :Ea combination. R values very close to the experimental uncertainty (R=1.0-2.0) were observed with rmGAPDH, and R values equal 1 were observed with bsGAPDH. Two types of bsGAPDH enzyme were used: the wild type and the S mutant. The S mutant has L187A, P188S replacements and binds the NADH with three times lesser affinity (Clermont et al., 1993; Corbier *et al.*, 1990). No significant difference in the channeling ratio was observed between the mutant and the wild type. Again we emphasize that low R values are not evidence of the lack of NADH channeling. This is more fully described in chapter 5.

### 2.3.2 Non-Channeling Control Experiments: Enzyme Buffering Experiments with Dehydrogenases of the same Chiral Specificity.

Enzyme buffering experiments with enzymes of the same chiral specificity (enzyme buffering, control experiments) offer two important types of information: 1) a measure of the errors involved in the companion enzyme buffering tests with enzymes of opposite chiral specificity (potential channeling enzymes) and 2) a direct measure of the free concentration of NADH, $[NADH]_f$, in equilibrium with any Ed concentration used in the latter experiments.

However, accuracy in determining [NADH]f by these control experiments depends on the of the absence of channeling or other anomalous kinetics with these control experiments. The absence of channeling with these control experiments seems to

be a good hypothesis, but does need to be tested whenever practical. One way of doing this is to compare the calculated $K_d$ from such control experiments with the $K_d$ determined by independent methods. Another way is to perform enzyme buffering control experiments using at least two different second enzymes for the same enzyme under test. Data of this nature are given in the Tables 2.2 (A-F). In the experiments with byGAPDH or rmGAPDH as Ed, two different non-channeling experiments were performed and compared to increase the precision and the reliability. ByGAPDH or rmGAPDH were paired with rmαGDH and βHADH, all of which are B type enzymes. Each Ea: Ed pair, represents an independent experiment, so the results from two different Ea:Ed combinations can be directly compared. The apparent Kd values, calculated from the two Ea:Ed combinations are reasonably close, indicating the precision in the approach.

The apparent Kd value calculated for rmGAPDH is higher than the value reported in the literature (Wilder *et al.*, 1989). RmGAPDH binds NAD and NADH with strong negative cooperatively (Bloch *et al.*, 1971) and with very high affinity for the first two binding sites (0.01-0.4 μM). NADH binds several times weaker than NAD. The apparent NADH Kd we measure with the control experiments is 0.8 and 0.9 μM . Several reasons may explain this difference from independent measures of this Kd. Some of these differences could be due to the different purification procedures and freshness of the enzymes. Our lab has experienced considerable variations due to these factors. However, it should be remembered that I measured the enzyme buffering on the very next day after determining the [NADH]f values, so that these values should accurately represent the equilibria with these Ed enzymes. Another likely factor is that the control

**Table 2.2 (A-F). Determining [NADH]f and apparent Kd using enzymes of the same chiral specificity.**

All measurements were performed in 50 mM Tris/HCl, pH=7.5, 2 mM EDTA, 10 mM 2-ME. The rates were measured at 25 °C, by following NADH absorbance at 340 nm. Total [NADH] in all measurements was 50 μM. In all measurements where phβHADH was used as Ea, [acetoacetyl-CoA] = 100μM. In all measurements where rmαGDH was used as Ea, [dihydroxyacetone phospahte] = 3mM. In measurement with phcMDH as Ea, [oxaloacetic acid] = 150 μM. $[NADH]_f$ and the apparent Kd were calculated as indicated in equations 2.3 and 2.4. All indicated rates were measured to within 15% precision as indicated in the Material and Methods.

Table 2.2.A Ea phβHADH: Ed byGAPDH

| Ed/μM | Ed.site/μM | vexp/(U/mg) | [NADH]f/μM | appKd/μM |
|---|---|---|---|---|
| 50 | 200 | 3.90 | 1.05 | 3.23 |
| 60 | 240 | 3.10 | 0.78 | 3.03 |
| 80 | 320 | 2.80 | 0.69 | 3.79 |
| 100 | 400 | 2.10 | 0.49 | 3.48 |
| 110 | 440 | 1.80 | 0.41 | 3.25 |
| 120 | 480 | 2.00 | 0.46 | 4.04 |
| | | | Kd/μM= | 3.47 |
| | | | stdev Kd ± | 0.38 |
| [NADH]tot/uM= βHADH | 50 | | | |
| Vmax/(U/mg)= | 16.2 ± 0.8 | | | |
| Km/(μM)= | 3.24 ± 0.3 | | | |

Table 2.2.B Ea rmαGDH:Ed byGAPDH

| Ed/μM | Ed.site/μM | vexp/(U/mg) | [NADH]f/μM | appKd/μM |
|---|---|---|---|---|
| 50 | 200 | 36.90 | 0.71 | 2.16 |
| 60 | 240 | 35.20 | 0.67 | 2.58 |
| 80 | 320 | 24.20 | 0.44 | 2.37 |
| 100 | 400 | 21.20 | 0.38 | 2.65 |
| 110 | 440 | 16.90 | 0.29 | 2.30 |
| 120 | 480 | 17.60 | 0.31 | 2.65 |
| | | | Kd/μM= | 2.46 |
| | | | stdev Kd ± | 0.21 |
| [NADH]tot/μM= rm αGDH | 50 | | | |
| Vmax/(U/mg)= | 230 ± 24 | | | |
| Km/(μM)= | 3.7 ± 0.3 | | | |

Table 2.2.C Ea phβHADH: Ed rmGAPDH

| Ed/μM | Ed.site/μM | vexp/(U/mg) | [NADH]f/μM | appKd/μM |
|---|---|---|---|---|
| 50 | 200 | 1.20 | 0.25 | 0.76 |
| 60 | 240 | 1.00 | 0.21 | 0.79 |
| 70 | 280 | 0.90 | 0.18 | 0.85 |
| 80 | 320 | 0.75 | 0.15 | 0.83 |
| 90 | 360 | 0.64 | 0.13 | 0.80 |
| 100 | 400 | 0.55 | 0.11 | 0.77 |
| 110 | 440 | 0.40 | 0.08 | 0.62 |
| 120 | 480 | 0.57 | 0.11 | 0.99 |
| | | | Kd/μM= | 0.80 |
| | | | stdev Kd ± | 0.10 |
| [NADH]tot/uM= βHADH | 50 | | | |
| Vmax/(U/mg)= | 17 ± 1.2 | | | |
| Km/(μM)= | 3.24 ± 0.3 | | | |

Table 2.2.D Ea rmαGDH: Ed rmGAPDH

| Ed/μM | Ed.site/μM | vexp/(U/mg) | [NADH]f/μM | appKd/μM |
|---|---|---|---|---|
| 50 | 200 | 15.1 | 0.27 | 0.82 |
| 60 | 240 | 11.2 | 0.20 | 0.76 |
| 70 | 280 | 9.7 | 0.17 | 0.79 |
| 80 | 320 | 8.3 | 0.15 | 0.79 |
| 90 | 360 | 6.6 | 0.11 | 0.71 |
| 100 | 400 | 5.4 | 0.09 | 0.65 |
| 110 | 440 | 5.3 | 0.09 | 0.71 |
| 120 | 480 | 4.4 | 0.08 | 0.65 |
| | | | Kd/μM= | 0.74 |
| | | | stdev Kd ± | 0.06 |
| [NADH]tot/μM= rm αGDH | 50 | | | |
| Vmax/(U/mg)= | 220 ± 20 | | | |
| Km/(μM)= | 3.7 ± 0.3 | | | |

Table 2.2.E Ea phβHADH: Ed rmαGDH

| Ed/μM | Ed.site/μM | vexp/(U/mg) | [NADH]f/μM | appKd/μM |
|---|---|---|---|---|
| 55 | 110 | 3.15 | 0.74 | 0.91 |
| 70 | 140 | 2.53 | 0.57 | 1.04 |
| 80 | 160 | 2.10 | 0.46 | 1.02 |
| 90 | 180 | 1.75 | 0.37 | 0.98 |
| 100 | 200 | 1.30 | 0.27 | 0.82 |
| 120 | 240 | 1.15 | 0.24 | 0.90 |
| | | | Kd/μM= | 0.95 |
| | | | stdev Kd ± | 0.09 |
| [NADH]tot/uM= βHADH | 50 | | | |
| Vmax/(U/mg)= | 17.2 ± 0.6 | | | |
| Km/(μM)= | 3.24 ± 0.3 | | | |

Table 2.2.F Ea phcMDH:Ed phLDH

| Ed/μM | Ed.site/μM | vexp/(U/mg) | [NADH]f/μM | appKd/μM |
|---|---|---|---|---|
| 60 | 240 | 12.4 | 0.27 | 1.05 |
| 80 | 320 | 9.8 | 0.22 | 1.17 |
| 100 | 400 | 6.8 | 0.15 | 1.04 |
| 120 | 480 | 6 | 0.13 | 1.13 |
| | | | Kd/μM= | 1.10 |
| | | | stdev Kd ± | 0.06 |
| [NADH]tot/μM= phcMDH | 50 | | | |
| Vmax/(U/mg)= | 420 ± 20 | | | |
| Km/(μM)= | 9 ± 0.55 | | | |

experiments measure the apparent Kd at a specific ratio of total enzyme and NADH – ratios corresponding to those in the enzyme buffering experiments with enzymes of opposite chiral specificity. For enzymes with cooperative binding, our Kd values will be a complex average of the various stepwise Kd values of the enzyme. Another possibility is that in my hands the charcoal treatment used to prepare apo rmGAPDH was inadequate to remove extremely tightly bond cofactors or the cofactor degradation product. Binding was so tight that it was also undetected in the test I used to measure the residual NAD(H). Moreover the enzymatic approach used would not even detect the NAD(H) degradation products. An argument in support of this is the ratio of 280/260 nm absorbance measured on the charcoal treated enzyme. The highest ratios reported in the literature are 2.0-2.1 (Bloch et al., 1971; Scheek & Slater, 1982), the best ratios we measured were 1.7-1.8. In contrast to rmGAPDH, byGAPDH has no negative cooperatively in NADH binding (Cook & Koshland, 1970; Stallcup & Koshland, 1973) and binds NADH with moderate affinity. The apparent Kd value we measured for byGAPDH is at least five fold lower than those we found in the literature. The differences are most likely due to the different experimental conditions. Our measurements were in the low ionic strength, 50 mM Tris/HCl, pH = 7.5 buffer. The measurements reported in the literature are at much higher ionic strength, pH, and in phosphate buffer. All three factors, ionic strength, phosphate buffer, and higher pH are detrimental to byGPADH stability and NADH binding. We observed (as well as others (Srivastava & Bernhard, 1985; Wilder et al., 1989)) that increase in the ionic strength decreases the NADH binding affinity. Phosphate ions tend to interact strongly with GAPDH, possibly altering NADH affinity (our observation and others ((Bloch et al., 1971; Ward & Winzor, 1983)). ByGAPDH is

less stable at pH=8.0 and above (our observation and, (Byers, 1982)). The apparent Kd values measured in non-channeling with all other NAD(H) dehydrogenases were very close to the values reported in the literature. In the non-channeling experiments with rmαGDH as Ed, Ea was βHADH. The apparent Kd value calculated for rmαGDH is in good agreement with values reported in the literature (Srivastava et al., 1989). In all non-channeling experiments with various LDH as Ed (A type enzymes), the Ea was phcMDH (data not shown). The apparent Kd measured for phLDH, pmLDH are in good agreement with literature reported values (Dalziel, 1975; Holbrook *et al.*, 1975). Control non channeling experiments are performed with the same conditions as the channeling experiments and provide an excellent reference point. Several control non channeling experiments can be used in parallel increasing the quality of this control. [NADH]f values from non channeling experiments are independent of any complexities of NADH binding by the specific enzyme studied. Thus these measurements make enzyme buffering tests robust and a reliable approach to study channeling.

### 2.3.3 Ea Steady State Parameters for the Oxidized Substrate B in Enzyme Buffering Experiments

The most acceptable kinetic mechanism for NADH channeling (Chapter 5, Fig. 5.1) shows that the cosubstrate B is competitive with the first product, the apo-Ed. This product must necessarily be present at quite high concentrations in the enzyme buffering experiments to ensure that the majority of NADH is bound to Ed. To the extent that the apo-Ed inhibition of v in the enzyme buffering experiments is due to the product inhibition by Ed, increasing [B] should attenuate this inhibition. Data in Fig. 2.2 B shows that this is the case. However, increasing [B] also introduces substrate inhibition,

**Figure 2.2 (A-B). Pyruvate profiles for phLDH in the enzyme buffering and free NADH experiments.**

(A) Ed was byGAPDH (60μM and 117μM) and Ea was phLDH. The apparent Km for the substrate B ($appK_b$) was measured in the two channeling reactions with Ed = 60 μM (○) and Ed = 117 μM (■). The pyruvate inhibition is reduced in both channeling experiments. **(B)** The corresponding R values calculated using equations 2.1 and 2.2. Reduced pyruvate inhibition in the channeling relative to the free reaction, results in the increased R values (Ed=60μM ■, Ed=117 μM ○) with increase in pyruvate. All measurements were in 50 mM Tris/HCl, pH = 7.5, 2 mM EDTA, 10 mM 2-ME. The rates were measured at 25 °C, by following NADH absorbance at 340 nm. Total [NADH] in all measurements was 50 μM. The error bars, ± 7.5 % of the measured values, indicated the experimental precision. The velocity is expressed as U/mg of Ea. One unit U is defined as a μmol of NADH oxidized in one minute.

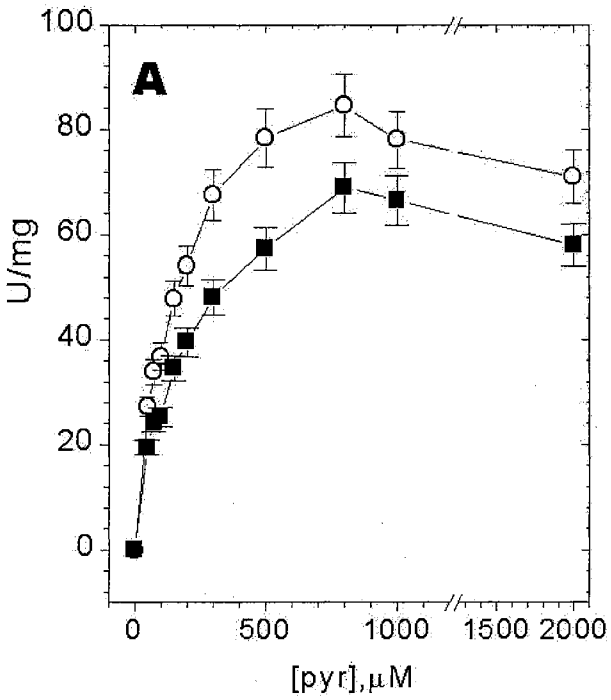
A
U/mg
100
80
60
40
20
0
0
500
1000
1500
2000
[pyr],μM

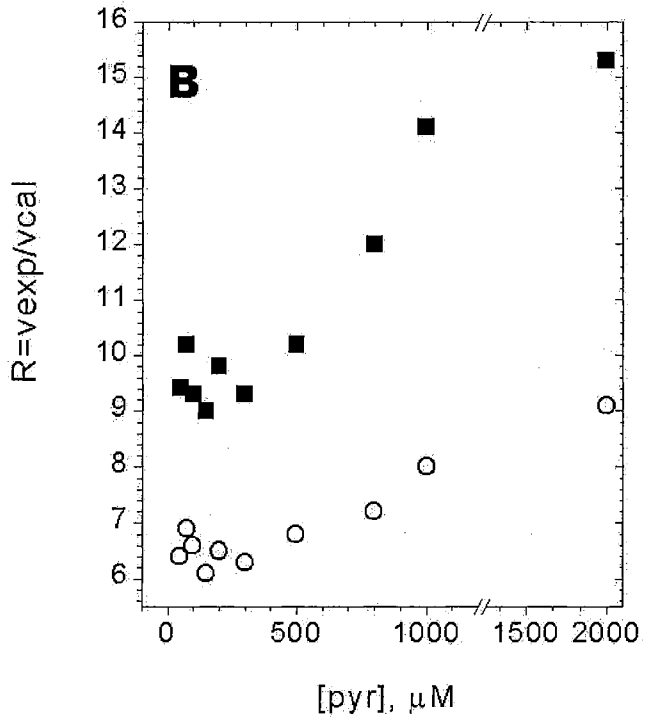
B
R=vexp/vcal
16
15
14
13
12
11
10
9
8
7
6
0
500
1000
1500
2000
[pyr], μM

which is well documented for these dehydrogenases in the free NADH experiments in the absence of Ed. Thus increasing [B] higher cannot increase R indefinitely. This is unfortunate since it might otherwise be a means of greatly enhancing the sensitivity and applicability of the enzyme buffering method. Aside from the possibility of reducing the apo-Ed inhibition by increasing [B], the apparent $K_b$ in the enzyme buffering experiments offers the possibility of another criterion for anomalous kinetics. The second channeling criteria presented is the apparent Km of the Ea for its oxidized substrate (B) in the channeling reaction system. For an ordered Bi-Bi steady-state mechanism adding reactants in the sequence of A followed by B, the apparent $K_b$ is given by Eqn 2.5 reproduced here

$$\text{app}K_b = \left(\frac{[\text{NADH}]_f + K_{ia}}{[\text{NADH}]_f + K_a}\right) \cdot K_b \qquad (2.5)$$

In an ordered Bi-Bi mechanism, the Km of B ($K_b$) is dependent on the concentration of coenzyme NADH as given by Eqn 2.5. The Kd values of the Ed-NADH complex presented in Table 2.3 are apparent Kd values calculated from non-channeling experiments where Ea and Ed were of the same chiral specificity (Eqns 2.3 and 2.4). With byGAPDH as donor enzyme, large disparities are observed between the $K_b$ from the enzyme buffering experiment and the $K_b$ expected for the classical path utilizing only free NADH. This is in keeping with the R criterion for channeling systems (Table 2.1). However, with rmGAPDH as the donor enzyme, it is not clear whether the differences in these two $K_b$ values is significantly larger than experimental error, though the result with pmLDH as Ea is promising.

**Table 2.3 (A-B) Evaluation of channeling by measuring apparent $K_b$ of Ea in the enzyme buffering experiments.**

The table summarizes values used for evaluation of channeling in enzyme buffering tests according to Eqn 2.5. **(A)** phLDH and pmLDH as Ea were paired with byGAPDH as Ed. **(B)** phLDH and pmLDH as Ea were paired with rmGAPDH as Ed. The Kd for Ed-NADH were calculated using non-channeling experiments and the equation 2.3. All other parameters were calculated as the best-fit values for the Michaelis-Menten hyperbolic equation. All measurements were performed in 50 mM Tris/HCl, pH=7.5, 2 mM EDTA, 10 mM 2-ME. The rates were measured at 25 °C, by following NADH absorbance at 340 nm. Total [NADH] in all measurements was 50 μM. The Eqn 2.5 was used in calculating phLDH and pmLDH app$K_b$ for pyruvate in case that there is no channeling and $[NADH]_f$ is the only NADH form available.

**Table 2.3 A byGAPDH as Ed**

| Reaction Type | Ea parameters | Ea=phLDH Ed=byGAPDH, 60 μM | Ea=phLDH Ed=byGAPDH, 117 μM | Ea=pmLDH Ed=byGAPDH, 117 μM |
|---|---|---|---|---|
| Enzyme Buffering: | $appK_b$, μM | 165 ± 17 | 177 ± 20 | 313 ± 32 |
| | V(pyr),U/mg | 103 ± 5 | 76.5 ± 4 | 322 ± 10 |
| Free NADH reaction | Km(NADH), μM | 7.9 ± 0.9 | 7.9 ± 0.9 | 8.2 ± 1.2 |
| | Kd(NADH), μM | 1.01 ± 0.09 | 1.01 ± 0.09 | 3.2 ± 0.6 |
| | V(pyr)free, U/mg | 152 ± 19 | 152 ± 19 | 321± 40 |
| Predict. $appK_b$, Eqn 2.5, μM | | 32.31 | 25.66 | 215 |

**Table 2.3 B rmGAPDH as Ed**

| Reaction Type | Ea parameters | Ea=phLDH Ed=rmGAPDH, 60 μM | Ea=pmLDH Ed=rmGAPDH, 60 μM |
|---|---|---|---|
| Enzyme Buffering: | $appK_b$, μM | 29 ± 5.2 | 195 ± 27 |
| | V(pyr),U/mg | 5.2 ± 0.16 | 16.4 ± 0.72 |
| Free NADH Reaction | Km(NADH), μM | 7.8 ± 0.9 | 8.2 ± 1.2 |
| | $K_d$(NADH), μM | 1.01 ± 0.09 | 3.2 ± 0.6 |
| | V(pyr)free, U/mg | 140 ± 15 | 353± 40 |
| Predict. $appK_b$, Eqn 2.5, μM | | 21.32 | 143 |

### 2.3.4 Enzyme Buffering Experiments with Variable or Fixed [Ed]/[NADH] Ratio.

There are two strategies in obtaining enzyme buffering data, the constant [Ed]/[NADH] ratio method and the fixed total [NADH], but variable [Ed] method. In the constant ratio experiments, both total [NADH] and [Ed] are increased but the (total [Ed])/(total [NADH]) ratio is kept constant. In the fixed [NADH] method, the total [NADH] in the experiment is kept constant while [Ed] is increased. We used both approaches to describe the properties of channeling reaction and the enzyme buffering test. The constant ratio method provides data that closely approximate the Michaelis-Menten equation. A similar strategy (constant ratio of substrate to inhibitor) is common practice to provide a Michaelis-Menten response of enzyme rates. Hence, this constant ratio method is good for a quick graphical interpretation of the enzyme buffering data and gives apparent Km and V values for the Ed-NADH substrate ($appK_a^b$ and $appV^b$) where the superscript b denotes Ed-bound NADH, the A substrate. These data are shown in Table 2.4 and Fig. 2.3. As indicated by model equations discussed in chapter 5, the $appK_{mb}$ appears to be close to the true $K_{mb}$, but the $V_b$ is substantially lower than the true value. This is due to the fact that the substantial inhibition by apo-Ed is included in these $v_{exp}$. Using the Michaelis-Menten equation for these data does not take this inhibition into consideration whereas the model equations and analyses in chapter 5 do.

As mentioned earlier, the constant total [NADH] method with variable [Ed] invariably gives higher R values in spite of the inhibition by Ed. Obviously the reduction in $[NADH]_f$ has a bigger impact on the R value than does the reduction in $v_{exp}$ from this

**Table 2.4 (A-B) Enzyme buffering measurements with constant (total [Ed]/total [NADH]) ratio.**

**(A)** The Ea is phLDH, the Ed is byGAPDH. The [byGAPDH]/[NADH] ratio was 1.25, or in terms of byGAPDH-NADH binding sites, the [byGAPDH-NADH sites]/[NADH] ratio was 5. $[NADH]_f$ and the $[NADH]_b$ values were calculated using Kd = 3.3 ± 0.8 μM for each byGAPDH NADH binding site (Table 2.2 A). The $v_{cal}$ values were calculated using Eqn. (2.1) and phLDH $K_{NADHf}$ and $V_{NADHf}$ equal 7.8 ± 0.9 μM and 125 ± 15 U/mg respectively (Table 2.1). The R values were calculated from $v_{exp}$ and $v_{cal}$ using the equations 2.1 and 2.2. The total [pyruvate] was 630 μM. **(B)** Ea is rmLDH and Ed is rmαGDH. The [rmαGDH]/[NADH] ratio was 2 or in terms of rmαGDH binding sites, [rmαGDH-NADH site]/[NADH] ratio was 4. The $[NADH]_f$ and the $[NADH]_b$ values were calculated using Kd=0.96 ± 0.096μM for each rmαGDH-NADH-site (Table 2.2 E). The $v_{cal}$ values were calculated using equation 2.1 and phLDH $K_{NADHf}$ and $V_{NADHf}$ equal 7.8 ± 0.9 μM and 125 ± 15 U/mg respectively (Table 2.1). The [pyruvate] in the measurements was equal to 150 μM. All rates were expressed as U/mg of Ea. One unit is defined as a μmol of NADH oxidized in one minute. All measurements were in 50 mM Tris/HCl, pH=7.5, 2 mM EDTA, 10 mM 2-ME. The rates were measured at 25 °C, by following NADH absorbance at 340 nm.

**Table 2.4 A Ed byGAPDH:Ea phLDH**

| [NADH], μM | byGAPDH tetramer, μM | [NADH]f, μM | [NADH]b, μM | % NADHf | vexp, U/mg | vcal, U/mg | R |
|---|---|---|---|---|---|---|---|
| 0 | 0 | 0 | 0 | | 0 | 0 | |
| 5 | 6.25 | 0.81 | 4.19 | 16.12 | 20.60 | 11.71 | 1.76 |
| 7 | 8.75 | 0.85 | 6.15 | 12.18 | 24.80 | 12.31 | 2.01 |
| 10 | 12.5 | 0.89 | 9.11 | 8.91 | 32.52 | 12.82 | 2.54 |
| 15 | 18.75 | 0.92 | 14.08 | 6.16 | 38.80 | 13.24 | 2.93 |
| 20 | 25 | 0.94 | 19.06 | 4.71 | 55.30 | 13.47 | 4.11 |
| 35 | 43.75 | 0.97 | 34.03 | 2.76 | 61.70 | 13.77 | 4.48 |
| 50 | 62.5 | 0.98 | 49.02 | 1.95 | 75.26 | 13.90 | 5.42 |
| 60 | 75 | 0.98 | 59.02 | 1.63 | 73.40 | 13.95 | 5.26 |

**Table 2.4 B Ed rmαGDH : Ea rmLDH**

| [NADH], μM | rmαGDH dimer,μM | [NADH]f, μM | [NADH]b μM | % NADHf | vexp U/mg | vcal U/mg | R |
|---|---|---|---|---|---|---|---|
| 0 | 0 | 0 | 0 | | 0 | 0 | |
| 1 | 2 | 0.23 | 0.77 | 22.74 | 6.50 | 6.88 | 0.94 |
| 2 | 4 | 0.26 | 1.74 | 13.17 | 16.00 | 7.91 | 2.02 |
| 3 | 6 | 0.28 | 2.72 | 9.29 | 14.00 | 8.34 | 1.68 |
| 4 | 8 | 0.29 | 3.71 | 7.18 | 22.50 | 8.57 | 2.62 |
| 5 | 10 | 0.29 | 4.71 | 5.85 | 21.00 | 8.73 | 2.41 |
| 6 | 12 | 0.30 | 5.70 | 4.94 | 24.00 | 8.83 | 2.72 |
| 7 | 14 | 0.30 | 6.70 | 4.27 | 26.00 | 8.91 | 2.92 |
| 8 | 16 | 0.30 | 7.70 | 3.76 | 24.00 | 8.96 | 2.68 |
| 9 | 18 | 0.30 | 8.70 | 3.36 | 29.00 | 9.01 | 3.22 |
| 10 | 20 | 0.30 | 9.70 | 3.04 | 23.80 | 9.05 | 2.63 |
| 15 | 30 | 0.31 | 14.69 | 2.05 | 32.00 | 9.16 | 3.49 |
| 30 | 60 | 0.31 | 29.69 | 1.04 | 34.00 | 9.28 | 3.66 |

**Figure 2.3 (A-B). Enzyme buffering measurements with constant (total [Ed]/total [NADH]) ratio.**

The figure shows the data given in the table 2.4 (A-B). **(A)** Ea is phLDH and Ed is byGAPDH (Table 2.4 A). The [byGAPDH]/[NADH] ratio was 1.25, or in terms of byGAPDH-NADH binding sites, the [byGAPDH-NADH sites]/[NADH] ratio was 5. The $v_{exp}$ (○)data were fitted to Michaelis-Menten model equation giving an apparent $K_{Ed\text{-}NADH}$ value of 17.97 ± 2.5 μM. The $v_{cal}$ (●) values were calculated using Eqn. (2.1), $K^{f}_{NADH}$ and $V^{f}_{NADH}$ for phLDH equal 7.8 ± 0.9 μM and 125 ± 15 U/mg respectively, and the $[NADH]_f$ values given in the Table 2.2 A. **(B)** The Ea is rmLDH, the Ed is rmαGDH. The figure represents the data given in the Table 2.4 B. The [rmαGDH]/[NADH] ratio was 2, or in terms of rm-αGDH binding sites, [rm-αGDH-NADH site]/[NADH] ratio was 4. The $v_{exp}$ (■)data were fitted to Michaelis-Menten model equation giving apparent $K_{Ed\text{-}NADH}$ value 4.4 ± 0.4 μM. The $v_{cal}$ (●) values were calculated using equation 2.1, $K^{f}_{NADH}$ and $V^{f}_{NADH}$ for phLDH equal 4.4 ± 0.4 μM and 140 ± 10 U/mg respectively, and the $[NADH]_f$ values given in the Table 2.1 E. The [pyruvate] = 150 μM. All rates were expressed as U/mg of Ea. All measurements were in 50 mM Tris/HCl, pH = 7.5, 2 mM EDTA, 10 mM 2-ME. The rates were measured at 25 °C, by following NADH absorbance at 340 nm. The error bars, ± 7.5 % of the measured values, indicate the experimental precision.

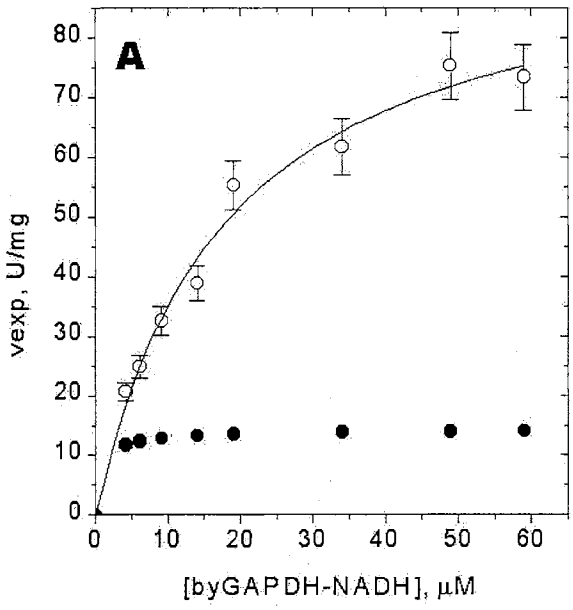
A
vexp, U/mg
[byGAPDH-NADH], μM
0
10
20
30
40
50
60
70
80

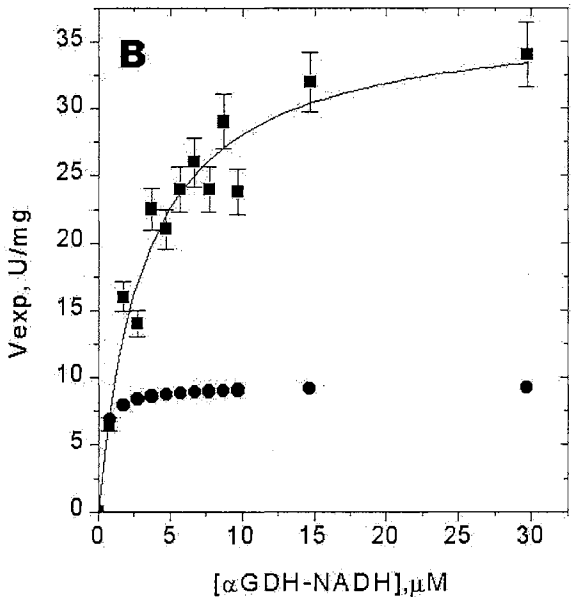
B
Vexp, U/mg
[αGDH-NADH],μM
0
5
10
15
20
25
30
35

inhibition. Thus this method for obtaining enzyme buffering data provides the advantages of larger R values and a direct measure of the apo-Ed inhibition, which may be useful in interpreting mechanisms of NADH channeling.

It is helpful to consider the likely mechanisms of inhibition by apo-Ed here, although this will be more fully discussed in chapter 5. The first mechanism of inhibition considered is that revealed by Fig. 5.1. It can be seen that Ed competes with Ed-NADH for Ea, forming a dead-end complex at the beginning of the reaction scheme. This is imminently reasonable, for if Ed-NADH forms a complex with Ea, it is most likely that the same docking surfaces are involved in forming the dead-end complex, Ed-Ea. A second mechanism for this inhibition is that Ed is the first product of the most likely reaction mechanism (chapter 5, Fig. 5.1). Furthermore, this inhibition is unavoidable in the enzyme buffering experiments since excess Ed must be present to ensure that $[NADH]_f$ is far below its Km with Ea. These inhibition patterns are shown in Figures 2.4 through 2.6, for Ed as byGAPDH, rmGAPD, and rmαGDH, repectively.

**Figure 2.4 (A-D) Apo Ed inhibition in enzyme buffering experiments with byGAPDH as Ed.**

Data with constant total [NADH] = 50 μM. The figure shows byGAPDH as Ed and phLDH (**A**), pmLDH (**B**) and hlADH (**C**) as Ea. The figures (**A**)-(**C**) show measured $v_{exp}$ (■) and corresponding $v_{cal}$ (○), calculated using Eqn 2.1 and the $K_{NADH}$ and $V_{NADH}$ values given in the Table 2.1. For all three Ea, the $v_{exp}$ decreases with the increase in apo-byGAPDH faster than $v_{cal}$, indicating that apo-Ed affects the $v_{exp}$ beyond what is predicted by simple decrease in $[NADH]_f$. (**D**) R values as a function of increasing [Ed] for Ea=phLDH (○), Ea=pmLDH (□), and Ea=hlADH (■). R values for each of the three Ea Ed pair were calculated using eqn. 2.2. For each of the three Ea-Ed pairs the R values appear to approach an asymptotic maximum. All rates were expressed as U/mg of Ea. All measurements were in 50 mM Tris/HCl, pH=7.5, 2 mM EDTA, 10 mM 2-ME. The rates were measured at 25 °C, by following NADH absorbance at 340 nm. The error bars, ± 7.5 % of the measured values, show the experimental precision.

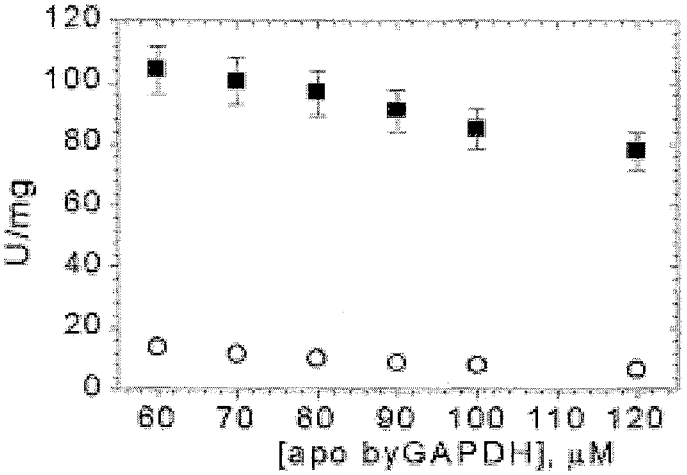
120
100
80
60
40
20
0
U/mg
60 70 80 90 100 110 120
[apo byGAPDH], μM

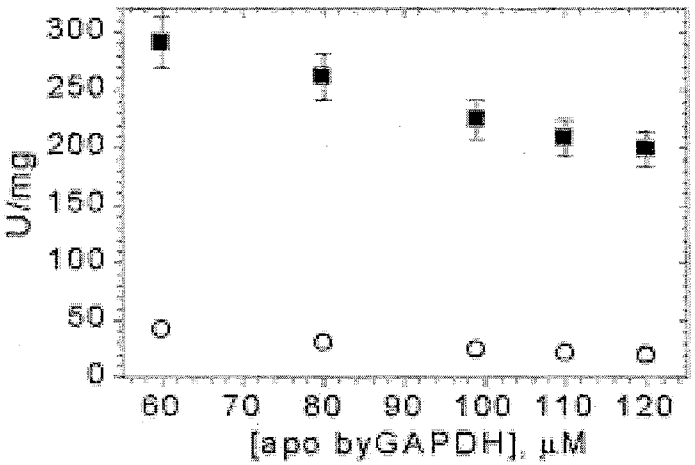
300
250
200
150
100
50
0
U/mg
60 70 80 90 100 110 120
[apo byGAPDH], μM

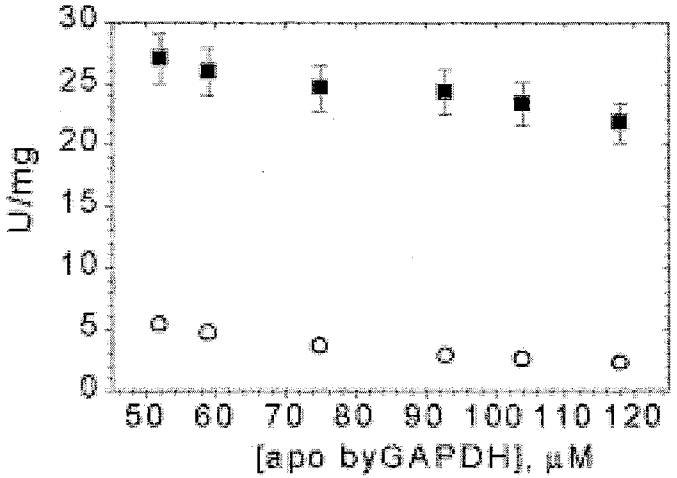
30
25
20
15
10
5
0
U/mg
50 60 70 80 90 100 110 120
[apo byGAPDH], μM

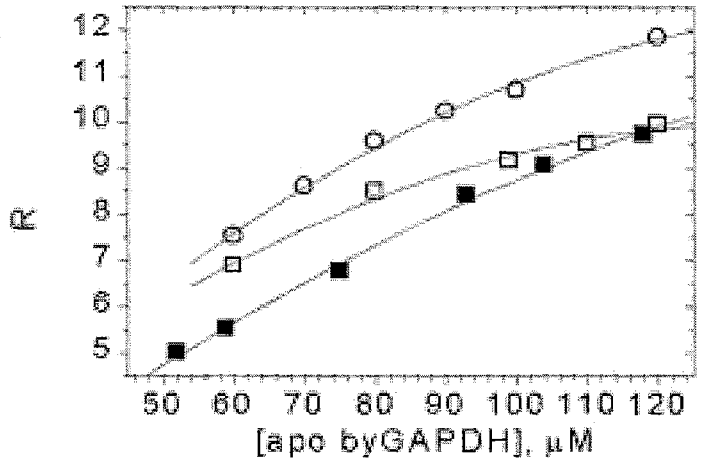
12
11
10
9
8
7
6
5
R
50 60 70 80 90 100 110 120
[apo byGAPDH], μM

**Figure 2.5 (A-D). Apo Ed Inhibition in the Enzyme Buffering Experiments with rmGAPDH as Ed.**

Data with constant total [NADH] = 50 μM. The figure shows rmGAPDH as Ed, and phLDH **(A)**, pmLDH **(B)** and phcMDH **(C )** as Ea. The figures **(A)-(C )** show measured $v_{exp}$ (■) and corresponding $v_{cal}$ (○). The $v_{cal}$ was calculated using the Eqn 2.1 and the $K_{NADH}$ and $V_{NADH}$ values given in Table 2.1. For all three Ea, the $v_{exp}$ decreases steeply with increasing apo-rmGAPDH, indicating inhibition by apo-Ed. **(D)** R values as a function of increasing [Ed] for Ea=pmLDH (○), Ea=phcMDH(□) and Ea=phLDH (■). R values for each of the three Ea Ed pair were calculated using Eqn. 2.2. For each of the three Ea-Ed pairs the R values appear to converge to an asymptotic maximum. All rates were expressed as U/mg of Ea. All measurements were in 50 mM Tris/HCl, pH=7.5, 2 mM EDTA, 10 mM 2-ME. The rates were measured at 25 °C, by following NADH absorbance at 340 nm. The error bars, ± 7.5 % of the measured values, show the experimental precision.

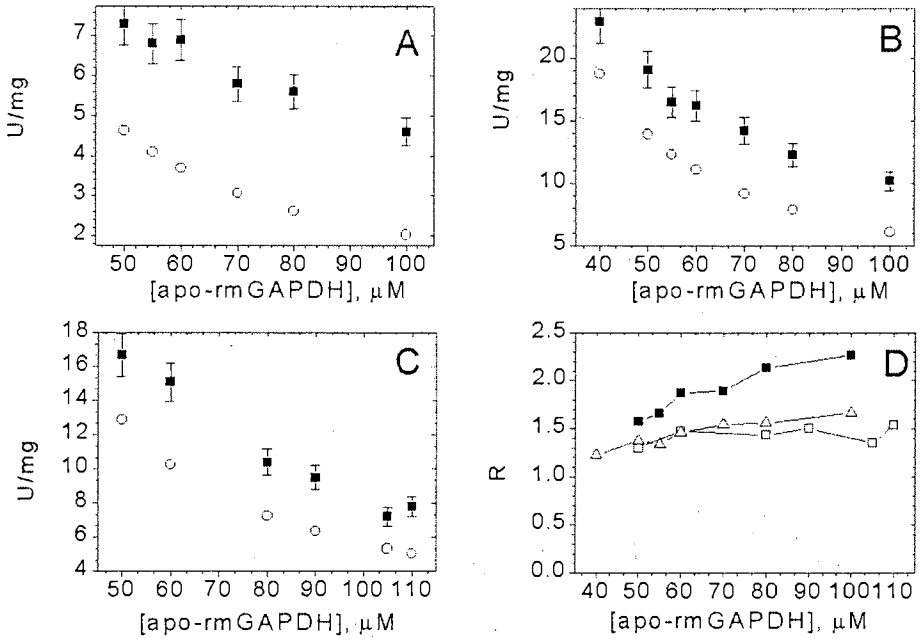
A
B
C
D
U/mg
U/mg
U/mg
R
[apo-rmGAPDH], μM
[apo-rmGAPDH], μM
[apo-rmGAPDH], μM
[apo-rmGAPDH], μM

**Figure 2.6 (A-C). Apo Ed Inhibition in Enzyme Buffering Experiments with rmαGDH as Ed.**

Data with constant total [NADH] = 50 μM. Ed was rmαGDH with Ea as rmLDH **(A)**, phLDH **(B)**. The figures **(A)-(B)** show measured vexp (□) and corresponding vcal (●), calculated using Eqn 2.1 and the $K_{NADH}$ and $V_{NADH}$ values given in the Table 2.1. For both Ea, the $v_{exp}$ decreases with increase in apo-rmGAPDH, indicating inhibition by apo-Ed. **(C)** R values as a function of increasing [Ed] for Ea=phLDH (○), Ea=rmLDH (■). R values for each of the Ea-Ed pair were calculated using Eqn. 2.2. Each of the R values appear to converge to an asymptotic maximum. All rates were expressed as U/mg of Ea. All measurements were in 50 mM Tris/HCl, pH=7.5, 2 mM EDTA, 10 mM 2-ME. The rates were measured at 25 °C, by following NADH absorbance at 340 nm. The error bars, ± 7.5 % of the measured values, show the experimental precision.

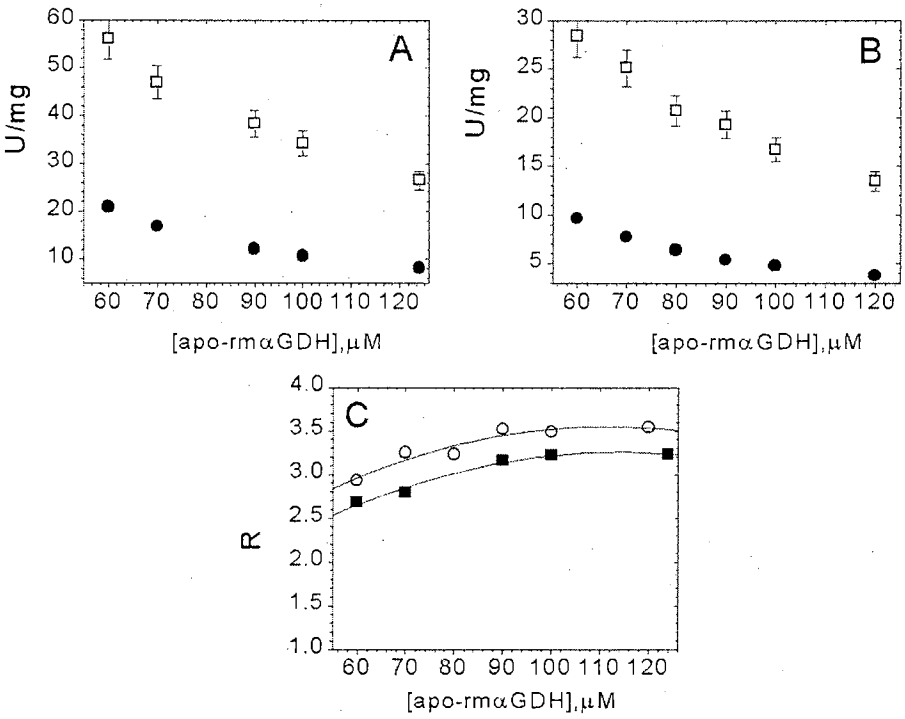
A
B
C
U/mg
U/mg
R
[apo-rmαGDH],μM
[apo-rmαGDH],μM
[apo-rmαGDH],μM

## 2.4 Discussion and Conclusions

Table 2.1 summarizes our enzyme buffering data for the range of enzyme pairs examined. This summary organizes the results around each donor enzyme and a range of acceptor enzymes. It condenses much of the data by considering single concentrations or a small range of Ed . This Table demonstrates NADH channeling between some enzyme pairs using the most rigorous criterion, the ratio $R = v_{exp}/v_{cal}$, where $v_{cal}$ is the velocity calculated assuming no channeling. Included in this group are the αGDH-LDH pair that has been most extensively researched and disputed. We find modest, but significant evidence of channeling in this pair. The strongest evidence of NADH channeling, however occurs between phLDH and byGAPDH. The high R value with phLDH as donor is undoubtedly due to the very much more favorable (higher) $K_m$ for NADH that byGAPDH has relative to the other dehydrogenases. Table 2.1 also shows that NADH channeling when evident is not discriminating with respect to the phylogenic form of the paired enzymes. The table also shows that many dehydrogenase pairs exhibit no evidence of channeling by the R criterion. However, several considerations indicate that NADH channeling occurs even in these cases with $R \approx 1$. The most persuasive of these derive from analysis of the NADH channeling, kinetic models discussed in chapter 5. We show there that the R value is limited in magnitude by the kinetic and dissociation constants of the enzymes. This limitation is independent of the extent of channeling in the system. Thus R is a rigorous criterion of NADH channeling with favorable enzyme constants, but is a very insensitive criterion otherwise. Another, but less rigorous, indication that

channeling is likely even when R is low is from Table 2.1 On occasion this table shows strong evidence that NADH channeling occurs across different phylogenic divisions, e.g., phLDH to byGAPDH, yet virtually no evidence of this between the same enzymes and phylum, e.g., phLDH with rmGAPDH or rmLDH with rmGAPDH. It doesn't seem reasonable that such a remarkable phenomenon as NADH channeling would evolve without a physiological role – a role that can only occur between enzymes of the same species. In any event, better criteria of NADH channeling are needed. Such research is being pursued in our lab with optimistic prospects.

Table 2.1 addresses, to some extent, the question of how reliable the estimates of $[NADH]_f$ are for our enzyme buffering experiments. Inaccurate $[NADH]_f$ values will give nearly proportional inaccuracies in the channeling criterion R. Our study of this general question is quite superficial since the literature control experiments leave little doubt of the accuracy of $K_d$ and hence $[NADH]_f$ in many cases. Our approach to this problem was to use the control experiments to determine the effective $[NADH]_f$ present in our enzyme buffering experiments. This approach circumvents possible problems caused by $K_d$ values varying with the concentration of Ed. On the other hand, it is based on the very likely, but not definitively proven assumption that NADH channeling does not occur between enzymes of the same chiral specificity.

We found good correlation of our calculated Kd's with literature values in some cases, but not all. For example, in the experiment with the highest R (phLDH to byGAPD), the Kd of the phLDH donor was in close agreement with literature values. In cases, where there was not good agreement with literature values, numerous good reasons

for these differences exist. In addition, we found good agreement between $[NADH]_f$ values from a given Ed determined with two different control enzymes.

Fig. 2.2 shows that increasing [B] increases the channeling criterion R. This effect is most likely due to the fact that B reduces the inhibition by apo-Ed. This competitive nature of B with apo-Ed is predicted by the kinetic mechanism we propose in chapter 5. However, increasing [B] is not successful with all enzyme pairs (data not shown). This may be due to the fact that at the high [B] values needed to effectively compete with apo-Ed, substrate inhibition becomes significant.

Table 2.3 examines the usefulness of the apparent $K_b$ from the enzyme buffering experiments to witness anomalous kinetics and thus indirectly indicate NADH channeling. The apparent $K_b$ does show anomalous behavior for those enzymes and reactions directions having R significantly greater than 1. For the two cases with $R \approx 1$, there is little difference in one of these and a quite possible difference in the second case. More experiments would be needed to be sure of this last case.

Table 2.4 and Fig. 2.3 illustrate how the data with constant ratio of total Ed to total NADH provide data similar to Michaelis-Menten kinetics. Although the Michaelis-Menten behavior is not mathematically exact, it appears to be adequate within the experimental error. However, the apparent $V_m$ from analysis of these curves is a very substantially reduced value from the most probable value since these data ignore the simultaneous inhibition by apo-Ed that occurs with these experiments. In other words, this inhibition is hidden by this method of gathering the kinetic data. As described in chapter 5, analysis of the combined enzyme buffering data from both constant ratio and constant [NADH]f methods indicates that the $V_{NADHb}$ value is most likely equal to the

$V_{NADHf}$ where the subscripts b and f denote the bound and free NADH kinetic paths, respectively.

Figures 2.4 – 2.6 demonstrate how the method of increasing [Ed] at constant total [NADH] gives increasing R values, which appear to reach a maximum value. This method invariably gives higher R values than achievable by the alternative method of the enzyme buffering experiments, a fact that can also be predicted by analysis of the kinetic models. Features of the inhibition by apo-Ed are also revealed by these data. These features are reproduced by the kinetic model we provide in chapter 5 and are very helpful in distinguishing alternative kinetic models.

Enzyme buffering data are valuable for additional reasons. The conditions of these experiments are enormously closer to physiological conditions with respect to the relative values of enzyme binding site concentrations and total [NADH] in vivo (Ushiroyama et al., 1992) than conventional steady-state enzyme kinetic data.

## 2.5 References


Arias, M. W. & Pettersson, G. (1997). Mechanism of NADH transfer between alcohol dehydrogenase and glyceraldehyde-3-phosphate dehydrogenase. *Eur J Biochem* **250**, 158-62.

Arias, W. M., Pettersson, H. & Pettersson, G. (1998). Mechanism of NADH transfer among dehydrogenases. *Biochim Biophys Acta* **1385**, 149-56.

Bloch, W., MacQuarrie, R. A. & Bernhard, S. A. (1971). The nucleotide and acyl group content of native rabbit muscle glyceraldehyde 3-phosphate dehydrogenase. *J Biol Chem* **246**, 780-90.

Byers, L. D. (1982). Glyceraldehyde-3-phosphate dehydrogenase from yeast. *Methods Enzymol* **89 Pt D**, 326-35.

Chock, P. B. & Gutfreund, H. (1988). Reexamination of the kinetics of the transfer of NADH between its complexes with glycerol-3-phosphate dehydrogenase and with lactate dehydrogenase. *Proc Natl Acad Sci U S A* **85**, 8870-4.

Clermont, S., Corbier, C., Mely, Y., Gerard, D., Wonacott, A. & Branlant, G. (1993). Determinants of coenzyme specificity in glyceraldehyde-3-phosphate dehydrogenase: role of the acidic residue in the fingerprint region of the nucleotide binding fold. *Biochemistry* **32**, 10178-84.

Cook, R. A. & Koshland, D. E., Jr. (1970). Positive and negative cooperativity in yeast glyceraldehyde 3-phosphate dehydrogenase. *Biochemistry* **9**, 3337-42.

Corbier, C., Clermont, S., Billard, P., Skarzynski, T., Branlant, C., Wonacott, A. & Branlant, G. (1990). Probing the coenzyme specificity of glyceraldehyde-3-phosphate dehydrogenases by site-directed mutagenesis. *Biochemistry* **29**, 7101-6.

Cori, C. F., Velick, S. F. & Cori, G. T. (1950). The Combination of Diphosphopyridine Nucleotide with Glyceraldehyde Phosphate Dehydrogenase. *Biochim. Biophys. Acta* **4**, 160-169.

Dalziel, K., (1975). Kinetics and Mechanism of Nicotinaamide-Nucleotide-Linked Dehydrogenases. 3rd Edn. Vol. XI. The Enzymes (Boyer, P. A., ed.) New York: Academic Press.

Fukushima, T., Decker, R. V., Anderson, W. M. & Spivey, H. O. (1989). Substrate channeling of NADH and binding of dehydrogenases to complex I. *J Biol Chem* **264**, 16483-8.

Holbrook, J. J., Liljas, S., Steindel, S. J. & Rossman, M. G., (1975). Lactate Dehydrogenase. 3rd edn. Vol. XI. The Enzymes (Boyer, P. A., ed.) New York: Academic Press.

Lynen, F., Henning, U., Bublitz, C., Sörbo, B. & Kröplin-Rueff, L. (1958). *Biochemische Zeitschrift* **330**, S269-295.

Mahler, H. R. & Elowe, D. (1954). *Biochim. Biophys. Acta* **14**, 100-107.

Nygaard, A. P. & Rutter, W. J. (1956). Interaction of Pyridine-Nucleotide Linked Enzymes. *Acta Chem. Scand.* **10**, 37-48.

Scheek, R. M. & Slater, E. C. (1982). Glyceraldehyde-3-phosphate dehydrogenase from rabbit muscle. *Methods Enzymol* **89 Pt D**, 305-9.

Spivey, H. O. & Ovadi, J. (1999). Substrate channeling. *Methods* **19**, 306-21.

Srivastava, D. K. & Bernhard, S. A. (1984). Direct transfer of reduced nicotinamide adenine dinucleotide from glyceraldehyde-3-phosphate dehydrogenase to liver alcohol dehydrogenase. *Biochemistry* **23**, 4538-45.

Srivastava, D. K. & Bernhard, S. A. (1985). Mechanism of transfer of reduced nicotinamide adenine dinucleotide among dehydrogenases. *Biochemistry* **24**, 623-8.

Srivastava, D. K., Bernhard, S. A., Langridge, R. & McClarin, J. A. (1985). Molecular basis for the transfer of nicotinamide adenine dinucleotide among dehydrogenases. *Biochemistry* **24**, 629-35.

Srivastava, D. K., Smolen, P., Betts, G. F., Fukushima, T., Spivey, H. O. & Bernhard, S. A. (1989). The Direct Transfer of NADH between α-Glycerol Phosphate Dehydrogenase and Lactate Dehydrogenase. Fact or Misinterpretation? *Proc. Natl. Acad. Sci., USA* **86**, 6464-6468.

Stallcup, W. B. & Koshland, D. E., Jr. (1973). Half-of-the sites reactivity and negative co-operativity: the case of yeast glyceraldehyde 3-phosphate dehydrogenase. *J Mol Biol* **80**, 41-62.

Svedruzic, Z. M. & Spivey, H. O. (2000). Evidence for NADH Channeling Between Dehydrogenases and Inadequacy of Non-Channeling Models. *In preparation.*

Ushiroyama, T., Fukushima, T., Styre, J. D. & Spivey, H. O. (1992). Substrate Channeling of NADH in Mitochondrial Redox Processes. In *From Metabolite, to Metabolism, to Metabolon* (Stadtman, E. R. & Chock, P. B., eds.), *Curr Top Cell Regul* 33, pp. 291-307. Academic Press, New York.

Ward, L. D. & Winzor, D. J. (1983). Thermodynamic studies of the activation of rabbit muscle lactate dehydrogenase by phosphate. *Biochem J* **215**, 685-91.

Wilder, R. T., Venkataramu, S. D., Dalton, L. R., Birktoft, J. J., Trommer, W. E. & Park, J. H. (1989). Catalytic mechanism and interactions of NAD+ with glyceraldehyde-3- phosphate dehydrogenase: correlation of EPR data and enzymatic studies. *Biochim Biophys Acta* **997**, 65-77.

Wu, X., Gutfreund, H., Lakatos, S. & Chock, P. B. (1991). Substrate Channeling in Glycolysis: A Phantom Phenomenon. *Proc. Natl. Acad. Sci. USA* **88**, 497-501.

You, K. (1982). Stereospecificities of the pyridine nucleotide-linked enzymes. *Methods Enzymol* **87**, 101-26.

You, K. S. (1985). Stereospecificity for nicotinamide nucleotides in enzymatic and chemical hydride transfer reactions. *CRC Crit Rev Biochem* **17**, 313-451.

# CHAPTER 3 Equilibrium Interaction between Dehydrogenases

## 3.1 Introduction

Substrate channeling by definition requires a complex of the two enzymes at least transiently during the catalytic reaction. This chapter presents equilibrium association experiments pursued in an attempt to describe the interactions between NAD(H) dehydrogenases active in channeling. The association experiments were directed to address the following goals:

i) test for interactions between NAD(H) dehydrogenases

ii) determine the association constants and stoichiometries of the complexes.

iii) test the NAD(H) effects on these interactions.

iv) utilize knowledge of the association properties of these dehydrogenases to reveal details of the kinetic mechanisms of NADH channeling.

If specific associations are found between those enzymes, which the enzyme buffering data indicate channel NADH, this would provide strong, supplementary evidence in support of the channeling. In fact the inability to detect such enzyme complexes in the few experiments attempted was a major criticism of the validity of NADH channeling. Enzyme complexes between the soluble mitochondrial matrix enzymes and purified complex I were demonstrated along with NADH channeling (Ushiroyama *et al.*, 1992). NADH concentrations in excess of the enzymes dissociated these complexes. However, complex I is an atypical dehydrogenase that can only be

purified in an active form from the mitochondrial membrane as a detergent stabilized suspension – an aggregate of multiple complex I molecules. It is atypical also in having more than 40 different subunits most of which are thought to provide structural functions adapting the enzyme to the membrane phase and interactions with other components of the electron transfer system. Thus binding of soluble enzymes to these especially elaborate complexes is not likely to be similar to the interactions between the very much smaller and structurally simpler "soluble" dehydrogenases.

There have been two unsuccessful attempts to demonstrate complexes between LDH and αGDH (Brooks & Storey, 1991b; Wu *et al.*, 1991). The experiments of Wu and co-authors were performed with large excesses of NADH relative to the enzyme binding site concentrations. The experiments of Brooks and Storey were also deficient in design for detecting weak interactions. Subsequently, Yong *et al.* (Yong *et al.*, 1993) reported a potentially very significant study using a modified Hummel-Dreyer method capable of detecting weak associations. They reported that strong association of LDH and αGDH occurred at with ratios of NADH/Ed ≈ 0.5, but not with excess NADH or in the absence of NADH. This biphasic modulation of this enzyme association has widespread and significant implications. However, the project leader was retiring and did not plan to pursue these studies further. Also this study was limited to one enzyme pair, utilized only one experimental method and only a few NADH concentrations. Thus the validity and the generality of this effect among putative NADH channeling dehydrogenases remained to be explored.

We report measurements by analytical ultracentrifugation, agarose gel electrophoresis, and PEG coprecipitation methods that have been especially sensitive in detecting macromolecular associations. Data were obtained for enzymes in both pure buffer solutions like those used in the enzyme buffering experiments and in media containing polymers or sucrose, which are known to enhance weak interactions between some macromolecules (Zimmerman & Minton, 1993; Crothers & Fried, 1981; Ashmarina *et al.*, 1994).

## 3.2 Materials and Methods

*Materials.* Ultra pure, high strength agarose was purchased from Biorad (Bio-Rad Laboratories, Hercules, CA). PEG 6000 and other chemicals were purchased from Sigma Chem. Co., St. Louis, MO, unless otherwise indicated. Both NAD and NADH were of 99% or better purity, as claimed by the manufacturer. D (-)3-phosphoglyceric acid 98% pure as claimed by manufacturer was obtained as tri(cyclohexylammonium) salt. ATP was disodium salt grade I. BSA was RIA grade, fraction V powder. Activated charcoal was hydrochloric acid-washed, cell culture tested. Ammonium sulfate suspensions of phLDH, rmGAPDH, and pmLDH were purchased from Sigma and used without further purification. Baker's yeast 3-phosphoglyceric phosphokinase was a suspension in 3.0 M $(NH_4)_2SO_4$. RmGAPDH, phLDH, pmLDH, phcMDH, rm-aldolase, and *Leuconostoc Mesenteroides* glucose-6-phosphate dehydrogenase were purchased form Sigma and used without further purification. RmGAPDH, phLDH, and pmLDH gave single bands in coomassie SDS PAGE analysis. *Bs*GAPDH and byGAPDH were purchased form Sigma as lyophilized powders. Rm-αGDH was purchased from Sigma or ICN on different occasions. Prior to use in analytical ultracentrifuge (AUC) studies, byGAPDH was purified from a small molecular weight contaminant on Sephadex G100 column.

*Buffers and Solutions.* Throughout this section Tris/HCl pH=7.5 buffer refers to 50 mM Tris/HCl pH=7.5, 2mM EDTA, 10 mM 2ME, unless otherwise indicated. The buffer pH was adjusted at room temperature. To prevent $Cl_2$ production in the agarose electrophoresis experiments, the Tris buffer was replaced with 50 mM MOPS/KOH buffer at pH = 7.0 containing 2 mM EDTA and 10 mM 2ME. NADH stock solutions

were prepared in 120 mM $Na_2CO_3$ buffer in a light isolated container and used within two weeks of preparation. NAD was prepared fresh before each measurement, and used within 8 hours from preparation. ATP was prepared as a 100 mM stock solution in 10 mM EDTA, 50 mM Tris/HCl, stored at -20 °C, and used within 3 months of preparation. The 3-phosphoglycerate was prepared as a 300 mM solution in 300 mM Tris base, and stored at -20 °C.

*Apo-enzyme preparations.* Prior to any of the described measurements the primary dehydrogenases (all except the NADH regenerating enzyme, lm-glucose-6-P dehydrogenase) were treated with one milligram of charcoal/milligram of protein. The procedure was repeated twice for rmGAPDH. Measurements of absorbance ratio at 280/260 nm showed that the treatment routinely produced the highest achievable ratios. The reliability of measured absorbance ratios at 280/260 nm for charcoal treated proteins was tested enzymatically. Residual NADH can be detected by incubating 100 -200 μM protein sites in the assay buffer and following absorbance at 340nm for 30 min after addition of the substrate specific for the observed protein. NAD was assayed similarly by using *Leuconostoc mesenteroides* glucose-6-phosphate dehydrogenase. After charcoal treatment, 100 μM of protein NAD(H) sites was incubated in the assay buffer in presence of 2 mM glucose-6-phosphate. Presence of NAD can be detected by following increase in absorbance at 340 nm for 30 minutes after addition of an excess of *Leuconostoc mesenteroides* glucose-6-phosphate dehydrogenase. These measurements showed that charcoal treatment produces >90 % of the enzyme in the apo-form. The protein concentrations were determined by absorbance at 280 nm, using the following

absorptivities ($M^{-1}$ $cm^{-1}$): rm-αGDH 4.78 $10^4$; phLDH 1.7 $10^5$; rmLDH 1.75 $10^5$; rmGAPDH 1.16 $10^5$, and byGAPDH 1.3.

*Enzyme assays.* Enzyme activities were measured by following absorbance at 340 nm. Each activity measurement was repeated three times to see whether measurements were reproducible to within 15%. If reproducibility was poorer than 15%, the measurements were tested for specific problems and repeated until this reproducibility was achieved. In all calculations an enzyme unit is defined as 1 μmol of NADH oxidized per minute, while specific activity is expressed as units per mg of protein at 25°C. The NADH molar absortivity was assumed to be 6.22 $10^3$ $M^{-1}$ $cm^{-1}$. All assay mixtures had 1 mg/ml BSA to prevent denaturation of the assayed protein due to absorption on the container surfaces or other deleterious reactions. The total NADH absorbance was recorded before each assay, and the reaction rate was calculated from the initial velocity slope. (disappearance of the first 15% of the total NADH absorbance).

For all GAPDH activity measurements, the assay mixture had 3 mM 3-phosphoglycrate, 1 mM ATP, 2 mM $MgCl_2$, and 10 U/ml of 3-phosphoglycerate kinase (PGK). NADH was 100 μM for the specific activity measurements unless otherwise indicated. The assay buffer was Tris/HCl pH=7.5 with 1.0 mg/ml of BSA. With these assays, the specific activity measured for rmGAPDH was 94 ± 10 U/mg. Unless otherwise indicated, all LDH assay mixtures were prepared with 630 μM pyruvate, and 100 μM NADH in Tris/HCl pH=7.5. The specific activities (U/mg enzyme) of enzymes assayed were: rmGAPD, 94 ± 10; phLDH, 130 ± 15; and pmLDH, 430 ± 30.

*Measurements.* All absorbance measurements were done on a Shimadzu 160uv spectrophotometer at 25°C.

*Polyethylene Glycol co-precipitation measurements.* The samples were prepared in 50 mM Tris/HCl pH=7.5, 1 mM EDTA, 10 mM 2ME and 10% w/v of PEG 6000 in indicated concentrations and incubated on ice for 20 min. The samples were then spun for 40 min at 14,000 g in a microcentrifuge within a 5°C room. After the centrifugation the supernatant and the pellets were promptly separated, and pellets were resuspended in an equal volume of buffer. The activities of both enzymes were measured in the pellets and in the supernatant and results were summed to check whether all expected activity was recovered. The results show 100% recovery to within experimental error. The specificity of co-precipitation was tested by incubating the proteins with control proteins that have closely similar molecular weight and net charge.

*Agarose Electrophoresis Experiments.* The agarose gels 1.5% (w/v) were prepared in water. One hour after pouring, the gel was incubated overnight in the MOPS buffer defined above prior to the run. The electrophoresis experiment was performed in the cold room and the gel buffer temperature was monitored and never exceeded 8°C. The wells were loaded with 300 μg (20 μL) of protein prepared in the same buffer plus 10% glycerol. All proteins were dialyzed in the MOPS/KOH buffer before the run. The run was performed with 70 V (20 cm between the electrodes), and during the run the buffer was re-circulated between anode and cathode compartments to prevent formation of ion gradients which can distort protein fronts.

*Analytical Ultracentrifugation*

*Sedimentation Equilibrium Measurements*. Equilibrium experiments at 20°C were performed in the An-60 Ti rotor of the XL-A instrument with "six-channel" centerpieces. The linearity of the instrument absorbance was tested with BSA solutions spun at 3,000 rpm. If the sample absorbance exceeded the instrument's linear range, the equilibrium profiles were analyzed on the shoulder of the protein absorbance peak, (295 and 307 nm). The An-60 Ti rotor accommodates 3 cells, each of which have 3 paired sectors (A, B, and C) allowing 9 different samples to be studied in one equilibrium experiment. The fourth hole contains the counterbalance and radial reference edges. LDH alone, GAPDH alone, and the mixture were placed in the three different cells, respectively. Concentrations of the enzymes were 2, 1, and 0.5 mg/ml in each enzyme for the sectors A, B, and C, respectively. Thus the mixture contained 2 mg/ml of each enzyme in sector A. NADH/enzyme binding site ratios of 0.25, 0.50, and 1.0 were used in separate experiments. The protein solutions also contained a NADH recycling mixture. The NADH recycling mixture was used to compensate for trace amounts of NADH oxidase activity that otherwise oxidized NADH extensively during the time period required for the experiments. The recycling mixture was prepared as 2 mM G6P, and 25-50 U of *Leuconostoc mesenteroides* G6PDH (unit defined as 1μmol of glucose oxidized per min at 25°C). With this recycling mixture, [NADH] remained at its initial value within detectable limits throughout the experiments. Sample volumes were such as to give column heights of about 2.5 mm and radial scans were obtained with radial stepsize of 0.003 cm and 4 repeats at each radius point. Since the absorbances at 280 nm of the more

concentrated samples were beyond the instrument linear range, equilibrium data were collected at 280, 295, and 305 nm for the equilibrium profiles at speeds of 7,000 and 10,900 rpm. Changing wavelength settings often gives small differences between specified and achieved wavelengths. To avoid this, the data for each wavelength were obtained in separate data files. Radial scans were also collected at 280 nm and 3,000 rpm speed to obtain loading absorbance values and at 280 nm and 40,000 rpm to obtain baseline absorbances. Accurate absorbance ratios between 280/295 and 295/307 nm were obtained by least-squares fits of segments of equilibrium data over absorbance ranges where the absorbances at both wavelengths were well within their linear response range.

The Beckman Multi-fit self-association program was used to characterize the individual enzymes as well as the enzyme mixture. The latter is justified since the two enzymes have virtually identical $M_r$ values. It is not strictly rigorous since the two enzymes have different absorptivities. However, an average absorptivity should be sufficient for these tests of hetero-association in this case, since any significant hetero-association deteriorated the Goodness of Fit criterion significantly. The Goodness of Fit from this program is the sum of squares of the weighted residuals divided by the number of degrees of freedom. Weighting factors were $1/\sigma_i^2$ where $\sigma_i$ is the standard deviation of the four repeat measurements at the i-th radial point. Thus the most probable value of the Goodness of Fit is 1.0 for data with only random errors of magnitude $\sigma_i$.

*Sedimentation Velocity Measurements in 10% PEG 6000.* Sedimentation velocity experiments in 10% (w/v) PEG 6000 were performed with a Beckman XL-A ultracentrifuge operating at 25°C. Sample cells used double sector charcoal-filled epon

centerpieces of 12 mm optical path and quartz windows. Three cells were used simultaneously in an An-60 Ti rotor to accommodate phLDH alone, rmGAPD alone, and the mixture of the two enzymes, respectively, in the separate cells. Each sample contained 1.0 mg/ml of individual enzymes in the Tris buffer containing 10% PEG with and without 100 mM NaCl. An initial rotor speed of 3000 rpm was used to obtain loading absorbances at 280 nm. The rotor was then accelerated to 40,000 rpm at which concentration profiles at 0.003 cm radial increments were obtained every 12 min. The period at 3000 rpm also permitted pelleting of any insoluble protein that might otherwise affect the sedimentation profiles. Although PEG induced precipitation experiments were performed at 4°C, ultracentrifuge experiments were performed at 25°C to avoid the very large viscosities of PEG solutions at 4°C. Otherwise the conditions were the same as for the precipitation experiments in PEG solutions. The sedimentation velocity experiment was repeated with the same conditions except for the addition of 100 mM NaCl in the Tris buffer. Seventeen and 11 scans were used for analysis of the no salt and 100 mM NaCl systems, respectively, with the programs "sedfit" (Schuck, P., 1998) and "SVEDBERG" (Philo, J. S., 1994). Fits with either program gave essentially identical results except for the plateau and sum of squares values for some of the samples, which had a significant plateau slope that SVEDBERG, but not sedfit allows for. On the other hand, sedfit allows for modeling self-associations, which our version of SVEDBERG does not. Therefore, all data shown in Table 3.2 were first analyzed with SVEDBERG to obtain best-fit values for the model of independent proteins with no interactions. The sedfit program available at the time only models self-associations for sedimentation

velocity data. However, best-fit values of sedimentation coefficients s and buoyant molar mass $M_b$ for LDH and GAPD enzymes were the same within experimental error (Table 3.2) when systematic errors of about 2% are considered. This permits us to use a self-association model for tests of hetero-association between these enzymes. Therefore, best-fit values from SVEDBERG were used with sedfit to test for hetero-associations in the enzyme mixture. The s value of the hypothetical hetero-dimer was fixed to be 1.59 times the s of the monomer since 1.59 is the two-thirds power of the ratio of molecular weights of dimer/monomer (= 2) – a relation closely followed by most globular proteins. The sedfit fits were first obtained with a negligibly low association constant $K_a$ (logKa = -10) and all parameters fixed at the best-fit values obtained from SVEDBERG except for the plateau absorbance, which was free. The fit was then repeated, but with a $K_a$ equivalent to 10% association at the loading concentration. The possibility of a hetero-association of the enzymes is judged by comparing the quality of fits (the root mean squared deviation) between these two results (two values of $K_a$). Numerous additional fits were explored using different strategies, e.g., fixing plateau absorbances at SVEDBERG values, floating various parameters, and fitting or not fitting for time independent noise.

## 3.3 Results

### 3.3.1 Sedimentation equilibrium analytical ultracentrifugation studies show no detectable interaction between several dehydrogenase pairs

AUC is a powerful method to study protein interaction (see, e.g., Hsu & Minton, 1991). Sedimentation equilibrium AUC experiments were used in our lab to test for interaction between three Ed:Ea pairs: byGAPDH and phLDH, phLDH and rmαGDH (Lehoux *et al.*, 2001), and phLDH and rmGAPDH (H.O. Spivey and A.P. Minton, unpublished results). ByGAPDH and phLDH exhibit unusually strong evidence of channeling in the enzyme buffering tests (Table 2.1). Results from equilibrium AUC experiments on this enzyme pair are reported in this thesis. (Sedimentation velocity data on the phLDH:rmGAPDH in 10% PEG are reported later in this chapter.).

Data were collected at three different ratios of NADH/enzyme binding sites since Yong et al. (1993) had reported that strong associations occur only with a ratio of 0.5 with the phLDH:rm-αGDH system. The Beckman Multi-fit self-association program was used to characterize the individual enzymes as well as the enzyme mixture as explained under Methods. Each enzyme was found to exhibit some self-dissociation of the native homo-tetramers both of which have $M_r$ values of about 142,000. This self-dissociation is confirmed by many equilibrium and sedimentation velocity experiments in our lab with enzymes from several different commercial sources. However, in spite of this complexity, fits to the model of a single non-associating component of $M_r$ about 110,00 were quite good by criteria of Goodness of Fit (Table 3.1) and residual plots. Fits to the

**Table 3.1 Equilibrum AUC data on byGAPDH and phLDH mixture.**

Apparent weight average molecular weights, appKw, are best-fit values with computed standard deviations. $K_a$ are the assumed association constants for the heterocomplex of byGAPDH-phLDH. G.F. = Goodness of Fit, which equals the sum of squares of the weighted residuals as defined under Methods. Experiments were at 20 °C, 7,000 rpm, at 1 mg/ml of each enzyme with ratio of [NADH]/[Binding sites] = 0.5 in the Tris/HCl buffer, pH 7.5. Data were recorded at 295 nm. Lack of hetero-complex formation is indicated by the larger (poorer) Goodness of Fit (G.F.) value with an assumed $K_a$ giving 10% association of the enzymes at 1 mg/ml.

| **$appM_w$** **kDa** | **$K_a$** **$M^{-1}$** | **G.F.** |
|---|---|---|
| **108.5 ± 0.9** | **0** | **3.7** |
| **97.4 ± 0.8** | **$6.8x10^3$** | **4.3** |

mixture were made using the apparent $M_r$ values of the individual proteins. Fits were again quite good assuming no hetero-association. The Goodness of Fit criterion is inversely proportional to the square of the standard deviation of absorbances at each radial point. Thus the residuals are less than two-fold higher than would give the most probable fit to a model that assumes no systematic errors. However, assuming 10% hetero-association at 1 mg/ml, equivalent to an association constant of $6.8 \times 10^3$ $M^{-1}$ caused a significant increase in the Goodness of Fit values at both 295 and 307 nm (poorer fit). These data are with commercial LDH that is not as pure or native as with good purifications made fresh in one's lab. However, they are with precisely the same enzymes that gave unusually high channeling criterion (R = 30-40) in the same buffer and gave expected results in the control (non-channeling) experiments. Furthermore, the NADH channeling kinetic data show nearly 100% saturation of Ea with the substrate Ed-NADH. Thus the enormously lower (undetectable) association of the enzymes in the absence of the catalytic reaction compared to that of the channeling data cannot be in question.

PhLDH and rmαGDH have been traditionally used in many studies of channeling between NAD(H) dehydrogenases (Brooks & Storey, 1991b; Chock & Gutfreund, 1988; Srivastava *et al.*, 1989; Wu *et al.*, 1990; Wu et al., 1991). Our AUC equilibrium data with varying ratios of NADH/binding sites have not been adequately analyzed yet since the molecular weights of these two enzymes differ by nearly two-fold and conservation of mass is unlikely to be accurate as described under Methods. We hope to complete and report these analyses in the very near future. AUC studies with excess NADH (Wu et

al., 1991) found no enzyme associations. Similarly no associations were detected using gel filtration studies (Brooks & Storey, 1991a; Wu et al., 1991) even though variable ratios of NADH/binding sites, were used by Brooks and Storey. Yong et al. (, 1993), using a Hummel-Dreyer method, did obtain evidence for a strong association of these enzymes with a ratio of NADH/binding sites = 0.5 (insignificant associations with ratios of 0 or 2.0), but these results have been subsequently shown to be due to an artifact (Lehoux et al., 2001). Combining these analytical ultracentrifuge results with the PEG precipitation and agarose electrophoresis experiments reported later in this thesis gives strong evidence against association of this enzyme pair in the absence of the catalytic reaction

Another interesting Ed:Ea pair to test for interaction was phLDH and rmGAPDH. The two proteins show relatively weak evidence of channeling based on the R criteria (Table 2.1). As shown later in this chapter, the phLDH and rmGAPDH are a unique pair that show interaction in the PEG co-precipitation and electrophoresis mobility shift experiments. Using a similar approach as described for byGAPDH and phLDH no interaction (with Kd $\leq$ 50$\mu$M) was found between phLDH and rmGAPDH in sedimentation velocity or equilibrium AUC studies (H.O Spivey and A. P. Minton unpublished data).

### 3.3.2 PEG co-precipitation experiments

#### 3.3.2.1 Introduction and results without NADH

The previous section described AUC studies that showed no detectable interaction between several enzyme pairs active in channeling including the phLDH-

byGAPD system with the highest R value (≈35) of any in our studies. PEG co-precipitation experiments can be used as an alternative approach to test for interactions between channeling dehydrogenases. Many reports have shown that PEG can enhance specific protein interactions (Ingham, 1984; Miekka & Ingham, 1980; Zimmerman & Minton, 1993). PEG can enhance molecular interaction by mimicking some of the conditions *in vivo*, specifically the volume excluding effects due to the extremely high concentrations of macromolecules (Zimmerman & Minton; Berg, 1990). PEG has this ability because it is very hydrophilic and hence very soluble and because it exists in aqueous solutions in a random coil conformation. A random coil has a very much larger excluded volume than a compact globular molecule of the same molecular weight.

PEG promoted interactions are most often shown to be specific (Ingham, 1984; Miekka & Ingham, 1980). Mitochondrial citrate synthase and mMDH are an example of the contribution of PEG to understanding of channeling phenomena. No detectable equilibrium association was found between mitochondrial citrate synthase and mMDH by a variety of methods (Srere *et al.*, 1978). However specific interaction between the two proteins can be observed in the presence of PEG (Halper & Srere, 1977; Merz *et al.*, 1987), or affinity agarose gel electrophoresis (Ashmarina *et al.*, 1994). The channeling observed within the PEG induced complexes proves their functional integrity (Datta *et al.*, 1985). Subsequently to the PEG experiments, channeling has been reported between citrate synthase and mMDH fusion protein (Lindbladh *et al.*, 1994) and the channeling mechanism has been suggested using molecular modeling studies (Elcock & McCammon, 1996).

Interactions between NAD(H) dehydrogenases were tested by following protein solubility in PEG. Associated proteins normally have significantly lower solubility than the individual proteins. Thus PEG concentrations can often be found in which the individual proteins are soluble, but the protein mixture with the same concentrations of individual enzymes as when alone will give considerable precipitation of both enzymes. In less favorable cases a small amount of one or both enzymes when alone will precipitate, but precipitation from the mixture will be considerably greater. Since the protein concentrations are only about 10 μM, it is unreasonable to invoke long range interactions for the precipitation. The only reasonable explanation for additional precipitation from the mixture is that the PEG induces formation of a new species (a complex between the proteins) that has lower solubility. A previous study showed that the protein complex has enormously lower solubility than the individual proteins (Merz et al., 1987). Consequently, the amount of associated complex remaining is solution is extremely low.

Our experiments were started by testing the solubility of individual proteins with increasing concentrations of PEG 6000. The proteins (1 to 2 mg/ml) were first incubated for 20 min on ice with increasing concentrations of PEG 6000. Following the incubation, insoluble and soluble proteins were separated by centrifugation. After the centrifugation the supernatant was removed from the pellets, and the pellets resuspended in the original volume of the assay buffer. The extent of protein insolubility was estimated by measuring protein activity in the pellets and the supernatant. Enzyme activity in the pellets indicates PEG induced precipitation. The sum of activities measured in the pellets

and the supernatant should be equal to the activity measured at the beginning of the co-precipitation experiment. This measurement is a control that indicates that there was no protein denaturation caused by the PEG treatment. Each of the analyzed enzymes will start to precipitate at a certain PEG concentration. The PEG concentration at which at least one of the proteins starts to precipitate, was chosen as the first PEG concentration in which co-precipitation from the protein mixture was tested. In the case of mutually induced co-precipitation, protein solubility in the mixture is lower than the solubility of the individual proteins.

The specificity of co-precipitation was tested by replacing one of the interacting components with its $M_r$ and pI analogue. It has been shown that protein PEG solubility is correlated with the protein $M_r$ and the net charge (Ingham, 1984). The analogue should not affect protein solubility if the co-precipitation was specific. Once specific co-precipitation was found, the experiments were repeated with lower PEG concentrations in an attempt to find optimal conditions with the minimal precipitation of the individual components and measurably high co-precipitation in from the mixture. The best PEG concentration is where both proteins are soluble when alone and co-precipitate when incubated together. Unfortunately such behavior was not observed for all proteins, so in some of the experiments it was necessary to subtract the background precipitation. The background precipitation is the protein precipitation in the absence of its co-precipitation partner.

Each of the three A type dehydrogenases: phLDH, pmLDH, pmcMDH were paired in separate experiments with each of the five B type dehydrogenases: byGAPDH,

bsGAPDH, rmαGDH, rmGAPDH or pmGAPDH for a total of 15 enzyme pairs tested. Co-precipitation was observed only between mammalian enzymes, e.g., phLDH with rmGAPDH (Fig. 3.1 (A-C)), or pmLDH with rmGAPDH (Fig. 3.2). PmGAPDH also co-precipitates with either phLDH or pmLDH (data not shown). This result is not surprising since sequence alignment shows that the rabbit and porcine GAPDH share 98.5% sequence identity. No co-precipitation was observed for phLDH or pmLDH with either byGAPDH, rmαGDH or bsGAPDH. No co-precipitation was observed for phcMDH with two B type enzymes tested: rmGAPDH, rmαGDH. The results of the co-precipitation experiments do not change if 50 mM Tris/HCl pH=7.5 is replaced with 50mM MOPS/KOH, pH = 7.5. The rmGAPDH and phLDH were originally chosen for the enzyme buffering experiments since both enzymes are most commonly covered in the literature and most readily available. Significant background precipitation, e.g. the precipitation in the absence of the companion protein, is observed with rmGAPDH (0.41 ± 0.04 mg/ml or 2.8 ± 0.3 μM with total protein 1.0mg/ml) and pmLDH (0.55 ± 0.06 mg/ml or 3.8 ± 0.4 μM with total protein 1.0 mg/ml). No background precipitation is observed with phLDH, making phLDH profiles very reproducible and easy to follow. The specificity of co-precipitation was tested by using the Mr and the pI analogues for one of the analyzed proteins. The phLDH ($M_r$ = 144 000, pI=5.1) can be replaced by bsGAPDH ($M_r$ = 144 000, pI=4.8) while rmGAPDH ($M_r$ = 142 000, pI=8.4) can be replaced by rm-aldolase ($M_r$ = 156 000, pI=8.2). Both controls showed no co-precipitation in the control experiment indicating that the co-precipitation is genuine and specific. The sum of the activities measured in the pellets and supernatants matches the

**Figure 3.1 (A-C) PEG induced precipitation between phLDH and rmGAPDH and control measurements.**

(A) PhLDH co-precipitation was followed as 1.0 mg/ml of rmGAPDH was titrated with the increasing concentration of phLDH, (○). In the control measurement rmGAPDH is replaced by rmALD (1.0 mg/ml or 6.4 μM) which is then titrated with the increasing concentration of phLDH (■). (B) rmGAPDH (1.0 mg/ml or 6.9 μM) co-precipitation in the presence of increasing concentration of phLDH (○) . In the control measurement ( ■), rmGAPDH (1.0 mg/ml or 6.9 μM) precipitation was monitored as phLDH was replaced by increasing concentration of *bs*GAPDH . (C ) rmGAPDH (■) and the phLDH (○) co-precipitation profiles from the figures (A) and (B) are combined to show the co-precipitation stoichiometry. The background precipitation (0.44 mg/ml or 3 μM) was subtracted from all rmGAPDH profiles shown. In all measurements, the two protein mixture was incubated for 15 min on ice in 50 mM Tris/HCl pH=7.5, 1 mM EDTA, 10 mM β-ME and 10% w/v of PEG 6000. The PEG insoluble protein was separated by centrifugation and the rmGAPDH activity was measured in the supernatant and in the pellets after suspending the pellets in buffer at a volume equal to that of the supernatants.

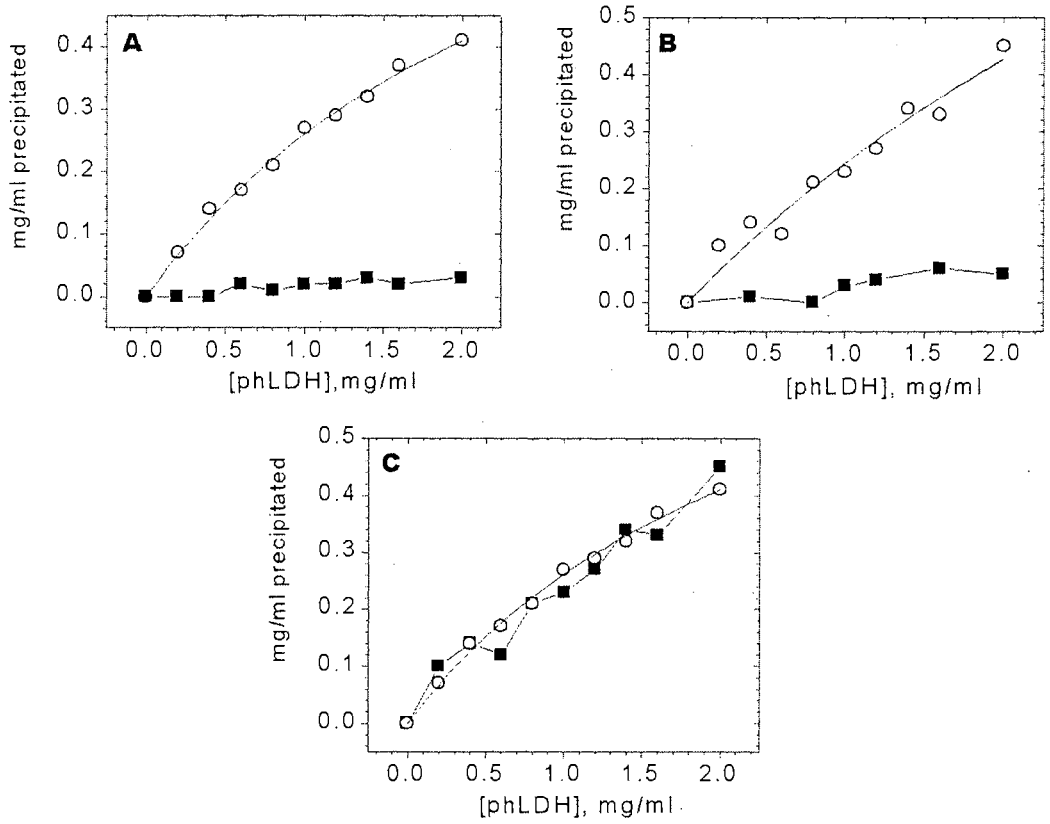
A
B
C
mg/ml precipitated
[phLDH], mg/ml
0.0
0.1
0.2
0.3
0.4
0.5
0.0
0.5
1.0
1.5
2.0

**Figure 3.2 PEG induced co-precipitation between pmLDH and rmGAPDH and control measurement.**

(○) Co-precipitation of rmGAPDH (1.0 mg/ml or 6.9 μM) when titrated with increasing concentrations of the pmLDH (0.6-1.2 mg/ml or 4.1-8.3 μM). (**x**) co-precipitation of pmLDH (1.0 mg/ml or 6.9 μM) when titrated with increasing concentrations of rmGAPDH (0.6-1.2 mg/ml or 4.1-8.3 μM). In the control experiment (■), pmLDH (1.0 mg/ml or 6.9 μM) precipitation was monitored in the presence of increasing concentration of rmALD (0.6-1.2 mg/ml or 3.8-7.7 μM). Background precipitation was subtracted from both rmGAPDH (0.41 mg/ml or 2.8 μM) and pmLDH (0.53 mg/ml or 3.7 μM) profiles. The procedure was the same as described in the legend of Fig. 3.1

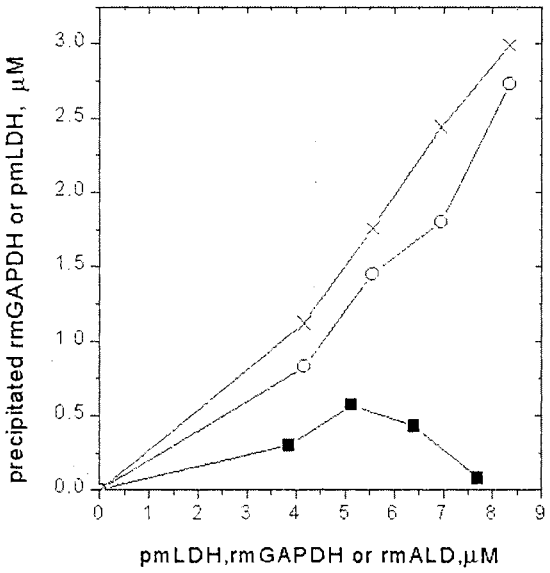
precipitated rmGAPDH or pmLDH, μM
3.0
2.5
2.0
1.5
1.0
0.5
0.0
0
1
2
3
4
5
6
7
8
9
pmLDH,rmGAPDH or rmALD,μM

original activity confirming protein stability throughout the experiment. The quantitative analysis of the co-precipitation between phLDH and rmGAPDH shows that two proteins precipitate roughly in 1:1 stoichiometry (Fig. 3.1 C). The quality of the pmLDH and rmGAPDH co-precipitation data is insufficient for quantitative stoichiometric calculations due to the extensive background precipitation, however it appears that the two proteins co-precipitate in 1:1 stoichiometry.

#### 3.3.2.2 PEG co-precipitation in the presence of NADH and NAD

Most of the enzyme interactions are modulated by metabolites (Beeckmans et al., 1989; Fahien et al., 1988; Fukushima et al., 1989). Metabolite mediated protein interactions can be a metabolic control mechanism in vivo. We tested how NAD and NADH affect co-precipitation between rmGAPDH and phLDH. Two protein PEG mixture was incubated with increasing concentration of NAD or NADH. The PEG induced co-precipitation was followed by measuring activity in the pellets and the supernatant as described in the previous section. The co-precipitation of phLDH and rmGAPDH is abolished with a stoichiometric concentration of NADH (Fig. 3.3 A). NAD on the other hand, affects the rmGAPDH-phLDH co-precipitation only slightly even when present in hundred fold excess (Fig. 3.3 B). NAD binds to most dehydrogenases with nearly 100-fold lower affintiy than NADH [Dalziel, 1975]. However, even with this lower affinity, the enzymes should have been saturated with the higher [NAD]. RmGAPDH is an exception in that it binds NAD tightly, but with large negative cooperativity to the successive subunits. Therefore, the lower effect of NAD on co-precipitation may be a real difference

**Figure 3.3 (A-B) The PEG induced co-precipitation between phLDH and rmGAPDH in the presence of increasing concentration of NADH (A) and NAD (B).**

**(A)** the precipitation of rmGAPDH (○) and phLDH (❑), in the presence of increasing concentration of NADH. **(B)** the precipitation of rmGAPDH (○) and phLDH (❑), in the presence of increasing concentration of NAD. The rmGAPDH precipitation in the absence of phLDH is indicated in the figure (●) and was not subtracted in the profiles shown. Proteins were present at 1.0 mg/ml (6.9 μM) in all measurements. Other procedures are as described in the legend of Fig. 3.1.

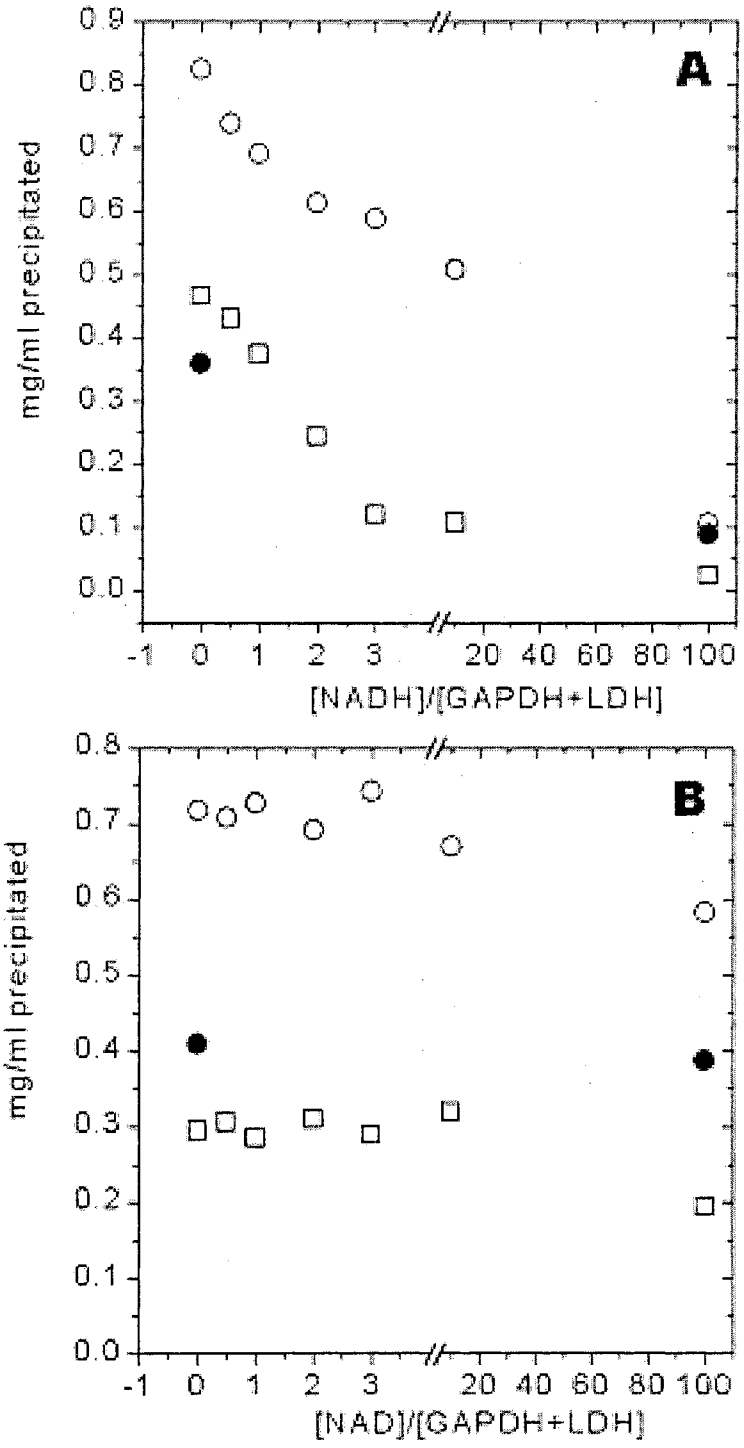
A
mg/ml precipitated
0.9
0.8
0.7
0.6
0.5
0.4
0.3
0.2
0.1
0.0
-1 0 1 2 3 20 40 60 80 100
[NADH]/[GAPDH+LDH]
B
mg/ml precipitated
0.8
0.7
0.6
0.5
0.4
0.3
0.2
0.1
0.0
-1 0 1 2 3 20 40 60 80 100
[NAD]/[GAPDH+LDH]

between the NAD and NADH bound enzymes, but a more thorough study would be needed to draw firm conclusions. The decrease in the co-precipitation with increase in NADH can be attributed to enzyme conversion to the holo form (Fig. 3.3 A). A different situation is observed with NAD. With increase in NAD, rmGAPDH is converted to the holo form, while phLDH remains in the apo-form. The decrease in co-precipitation with increase in NAD or NADH can be attributed either to the lack of interaction or to an increase in PEG solubility. It appears that both effects are present with NADH. NADH will abolish GAPDH background precipitation as well as rmGAPDH-phLDH co-precipitation . High NAD concentration does not affect the GAPDH background precipitation but will affect the co-precipitation suggesting that NAD directly competes with the protein interaction.

### 3.3.3 Sedimentation velocity AUC experiments in the presence of 10% PEG 6000

The evidence described above for association between potentially channeling dehydrogenases (dehydrogenases of opposite chiral specificity) prompted us to see if the solution phases as well as the precipitates of PEG solutions contained associated enzymes. For this purpose, we performed sedimentation velocity experiments with phLDH and rmGAPD alone and in a mixture. The experimental conditions were the same as used for the protein precipitations in PEG except for the temperature of 25°C for the sedimentation velocity experiments to avoid the very high viscosities of PEG solutions at 5°C. Also 100 mM NaCl was added to the Tris buffer in the second of the two sedimentation velocity experiments. Increased ionic strength from NaCl decreases the

amount of protein precipitated by PEG. Previous light scattering experiments on the oxaloacetate channeling enzymes malate dehydrogenase and citrate synthase (Merz, J. M. et al., 1987) revealed that exceedingly little enzyme complex exists in solutions in spite of extensive enzyme coprecipitation by [PEG]. Increasing ionic strength decreases coprecipitation of proteins by PEG, but conceivably could promote higher concentrations of associated enzymes in the solution phase. The second of our sedimentation velocity experiments tested this possibility using 100 mM NaCl in the Tris buffer. With the higher temperature (25°C) of the ultracentrifugation experiments, very little if any protein precipitated. In the experiment with no added NaCl, the initial absorbance plateau of the mixture was 10% lower than the sum of the corresponding absorbances of the individual enzymes. With the 100 mM NaCl system, however, these absorbances were the same within 1%. Therefore, approximately 10% of the protein may have precipitated from the enzyme mixture in the absence of NaCl, but we cannot be certain of this with only a 10% difference.

The sedimentation profiles for the individual enzymes were analyzed as described under MATERIALS and METHODS to obtain best-fit values of the sedimentation coefficient, buoyant molar mass, baseline offset, and the absorbance of the plateau at zero time. A fit to the slope of the plateau could also be obtained with the SVEDBERG program. The buoyant molar mass $M_b = M_r(1-\rho\bar{v}) = RTs/D$ where $\rho$ is density of the solution, $\bar{v}$ is the partial specific volume of the enzyme with molecular weight $M_r$, and s and D are the sedimentation and diffusion coefficients, respectively of the proteins. All other potential variables were fixed at experimental values. The resulting best-fits, and $M_b$ values were

the same for the two enzymes within the 2% experimental errors (Table 3.2) and the fits were of reasonable quality as judged both visually (Fig. 3.4) and by the root mean square (rmsd) values given in Table 3.2. Therefore, the data on the enzyme mixture can be modeled as a single species. Furthermore, a self-association model can exactly represent a hetero-associating system when the two proteins have the same s and $M_b$ values. Therefore, data from the enzyme mixture were also fitted with the "self-association" model assuming 10% of the equimolar proteins were in a 1:1 hetero-complex at the initial loading concentration of the enzymes (7.00 μM in each enzyme). The quality of these two fits (no association vs. 10% association) is used to test the hypothesis that the enzymes associate. Fig. 3.4 and Table 3.2 reveal that a considerably poorer fit is obtained when a 10% association is imposed. Very similar results were obtained with numerous other fitting strategies, e.g., fixing the s values of the monomer to best-fit SVEDBERG values, fitting to variable baseline offsets or base and meniscus positions. Although slightly different rmsd values were obtained with these different fitting strategies, all fits with 10% association were considerably poorer than fits assuming no association. When the s value of the hypothetical hetero-dimer was freed, the best-fit value of this parameter was close to that of the monomer, again indicating the absence of any hetero-dimer. Thus extensive hetero-association of the enzymes at these concentrations is unlikely even in PEG solutions where macromolecular associations should be more extensive than in polymer free solutions. Nearly maximal rates are observed for NADH channeling systems with [Ed-NADH] $\leq$ 20 μM in native enzyme and [Ea] $\leq$ 1 nM (Srivastava, D. K. and S. A. Bernhard, 1985). With these concentrations and the hetero-association

**Table 3.2 Sedimentation velocity results in 10% PEG solutions.**

PhLDH and rmGAPD (1 mg/ml each) were centrifuged at 40,000 rpm at 25 °C, with 10% PEG in the Tris buffer. Best fit values for individual enzymes are from the SVEDBERG program and results for mixtures are from the sedfit program referenced under EXPERIMENTAL METHODS. The sedimentation coefficients, s, are given in Svedberg units S. Square brackets indicate parameters that were fixed at values obtained on the mixture by SVEDBERG. Standard deviations given as ± values are based on random errors only. Real errors due to systematic and random sources are expected to be about 2% of the best-fit values. The root mean squared deviations (rmsd) = square root of (SSR/N), where SSR = sum($R_i^2$), $R_i$ is the residual at point I, and N is the number of degrees of freedom.

*The 10% association means that 10% of the total protein is associated at the loading concentration of the proteins (each at 1 mg/ml or 7.00 μM native tetramers). This corresponds to an association constant $K_a^{M,ha} = 1.77 \times 10^4\ M^{-1}$ on the molar scale (M) when formulated as a hetero-association (ha). The association constant used in the sedfit program is $K_a^{A,sa}$ on the absorbance scale (A) formulated as a self-association (sa). Hetero- and self- association constants are related by $K_a^{sa} = K_a^{ha}/4$. Association constants on the M and A scales are related by $K_a^A = 2K_a^M / \varepsilon_{avg}$ where $\varepsilon_{avg}$ is the average molar absorptivity of the two proteins. Therefore, with $\varepsilon_{avg} = 1.43 \times 10^5$, $K_a^{A,sa} = 3.56 \times 10^{-6} K_a^{M,ha} = 0.0630$, the value used in sedfit for the 10% association in this Table.

Table 3.2

| | $10^{-3}$ Buoyant Molar Mass | s S | rmsd |
|---|---|---|---|
| No NaCl | | | |
| phLDH alone | 25.0 ± 0.1 | 1.598 ± 0.001 | 0.0162 |
| rmGAPD alone | 26.3 ± 0.0.2 | 1.576 ± 0.002 | 0.0140 |
| Mixture, no association | [25.9] | [1.58] | 0.0244 |
| Mixture, 10% association* | [25.9] | [1.58] | 0.0793 |
| With 100 mM NaCl | | | |
| phLDH alone | 27.4 ± 0.2 | 2.595 ± 0.002 | 0.0131 |
| rmGAPD alone | 27.8 ± 0.2 | 2.525 ± 0.002 | 0.0093 |
| Mixture, no association | [27.9] | [2.55] | 0.0390 |
| Mixture, 10% association* | [27.9] | [2.55] | 0.0508 |

**Figure 3.4 Selected sedimentation velocity profiles of phLDH and rmGAPD mixtures.**

PhLDH and rmGAPD (1 mg/ml each) were centrifuged at 40,000 rpm at 25 °C, with 10% PEG in the Tris buffer as described under Experimental Methods. Solid curves are experimental data and dotted curves are best-fit data obtained from the sedfit program referenced under Experimental Methods. Buffer without added salt assuming: A, negligible association (log $K_a$ = -10.0) or B, 10% association at the loading concentration. Buffer with 100 mM NaCl assuming: C, negligible association or D, 10% association at the loading concentration. Good fits are observed assuming no association, in contrast to fits obtained assuming 10% association. Profiles shown are numbers 14 through 23 for the no salt experiments and profiles 10 through 19 for the experiments with 100 mM NaCl.

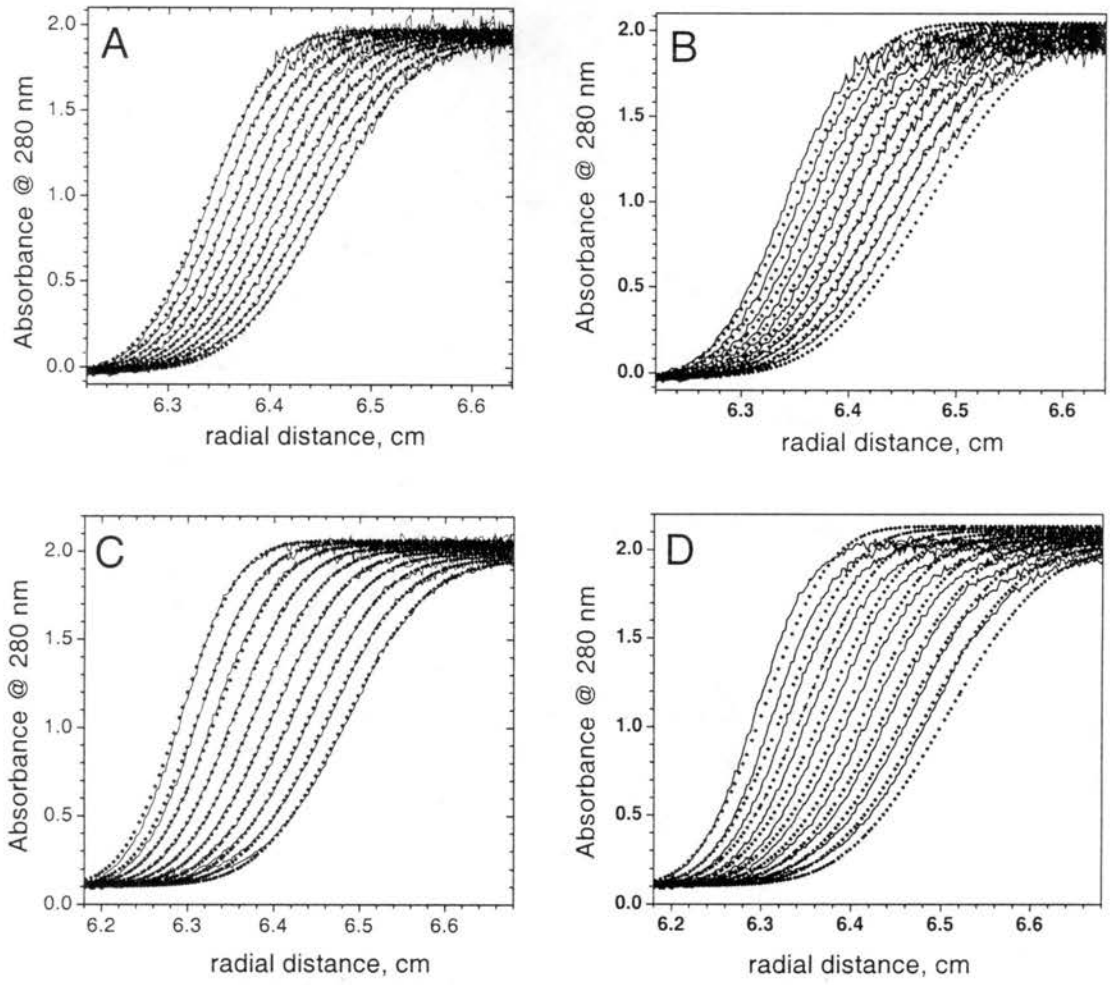
A
B
C
D
Absorbance @ 280 nm
radial distance, cm
0.0
0.5
1.0
1.5
2.0
6.2
6.3
6.4
6.5
6.6

constant of Table 3.2 ( $K_a^{M,ha} = 1.77x10^4\ M^{-1}$) Ea would only be 17% associated with Ed-NADH in enzyme buffering experiments unless one invokes kinetic mechanisms to alter the enzyme associations during the steady-state catalytic reaction. Thus we conclude that the Ed–NADH substrate is efficiently captured by Ea during the catalytic reaction although it is negligibly associated with Ea in the absence of this reaction.

If rates of the enzyme associations were slow relative to the rate of sedimentation, the enzyme association would not be observed. However, the enzyme buffering kinetic data indicate channeling and saturation of the acceptor enzyme by Ed-NADH within one minute of adding the second enzyme. In sharp contrast, the mixture of enzymes is present for at least one hour (for thermal equilibration of rotor and contents) before the sedimentation velocity experiments were started, and sedimentation at full speed lasts several hours. The very high pressures obtained in the cell during sedimentation velocity experiments can alter the extents of macromolecular associations. Ideally sedimentation velocity experiments at various speeds are desired to reveal such effects. Pressures within the cell vary with the square of the speed and the first power of column height. Therefore, pressures encountered in equilibrium runs are nearly 100-fold lower due to the 4 to 6-fold lower speeds and about 4-fold shorter columns. Hence the equilibrium experiments are not subject to uncertainties of pressure effects or of rates of association unless the latter are very much longer than 10 hrs.

### 3.3.4 Agarose Electrophoresis Mobility Shift Experiments

In parallel with the PEG co-precipitation experiments, the potential interactions between NAD(H) dehydrogenases were tested in electrophoresis mobility shift

experiments. PEG co-precipitation and the electrophoresis mobility shift experiments represent two independent methods to study interaction between NAD(H) · dehydrogenases. In contrast to PEG co-precipitation and enzyme buffering experiments, the mobility shifts were performed in MOPS/KOH instead of Tris/HCl to avoid development of $Cl_2$ at the anode. The electrophoresis experiments were used successfully in the past to demonstrate weak interaction between citrate synthase and mMDH (Ashmarina et al., 1994) as well as weak interactions between several other enzymes in the citric acid cycle (Beeckmans & Kanarek, 1981; Beeckmans et al., 1989). In the mobility shift experiments the molecular interaction is indicated by shifts in protein electrophoretic mobility induced by the presence of another protein. Protein or protein complex electrophoretic mobility is determined by its mass/charge ratio and its shape. The mobility shift experiments offer several unique advantages for detection of weak interactions. First the protein concentration used in the mobility shift experiment is limited only by protein solubility. In the phLDH and rmGAPDH experiments the proteins were at concentrations of 15 mg/ml or 104 μM. Very few protein interaction experiments will tolerate protein concentration that high. The second advantage of the mobility shift experiment is the gel matrix ability to promote weak interactions. It has been suggested that the gel matrix can promote some weak interactions by a cage effect or by adsorbing the interacting components on the matrix surface (Cann, 1996; Fried & Crothers, 1981; Zimmerman & Minton, 1993). Both the adsorption and the cage effects localize molecules, increasing the molecular collision frequency, and causing an apparent increase in the interaction affinity. Similar effects can exist *in vivo*, where molecular

clusters can produce an apparent increase in the interaction affinity by adsorbing the molecules or by limiting the molecular diffusion space.

The agarose electrophoresis experiments were used to test interaction between each one of the three A type dehydrogenase (phLDH, pmLDH, phcMDH) with each one of the four B type enzymes: byGAPDH, rmGAPDH, pmGAPDH and rmαGDH. Similar to the PEG co-precipitation studies interactions were observed between phLDH and rmGAPDH and between pmLDH and rmGAPDH (Figures 3.5 A and 3.7 A). The interaction specificity is demonstrated by replacing rmGAPDH with its pI and $M_r$ analogue rm-aldolase (Figures 3.5 B and 3.7 B). No mobility shifts were observed with phLDH when tested with byGAPDH or rmαGDH. Also no mobility shifts were observed with pmLDH paired with either byGAPDH or rmαGDH or with pmcMDH paired with either rmGAPDH or rmαGDH. Similar to PEG co-precipitation experiments, the interaction between phLDH and rmGAPDH is abolished with saturating NADH, but not with the saturating NAD (Fig. 3.6 A-B). The shifts were also abolished with increase in the ionic strength, e.g., adding 15 mM Na-Glu in the electrophoresis buffer, or doing the runs in 20 mM $KP_i$ pH=7.0. These results indicate that these interactions are ionic strength sensitive.

**Figure 3.5 (A-B) Agarose electrophoresis mobility shift experiment with phLDH and rmGAPDH (A) and the control mobility shift experiments with phLDH and rmALD (B) .**

**(A)** Lanes 1 and 8 contain phLDH only, lanes 3 and 6 contain rmGAPDH only. All other lanes contain both phLDH and rmGAPDH. The wells were loaded with 104 μM of rmGAPDH (15 mg/ml) and 76 μM (12mg/ml) of phLDH prepared in 20 μL of the running buffer plus 10% glycerol. The electrophoresis run time was four hours. PhLDH was loaded in the wells at the cathode side, rmGAPDH is loaded in the middle of the gel. During the run phLDH moves from cathode to anode crossing the rmGAPDH fronts. RmGAPDH moves from the middle of the gel towards the cathode crossing the incoming phLDH front. The mobility differences in phLDH front (lanes 1 and 8 relative to lanes 2, 4, 5, 7) and rmGAPDH fronts (lanes 3 and 6 relative to lanes 2, 4, 5, 7) indicate interaction. **(B)** The interaction specificity is demonstrated in the control experiment. Lanes 1 and 8 contain phLDH only, lanes 3 and 6 contain rmALD only. All other lanes contain both phLDH and rmALD. PhLDH was loaded in the wells on the cathode side. RmALD is loaded in the wells in the middle of the gel. During the run phLDH moves from cathode to anode crossing oppositely migrating rmALD fronts. The absence of mobility shifts when the two proteins fronts cross indicates no interaction. In both figures phLDH has two mobility fronts. The dominant first front corresponds to $H_4$ tetrameter isozyme, and the lagging front corresponds to the isozyme mixture $H_3M$. The H corresponds to LDH monomer predominant in heart tissues and M corresponds to monomer dominant in the muscle tissues. The

electrophoresis buffer was 50 mM MOPS/KOH containing 2 mM EDTA and 10 mM β-ME all at pH = 7.0. The temperature of the electrophoresis buffer was controlled to be 4 – 8°C and the electric field was 3.5 V/cm. The proteins were detected by coomassie staining.

---

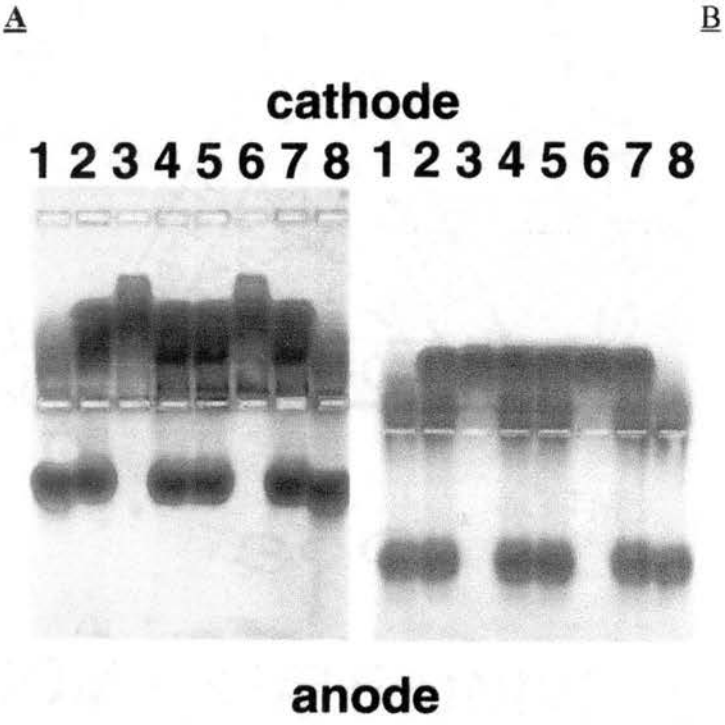

**Figure 3.6 (A-B) Electrophoresis mobility shift between rmGAPDH and phLDH in the presence of 2 mM NAD (A) and 2 mM NADH (B).**

In both gels lanes 1 and 8 contain phLDH only, lanes 3 and 6 contain rmGAPDH only. All other lanes contain both phLDH and rmGAPDH. The wells were loaded with 104 μM of rmGAPDH (15 mg/ml) and 76 μM (12mg/ml) of phLDH prepared in 20 μL of the running buffer plus 10% glycerol. PhLDH was loaded in the wells on the cathode side. RmGAPDH was loaded in the wells in the middle of the gel. During the run phLDH moves from cathode to anode crossing the rmGAPDH fronts. RmGAPDH moves from the middle of the gel towards the cathode crossing the phLDH front. The mobility differences in phLDH fronts (lanes 1 and 8 relative to lanes 2,4,5,7) and rmGAPDH fronts (lanes 3 and 6 relative to lanes 2,4,5,7) indicate interactions. In both figures phLDH has two mobility fronts. The dominant first front corresponds to $H_4$ tetrameter isozyme, and the lagging front corresponds to the isozyme mixture $H_3M$. H represents LDH monomer predominant in heart tissues, M represents monomer dominant in the muscle tissues. The experimental conditions were the same as described under Fig. 3.8.

A B

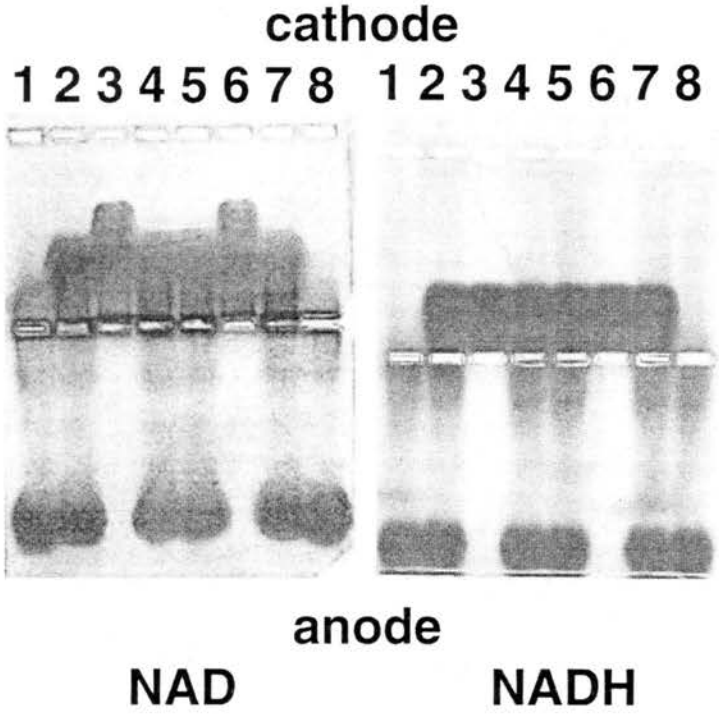

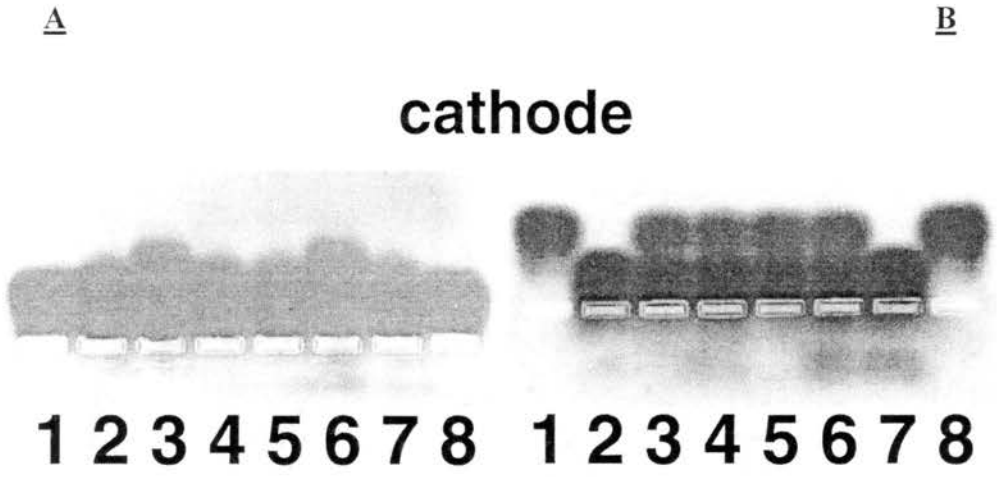


**Figure 3.7 (A-B) Mobility shift experiments with pmLDH and rmGAPDH (A), and the control mobility shift experiment between pmLDH and rmALD (B).**

In both gels the lanes 1 and 8 contain pmLDH alone, the lanes 3 and 6 (Fig A) and the lanes 2 and 7 (Fig B) contain rmGAPDH alone. All other lanes contain both pmLDH and rmGAPDH. The wells were loaded with 104 μM of rmGAPDH (15 mg/ml) and 62 μM (11 mg/ml) of phLDH prepared in 20 μL of the running buffer plus 10% glycerol Both proteins were loaded at the anode side of the gel. During the run both proteins run towards cathode. Interactions are indicated by the mobility differences between the free proteins fronts and the protein mixture fronts. The experimental conditions are the same as described under Fig. 3.8 except for an electrophoresis time of five hours.

## 3.4 Discussion and Conclusions

Describing interactions between NAD(H) dehydrogenases can help to understand the channeling mechanism and the enzyme buffering experiments. The sedimentation equlibrium AUC experiments were used to study possible interactions between three Ea-Ed pairs: byGAPDH and phLDH (section 3.3.1), rmαGDH and phLDH (Lehoux et al., 2001), and rmGAPDH and phLDH (H. O. Spivey and A. P. Minton unpublished results). All three Ea-Ed pairs show channeling in the enzyme buffering tests (Table 2.1). All three Ea-Ed pairs showed no detectable interaction, which indicates a Kd $\geq$ 100 μM. No interactions were observed in the absence of NADH, in subsaturating NADH or saturating NADH concentrations. This observation supports the Hummel-Dryer studies (Lehoux et al., 2001) which indicate that the previous report (Yong et al., 1993) of strong modulation of rmαGDH and phLDH interaction by NADH is an experimental artifact.

The absence of enzyme interactions is considered by some to be incompatible with NADH channeling (Keizer & Smolen, 1992). The reasons for this misimpression are discussed in chapter 5. The literature reports several cases where enzymes with protein substrates show no association in the absence of the catalytic reaction (absence of the cosubstrate). Effective channeling of phosphoribosylamine between glutamine phosphoribosylpyrophosphate amidotransferase and glycinamide ribonucleotide synthetase has been reported (Rudolph & Stubbe, 1995). The same study indicates no detectable equilibrium interaction between the channeling enzyme pair. The authors explained their results by introducing channeling with a short lived transient complex. Other examples involve enzyme-protein complexes that are imperative for the reaction

(electron transfer, or redox reactions of enzyme bound cystines or $FADH_2$), but are not seen in the absence of the reaction. For example very rapid electron transfer occurs between cytochrome c and cytochrome c peroxidase. Significantly, a complex can be easily observed at low ionic strengths, but none detected at physiological ionic strengths where the reaction is faster. Another example is E coli ribonucleotide reductase and thioredoxin, which do not form a detectable complex in the absence of their reaction, but must do so during their reaction in which thioredoxin reduces the cystines in the active site of the reductase (Holmgren, 1989; Mathews *et al.*, 1987). The final example is p-aminobenzoate synthase complex (PABA). Kinetic measurements demonstrate interactions between phosphoribosylamine amidotransferase and glycinamide ribonucleotide synthetase at concentrations as low as 10 nM in both enzymes. However, in the absence of the reaction no associations can be detected even with micromolar concentrations of the proteins (Roux & Walsh, 1992).

PEG co-precipitation and electrophoresis mobility shift experiments were used as an alternative approach to detect interaction between the dehydrogenase. Both methods are less quantitative than AUC, however both methods offer several unique advantages for detection of weak interactions. PEG has been reported to enhance specific protein interactions (Berg, 1990; Ingham, 1984; Miekka & Ingham, 1980; Zimmerman & Minton, 1993). The mobility shift experiments can handle exceptionally high protein concentrations and the gel matrix has been reported to enhance interactions by cage effects and by adsorption to the gel surface (Cann, 1996; Zimmerman & Minton, 1993). PEG co-precipitation experiments showed specific interaction between phLDH and both

rmGAPDH and phGAPDH, and between pmLDH and both rmGAPDH and pmGAPDH, i.e., between the mammalian forms of LDH and GAPDH. The sequence alignment shows that the rabbit and porcine GAPDH share 98.5% sequence identity. The enzymes co-precipitate in 1:1 stoichiometry. PEG induced co-precipitation can be abolished by stoichiometric concentration of NADH. NAD on the other hand affects co-precipitation only in millimolar concentrations. Sedimentation velocity AUC studies showed that the PEG complex exists only in an insoluble form as previously found for the MDH and citrate synthase enzymes (Merz et al., 1987). PEG co-precipitation studies in the presence of 100 mM NaCl indicated that the PEG co-precipitation is more sensitive to the increase in the ionic strength than the PEG induced protein precipitation of the individual enzymes. The presence of 100 mM NaCl will abolish the co-precipitation between phLDH and rmGAPDH but will only decrease the PEG induced precipitation of rmGAPDH. PEG induced interaction between rmGAPDH and phLDH or pmLDH was confirmed by the agarose electrophoresis mobility shift experiments. Like the co-precipitation experiments electrophoresis mobility shift experiments are affected by low concentrations of NADH but not by NAD.

The PEG co-precipitation and the mobility shift experiments did not show interaction between all analyzed dehydrogenases. Although PEG co-precipitation and the mobility shift experiments showed interaction only between mammalian LDH and GAPDH, we think that there could be specific interactions between other dehydrogenases. Both PEG co-precipitation and the mobility shift experiments are highly sensitive to the minute differences in protein properties. It is possible that we

observed interaction between mammalian enzymes due to the optimal combination of very specific protein properties like the net charge and solubility. Therefore, it is possible that additional optimization of PEG co-precipitation and mobility shift experiments could show interaction between other proteins. The effectiveness of PEG to induce enzyme interactions is dependent on the experimental conditions and protein properties (Ingham, 1984). The co-precipitation is most probable when proteins or protein complex are in buffer with pH close to its pI. The bigger the protein the more probable is the precipitation. The PEG experiments were performed in 50 mM Tris/HCl pH = 7.5, the buffer traditionally used for the enzyme buffering experiments. The solubility of mammalian GAPDH decreases rapidly as pH approaches 8. Low solubility of mammalian GAPDH as well as relatively large molecular mass of GAPDH, phLDH and pmLDH might have been factors that supported PEG induced co-precipitation. The mobility shift experiment are the most sensitive when interacting molecules are of the opposite net charge and large molecular mass. Protein electrophoretic mobility is proportional to the ratio of protein net charge and its molecular mass. PhLDH and rmGAPDH are of opposite net charge at pH of 7.5. PmLDH and rmGAPDH have unusually low electrophoretic mobility so that these two proteins stay in contact longer during the five hour experiment. In all other cases the protein migration distance is long and the two protein fronts stay in contact for a small fraction of the electrophoresis time. The sensitivity of the mobility shift experiments to detect interactions would be expected to increase as the two fronts stay in contact longer during their migration. PmLDH and

rmGAPDH have the longest protein contact time relative to the total protein migration distance.

The high conservation of NAD(H) dehydrogenase structures, especially the NAD(H) binding domain (the Rosmann fold, (Rossman *et al.*, 1975)), suggest the generality of weak interactions among dehydrogenases of opposite chiral specificity. The lowest sequence similarity within the GAPDH family has at least 50% identity (Harris & Waters, 1976). I have superimposed structures of several GAPDH dehydrogenases with RMS lower than 1 Å, indicating highly conserved backbone fold. In chapter 4 I show that GAPDH family has a specific pattern of the surface electric potentials. The backbone of several LDH as well as MDH structures can be superimposed with RMS lower than 1 Å. Chapter 4 shows that the pattern of surface electric potentials is conserved within the LDH and MDH families, though sequence similarity is very low. GAPDH ternary structure seems to be closely similar to other B type NAD(H) dehydrogenases: βHAD (Barycki *et al.*, 1999) and rmαGDH (Otto *et al.*, 1980).

## 3.5 References


Ashmarina, L. I., Pshezhetsky, A. V., Spivey, H. O. & Potier, M. (1994). Demonstration of Enzyme Associations by Countermigration Electrophoresis in Agarose Gel. *Anal. Biochem.* **219**, 349-355.

Barycki, J. J., O'Brien, L. K., Bratt, J. M., Zhang, R., Sanishvili, R., Strauss, A. W. & Banaszak, L. J. (1999). Biochemical characterization and crystal structure determination of human heart short chain L-3-hydroxyacyl-CoA dehydrogenase provide insights into catalytic mechanism. *Biochemistry* **38**, 5786-98.

Beeckmans, S. & Kanarek, L. (1981). Demonstration of Physical Interactions between Consecutive Enzymes of the Citric Acid Cycle and of the Aspartate-Malate Shuttle. A Study Involving Fumarase, Malate Dehydrogenase, Citrate Synthase and Aspartate Aminotransferase. *Eur. J. Biochem.* **117**, 527-535.

Beeckmans, S., Van Driessche, E. & Kanarek, L. (1989). The Visualization by Affinity Electrophoresis of a Specific Association between the Consecutive Citric Acid Cycle Enzymes Fumarase and Malate Dehydrogenase. *Eur. J. Biochem.* **183**, 449-454.

Berg, O. G. (1990). Influence of Macromolecular Crowding on thermodinamic activity: Solubility and Dimerisation Constants for Spherical and Dumbbell-Shaped Molecules in a Hard-Sphere Mixture. *Biopolymers* **30**, 1027-1037.

Brooks, S. P. & Storey, K. B. (1991). Re-evaluation of the glycerol-3-phosphate dehydrogenase/L-lactate dehydrogenase enzyme system. Evidence against the direct transfer of NADH between active sites. *Biochem J* **278**, 875-81.

Cann, J. R. (1996). Theory and practice of gel electrophoresis of interacting macromolecules. *Anal Biochem* **237**, 1-16.

Chock, P. B. & Gutfreund, H. (1988). Reexamination of the kinetics of the transfer of NADH between its complexes with glycerol-3-phosphate dehydrogenase and with lactate dehydrogenase. *Proc Natl Acad Sci U S A* **85**, 8870-4.

Dalziel, K. (1975) Kinetics and mechanisms of nicotinamide-nucleotide-linked dehydrogenases in The Enzymes (Boyer, P. D., Ed,) Third ed. Academic Press, New York. 1-60.

Datta, A., Merz, J. M. & Spivey, H. O. (1985). Substrate channeling of oxalacetate in solid-state complexes of malate dehydrogenase and citrate synthase. *J Biol Chem* **260**, 15008-12.

Elcock, A. H. & McCammon, J. A. (1996). Evidence for electrostatic channeling in a fusion protein of malate dehydrogenase and citrate synthase. *Biochemistry* **35**, 12652-8.

Fahien, L. A. & Kmiotek, E. (1979). Precipitation of complexes between glutamate dehydrogenase and mitochondrial enzymes. *J Biol Chem* **254**, 5983-90.

Fahien, L. A., Kmiotek, E. & Smith, L. (1979). Glutamate dehydrogenase--malate dehydrogenase complex. *Arch Biochem Biophys* **192**, 33-46.

Fahien, L. A., Kmiotek, E. H., MacDonald, M. J., Fibich, B. & Mandic, M. (1988). Regulation of malate dehydrogenase activity by glutamate, citrate, alpha-ketoglutarate, and multienzyme interaction. *J Biol Chem* **263**, 10687-97.

Fried, M. & Crothers, D. M. (1981). Equilibria and kinetics of lac repressor-operator interactions by polyacrylamide gel electrophoresis. *Nucleic Acids Res* **9**, 6505-25.

Fukushima, T., Decker, R. V., Anderson, W. M. & Spivey, H. O. (1989). Substrate channeling of NADH and binding of dehydrogenases to complex I. *J Biol Chem* **264**, 16483-8.

Halper, L. A. & Srere, P. A. (1977). Interaction between citrate synthase and mitochondrial malate dehydrogenase in the presence of polyethylene glycol. *Arch Biochem Biophys* **184**, 529-34.

Harris, J. I. & Waters, M., Eds. (1976). Glyceraldehyde-3-phosphate dehydrogenase. 3rd edit. Vol. XIII. The Enzymes. Edited by Boyer , P. D. I-XX vols. New York: Academic Press.

Hsu, C. S., Minton, A. P. (1991) A Strategy for Efficient Characterization of Macromolecular Heteroassociations via Measurement of Sedimentation Equilibrium. *J. Molec. Recog.* **4**, 93-104.

Holmgren, A. (1989). Thioredoxin and glutaredoxin systems. *J Biol Chem* **264**, 13963-6.

Ingham, K. C. (1984). Protein precipitation with polyethylene glycol. *Methods Enzymol* **104**, 351-6.

Keizer, J. & Smolen, P. (1992). Mechanisms of metabolite transfer between enzymes: diffusional versus direct transfer. *Curr Top Cell Regul* **33**, 391-405.

Lehoux, E. A., Baker, S. H., Svedruzic, Z., Hays, F. A. & Spivey, H. O. (2001). Evidence against the NADH-modulated complex formation between α-glycerol-3-phosphate dehydrogenase and lactate dehydrogenase. *In preparation.*

Lindbladh, C., Rault, M., Hagglund, C., Small, W. C., Mosbach, K., Bulow, L., Evans, C. & Srere, P. A. (1994). Preparation and kinetic characterization of a fusion protein of yeast mitochondrial citrate synthase and malate dehydrogenase. *Biochemistry* **33**, 11692-8.

Mathews, C. K., Sjoberg, B. M. & Reichard, P. (1987). Ribonucleotide reductase of Escherichia coli. Cross-linking agents as probes of quaternary and quinary structure. *Eur J Biochem* **166**, 279-85.

Merz, J. M., Webster, T. A., Appleman, J. R., Manley, E. R., Yu, H. A., Datta, A., Ackerson, B. J. & Spivey, H. O. (1987). Polyethylene glycol-induced heteroassociation of malate dehydrogenase and citrate synthase. *Arch Biochem Biophys* **258**, 132-42.

Miekka, S. I. & Ingham, K. C. (1980). Influence of hetero-association on the precipitation of proteins by poly(ethylene glycol). *Arch Biochem Biophys* **203**, 630-41.

Otto, J., Argos, P. & Rossmann, M. G. (1980). Prediction of secondary structure elements in Glycerol-3-phosphate dehydrogenase by comparison with other dehydrogenases. *Eur. J. Biochem.* **109**, 325-330.

Philo, J. (1994). Meassuring Sedimentation, Diffusion, and Molecular Weights of Small Molecules by Direct Fitting of Sedimentation Velocity Concentration Profiles. In

*Modern Analytical Ultracentrifugation* (Schuster, T. & Laue, T., eds.), pp. 350. Birkhauser, Boston Basel Berlin.

Rossman, M. G., Liljas, A., Branden, C.-I. & Banaszak, L. J. (1975). Evolutionary and Structural Relationships among Dehydrogenase. In *The Enzymes* 3rd edit. (Boyer, P. D., ed.), Vol. XI, pp. 61-102. Academic Press, New York.

Roux, B. & Walsh, C. T. (1992). p-Aminobenzoate synthesis in Escherichia coli: kinetic and mechanistic characterization of the amidotransferase PabA. *Biochemistry* **31**, 6904-10.

Rudolph, J. & Stubbe, J. (1995). Investigation of the mechanism of phosphoribosylamine transfer from glutamine phosphoribosylpyrophosphate amidotransferase to glycinamide ribonucleotide synthetase. *Biochemistry* **34**, 2241-50.

Schuck, P. (1998) Sedimentation analysis of noninteracting and self-associating solutes using numerical solutions to the Lamm equation. *Biophys. J.* **75**, 1503-1512.

Srere, P. A., Halper, L. A. & Finkelstein, M. B. (1978). Interaction of Citrate Synthase and Malate Dehydrogenase. In *Microenvironments and Metabolic Compartmentation* (Srere, P. A. & Estabrook, R. W., eds.), pp. 421-422. Academic Press, New York.

Srivastava, D. K., Bernhard, S. A. (1984) Direct Transfer of Reduced Nicotinamide Adenine Dinucleotide from Glyceraldehyde-3-phosphate Dehydrogenase to Liver Alcohol Dehydrogenase. *Biochemistry* **23**, 4538-4545.

Srivastava, D. K., Smolen, P., Betts, G. F., Fukushima, T., Spivey, H. O. & Bernhard, S. A. (1989). The Direct Transfer of NADH between α-Glycerol Phosphate Dehydrogenase and Lactate Dehydrogenase. Fact or Misinterpretation? *Proc. Natl. Acad. Sci., USA* **86**, 6464-6468.

Ushiroyama, T., Fukushima, T., Styre, J. D. & Spivey, H. O. (1992). Substrate Channeling of NADH in Mitochondrial Redox Processes. In *From Metabolite, to Metabolism, to Metabolon* (Stadtman, E. R. & Chock, P. B., eds.), Curr. Top. Cell Regul. Vol. 33, pp. 291-307. Academic Press, New York.

Wu, X., Chock, P. B., Lakatos, S. & Gutfreund, H. (1990). On the Mechanism of Transfer of NADH between Its Complexes with Glycerol-3-phosphate Dehydrogenase and with Lactate Dehydrogenase. *FASEB J.* **4**, A2303, Abst. #3524.

Wu, X., Gutfreund, H., Lakatos, S. & Chock, P. B. (1991). Substrate Channeling in Glycolysis: A Phantom Phenomenon. *Proc. Natl. Acad. Sci. USA* **88**, 497-501.

Yong, H., Thomas, G. A. & Peticolas, W. L. (1993). Metabolite-modulated complex formation between alpha-glycerophosphate dehydrogenase and lactate dehydrogenase. *Biochemistry* **32**, 11124-31.

Zimmerman, S. B. & Minton, A. P. (1993). Macromoleculare Crowding: Biochemical, Biophysical, and Physiological Consequences. *Annual Review of Biophysic and Biomolecular Structure* **22**, 27-65.

# CHAPTER 4 Molecular Modeling

## 4.1 Introduction

In the previous two chapters the channeling between two dehydrogenases has been analyzed by enzyme kinetics and protein association studies. This chapter describes molecular modeling studies designed to study channeling at the protein structure level. The approach was encouraged by the rich structural information on the NADH dehydrogenase family, and powerful molecular modeling tools developed in the last decade. Molecular modeling studies have been used in the past to study channeling between citrate synthase and mMDH (Elcock & McCammon, 1996) and between A and B type NAD(H) dehydrogenases (Srivastava *et al.*, 1985). The citrate synthase and mMDH channeling complex was constructed by docking the two protein structures. Brownian dynamic simulations with and without the electrostatic potential within the channeling complex showed that channeling is facilitated by the molecular electric field. The molecular modeling studies of the channeling between the NADH dehydrogenases are older and less extensive (Srivastava et al., 1985). The authors reported complementary surface potentials around the NAD(H) binding sites of A and B type dehydrogenases. The authors concluded that the conformations of these two types of NADH sites allowed direct transfer of the nicotinamide portion of NADH between docked dehydrogenases only if they were of opposite chiral specificity (A-B). The enzymes then had to dissociate from each other to allow the adenine moiety to undergo the anti-syn rotation after which the adenine could then be bound into its binding site on the acceptor enzyme.

It was impossible for any of the NADH to be transferred between two dehydrogenases of the same chiral specificity while the enzymes were docked – an essential step in order to retain the chiral specificity of this NADH channeling. However, Srivastava and co-authors did not describe the docking process and only vaguely described the docking surfaces as the surrounding of the NAD(H) binding site. Actually the authors did not make clear whether their analysis was performed using the native oligomeric enzyme forms or the individual subunits. The failure to report the docking process precisely makes the original study very hard to reproduce and analyze. In addition there were only three dehydrogenase structures known at the time of their studies. Our plan was to extend the original study by taking advantage of the recent progress in molecular modeling and the very much larger number of dehydrogenase structures known now. First we wanted to evaluate possible docking surfaces between A and B dehydrogenase pairs and show a detailed analysis of the docking process. Next we wanted to describe the electric potential and hydropathic properties of the docking surfaces to find the forces driving the docking process. Finally we wanted to map the channeling process, by describing the feasibility of the NAD(H) transfer between the channeling proteins.

## 4.2 Methods

All protein coordinates were downloaded from the protein data bank in Brookhaven. All molecular structures were visualized using the Insight II program package (Biosym, San Diego, CA). The surface potentials were calculated using the GRASP program (Honig & Nicholls, 1995), and the potential near the protein surface was calculated using the Delphi program (Honig & Nicholls, 1995). The surface hydropathic properties were calculated using the HINT program (Kellogg *et al.*, 1991).

All calculations were performed according to the default protocol in the program manuals. In the surface potential calculations by the GRASP and Delphi programs, the protein surface potentials were calculated by assigning charges to the four charged amino acids according to the program's charge assignment files. The relative electric permitivity of the protein interior was assumed to be 2, the surrounding water media was 80. The protein surfaces were calculated according to the algorithm of Connolly (Connolly, 1983). The surface hydropathic priorities were calculated by assigning each amino acid its LogP. The LogP value for each amino acid is the logarithm of the amino acid partition between aqueous and the n-octanol phases. In all hydropathic calculations the amino acid Log P values were assigned according to the program's LogP assignment file.

Channeling complexes between two dehydrogenases were built with the following guidelines:

1. Proposed channeling complex needs to be assembled so that NAD(H) could be transferred between the two proteins without escaping into the bulk phase.

2. Docking surfaces should have complementary shapes, surface potentials and/or hydropathic properties.
3. Interaction affinity is probably modulated by NAD(H).
4. Productive docking should happen between A and B type dehydrogenases, but not between B and B nor between A and A type dehydrogenases. The essential structural feature(s) supportive of channeling are expected to be conserved among all A type dehydrogenases, and all B types dehydrogenases.

The first and fourth requirements are due to the apparent stereospecificity of NADH channeling, which has only been observed between dehydrogenases of opposite chiral specificity. It is also based on the assumption that the mechanism reported by Srivastava et al. (1985) is valid. The stereospecificity of NADH channeling could alternatively be achieved by the fact that only A-B complexes have sufficient life-time for the transfer of NADH by proximity effects, e.g, by electrostatic channeling (Elcock & McCammon, 1996). Complementary surface charges act as a driving force for the complex formation and assure the specificity and stability of the complex. Complementary surface hydropathic properties and shape assure the stability of the complex. NAD(H) modulation of the extent of complex formation and the 1:1 stoichiometry are experimentally observed properties of the interaction between NAD(H) dehydrogenases that have been detected at equilibrium (chapter 3, and Fukushima *et al.*, 1989). The fourth guideline is also based on the experimental observation that NADH channeling only occurs between A and B type dehydrogenases.

## 4.3 Results

### 4.3.1 Channeling complex between porcine heart LDH and human GAPDH

The LDH-GAPDH channeling complex was constructed by docking structures of the pig heart LDH (A type , pdb 5LDH, resolution 2.7 Å, R = 0.196, (Grau *et al.*, 1981)) and human muscle GAPDH (B type, pdb 3GPD, resolution 3.5 Å, R = 0.33 (Mercer *et al.*, 1976)). The molecular modeling studies are designed to be a close match to the actual experiment which showed specific interaction between mammalian enzymes: rmGAPDH or pmGAPDH with either phLDH or pmLDH (chapter 3). The molecular modeling studies used the human muscle GAPDH since no other mammalian GAPDH crystal structure is currently available in the PDB. For all practical modeling purposes, the human GAPDH is a close match to the rmGAPDH (or pmGAPDH) since the two enzymes share 96% sequence identity and 98% sequence homology. Molecular modeling was used in the past to study channeling between phLDH: lobster GAPDH (Srivastava et al., 1985). That study is closely similar to my study, since hGAPDH and lobster tail GAPDH share over 70% amino acid sequence homology and the backbone of the two proteins superimpose with low RMS between the corresponding atoms. In contrast to the work of Srivastava and co-authors who appear to have worked on monomers, the current study constructed potential channeling complexes by docking tetrameric enzyme forms.

The structures of human GAPDH and pig heart LDH tetramers were manually docked using the program Insight II. The channeling complex of Figures 4.1 and 4.2 is a close match to the docking guidelines listed in the section 4.3.1. The constructed

channeling complex brings the docking surfaces in intimate contact forming a "channeling cavity" by interfacing the two NAD(H) sites (Figures 4.2 and 4.3). The channeling cavity surrounds the two NAD(H) binding sites but is partially open to the surrounding aqueous media. Fig. 4.2 shows that NAD(H) can be channeled between the two sites by free diffusion within the confines of the cavity. Incomplete closure of the channeling cavity (Fig. 4.2) suggests that NAD(H) diffusion out of the channeling cavity (e.g. leaky channeling) is limited but apparently possible. Matching the interfacing surfaces according to the surface potentials (Fig. 4.4) and hydropathic properties (Fig. 4.5) is challenging. The docking surfaces have weak electric potential (Fig. 4.4, area marked 2 and 3), with patches of unusual hydrophobicity (Fig. 4.5). The proposed docking surfaces of the individual enzymes have a number of amino acids of opposite charge in close proximity, which effectively cancels the electric fields of these surface areas. As a result the surface potential distribution and hydropathic properties on the docking surfaces of each enzyme are dispersed in small poorly defined patches (Fig. 4.4). With no dominant surface electric potentials, the surface analysis programs are of limited use, and the search for electrostatic complementarity has to be done on the level of individual amino acids (Table 4.1). The analysis successfully identified several complementary ion pairs at the protein interface (Table 4.1).

Building a proposed phLDH:hGAPDH channeling complex is a difficult task even with today's molecular modeling programs. A number of programs for automatically docking macromolecules have been written and have had some success. We haven't tried these yet and suspect that they will have difficulty with the weak interactions involved in

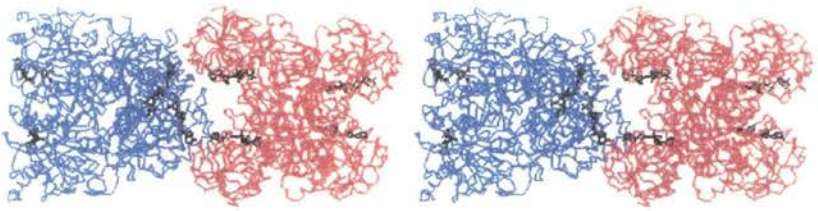

**Figure 4.1 The stereo image of the phLDH: hGAPDH channeling complex.**

The phLDH tetramer (5ldh, **(Grau et al., 1981)**) backbone is shown in blue; hGAPDH tetramer (3gpd, **(Mercer et al., 1976)**) is shown in red; and NAD molecules are shown in black. The GAPDH is positioned with its Q,R axis plane (Rossman et al., 1975) coplanar with the plane of paper. The LDH is positioned with its main symmetry axis in the plane of the paper (Holbrook et al., 1975; Rossman et al., 1975). The figure illustrates general orientation between the two proteins within the channeling complex. The image was generated using the Insight II program (Biosym, San Diego, CA).

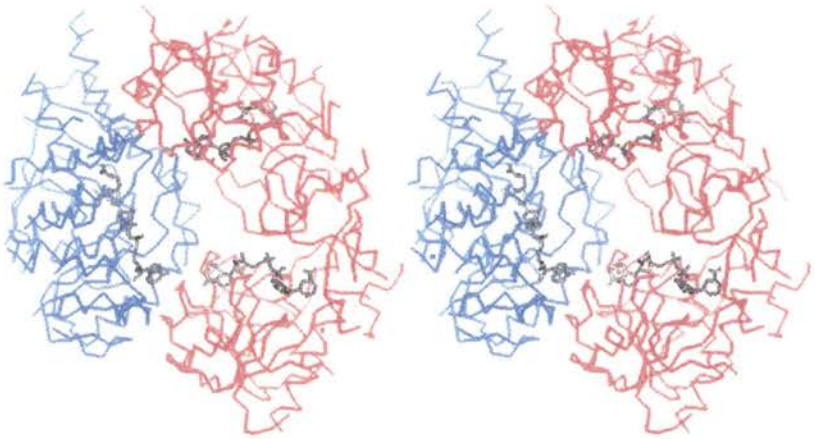

**Figure 4.2. The stereo image of the docking interface between the phLDH and hGAPDH.**

Figure 4.2 is a close up of figure 4.1 created in an attempt to show the interface between the docking surfaces and the "channeling cavity". The "channeling cavity" can be defined as the empty space enclosed between the two NAD(H) sites. The figure is created by "cutting" the protein structures at 38 Å radial from the center of the channeling cavity using the Insight II program (Biosym, San Diego, CA). The phLDH **(Grau et al., 1981)** backbone is shown in blue, hGAPDH **(Mercer et al., 1976)** is shown in red and the NAD molecules are shown in black. The figure shows structural complementarity of the docking surfaces in intimate contact. The channeling cavity completely encloses the NAD(H) binding sites and apparently acts as a cage for the free diffusion of NAD(H) between the two sites. The channeling cavity is also partially open to the surrounding aqueous media, however the opening appears too small for a significant NAD(H) escape and leaky channeling.

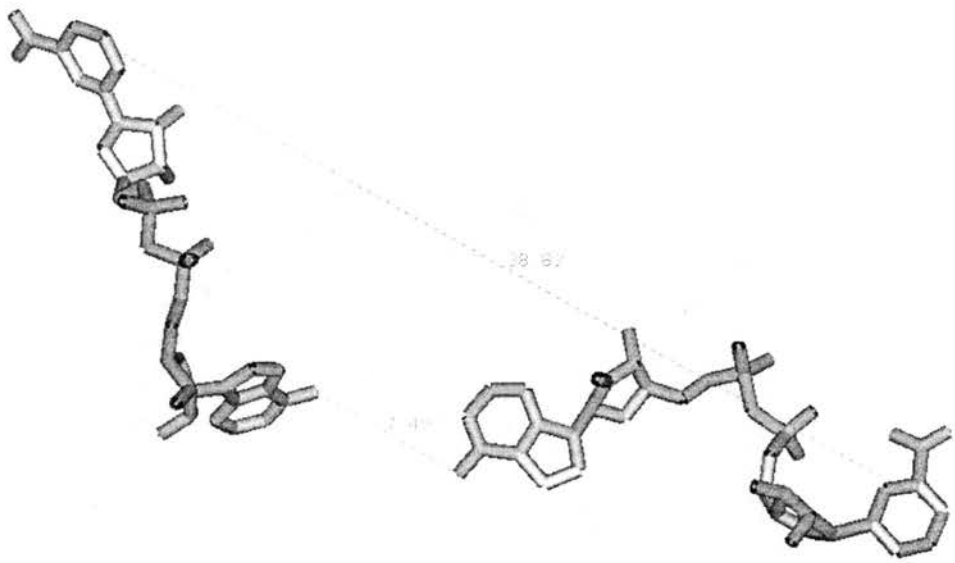

**Figure 4.3 Channeled NAD molecules within the phLDH: hGAPDH complex.**

The figure is a close up of the figure 4.2, with only "channeling" NAD molecules shown[1]. The left molecule is NAD bound to the A type dehydrogenase and the right molecule is NAD bound to the B type dehydrogenase. Two molecules are roughly related by a two fold symmetry axis as originally suggested (Srivastava et al., 1985). The dashed lines show distance between two most distal (nicotinamide C4) and the closest (adenine N6) parts of the two NAD molecules.

[1] The purpose of this figure is to illustrate distance and orientation between NAD(H) binding sites when two dehydrogenase are docked in a channeling complex. The relative orientation between two NAD(H) binding sites are illustrated by using NAD molecules present in the original protein structures. No NAD channeling was reported to this date, though there was a mention that it is possible (Srivastava & Bernhard, 1984). Although there could be some small difference in the conformation of the bound nucleotides for the purpose of this study those differences could be ignored.

**Figure 4.4 (A-B) The electric potentials on the phLDH (A) and hGAPDH (B) docking surfaces.**

The figure shows orthogonal views of the docking surfaces of: **A**, phLDH monomer (Grau et al., 1981) and **B**, hGAPDH dimer (Mercer et al., 1976). The figure is generated by "cutting" Fig. 4.2 in the middle of the channeling cavity orthogonal to the plane of the paper and then rotating the docking surfaces 90 degrees towards the reader. PhLDH is rotated about 20 degrees with its N terminal tail away from the reader. The NAD molecules are shown in green and the protein atoms as CPK spheres. The red and blue colors represent surface areas with negative and positive potentials, respectively. The color intensities are proportional to the surface potentials and span from -10.0 $k_BT/e$ to 10.0 $k_BT/e$, where $k_B$ is Boltzmann constant $k_B = 1.38\ 10^{-23}\ JK^{-1}$, T is the absolute temperature (298 K), and $e$ is the charge of an electron in C. The potentials are calculated using the Delphi program (Honig & Nicholls, 1995), and the picture was generated using Insight II program (Biosym, San Diego CA). The complementary docking surfaces for the channeling complex shown in Figure 4.1 and 4.2 are marked with numbers 2 and 3. The calculation shows that both docking surfaces are covered with a relatively weak electric field with poor complementarity between the two proteins. The complementary docking surfaces for the alternative channeling complex shown in the Figure 4.4 are marked with number 1. The area corresponds to the catalytic domains of the two proteins. The two surfaces match during the docking when phLDH inserts between the two hGAPDH domains. The process brings the two NAD(H) binding domains and catalytic domains in direct contact as described in the Figure 4.4.

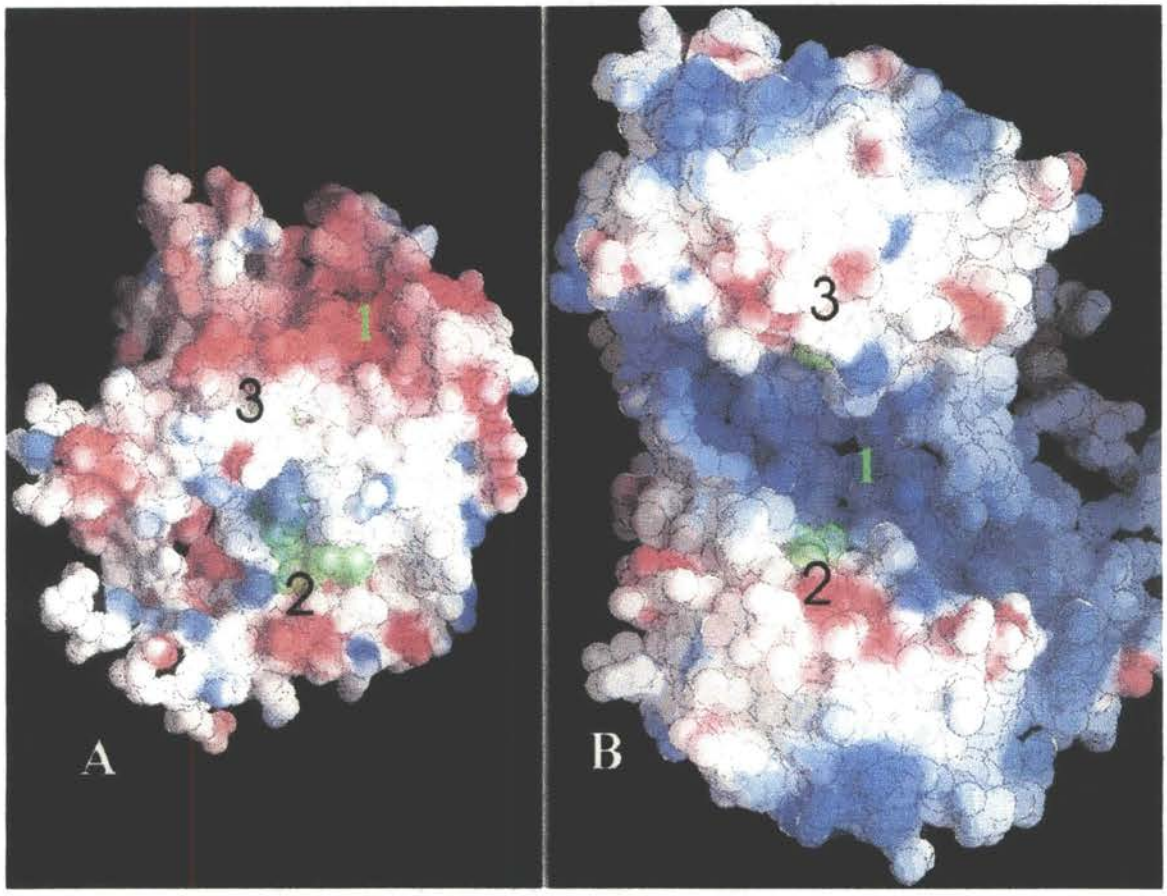
1
3
2
A
3
1
2
B

**Figure 4.5 (A-C) The hydropathic properties of the phLDH (A) and hGAPDH (B-C) docking surfaces.**

Figures (**A-B**) are orthogonal views of the docking surfaces of phLDH (**B**, (Grau et al., 1981)) and hGAPDH (A, (Mercer et al., 1976)) as suggested in Fig 4.2. The figures (**A-B**) are generated by "cutting" Fig. 4.2 in the middle of the channeling cavity orthogonal to the plane of the paper and then rotating the docking surfaces 90 degrees towards the reader. Figure (**C** ) shows hydropathic properties of the surrounding of hGAPDH NAD(H) binding site. Figures (**B-C**) are generated by "cutting" Fig. 4.2 in the middle of the channeling cavity orthogonal to the plane of the paper and then rotating the docking surfaces 90 degrees towards the reader. In all figures the NAD molecules are shown in green, the protein atoms are shown as CPK spheres. The red and blue colors represent surface areas with hydrophilic (red) or hydrophobic (blue) properties, respectively. The color intensity (the scale shown in the middle of the figure) is proportional to the surface LogP values, which are defined as the logarithm of the partition coefficient between the water and n-octanol. The surface hydropathic properties are calculated using the program HINT (Kellogg et al., 1991), and picture was generated using the program Insight II (Biosym, San Diego CA). The calculation showed that the docking surfaces as well as surrounding of the NAD(H) binding sites contain patches of unusual hydrophobicity.

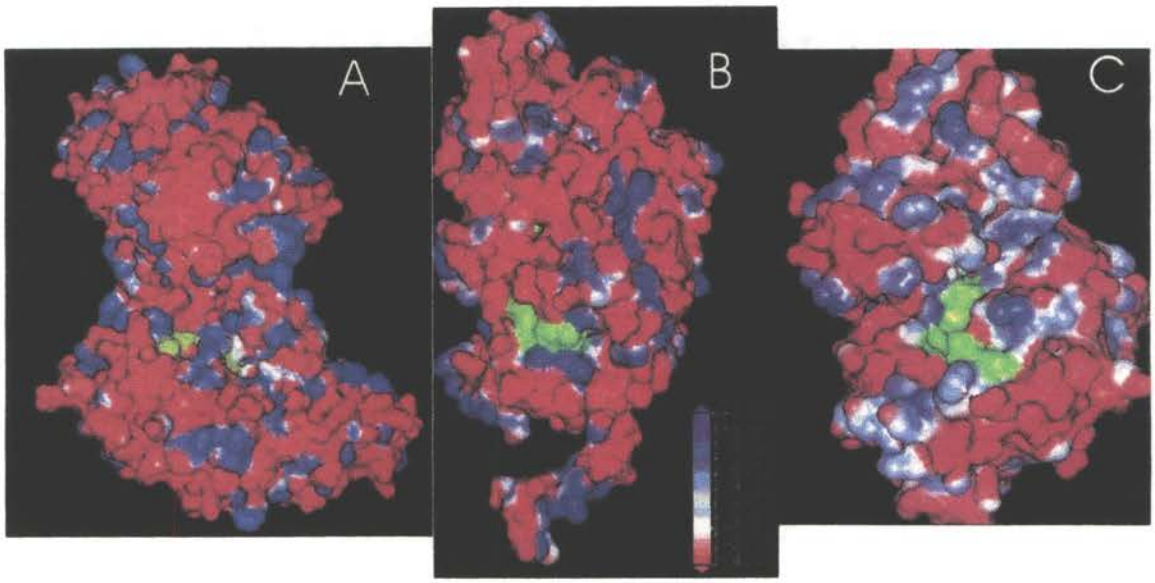
A
B
C

**Table 4.1 List of the amino acids in ion contact between the docking interface between phLDH and hGAPDH.**

| PhLDH | hGAPDH |
|---|---|
| Glu 56 | Lys 112 |
| Asp 57 | Lys 85 |
| Lys 58 | Asp 80 |
| Asp 84 | Lys 85 |
| Arg 115 | Asp 38 |
| Lys 241 | Asp 80 |

these complexes. However, manual docking of the enzymes are aided by the assumed mechanism that docks the enzymes so that at least part of the NADH molecule can be directly transferred between the two enzymes. The proposed structure for the docked enzyme pair has its strengths and weaknesses, however I think it is the best possible match to the docking guidelines described in the methods section. The strength of the proposed structure is that it brings two NAD(H) sites into proximity allowing unobstructed but controlled transfer of NAD(H) between the two sites (Fig. 4.2). The two proteins are in intimate contact and make a channeling cavity. The docking interfaces in the complex match several ion pairs. However, the proposed model offers no clear explanation for the NAD/NADH modulation of the interaction affinity. Another weakness is that the proposed complex offers no clear explanation for the A type-B type preference in channeling in the manner reported by Srivastava et al. (Srivastava et al., 1985). Finally the proposed complex offers no specific evaluation of the forces holding the complex together for the required time to allow the transfer of NADH. These weaknesses are being explored now by collaborators expert in molecular modeling.

An alternative complex (Fig. 4.6) can be proposed that alleviates most of these weaknesses. The alternative complex would involve a significant conformational change in the GAPDH structure upon docking of two proteins. The hGAPDH structure given in the PDB and analyzed in this study represents protein "squeezed" in the crystal lattice. The protein crystal structure is not necessarily the best representative for all protein conformations (structures) that can be formed by the protein backbone "breathing" in the solution. To form the alternative channeling complex, the GAPDH structure needs to

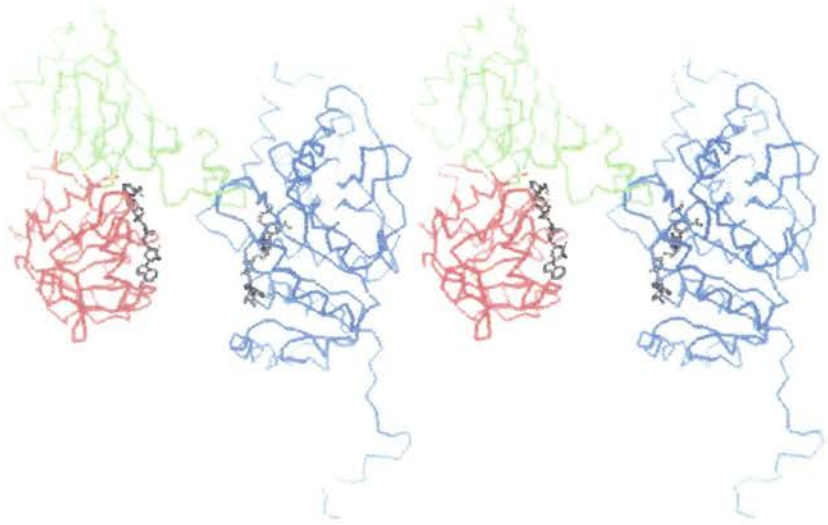

**Figure 4.6 The stereo image of the alternative channeling complex between phLDH and hGAPDH**

The stereo image shows one subunit of hGAPDH subunits (3gpd, **(Mercer et al., 1976)**) and one subunit of phLDH (5ldh, **(Grau et al., 1981)**) facing each other with their NAD(H) binding sites opposed. PhLDH is shown in blue, hGAPDH catalytic domain (amino acids 151-316) is shown in green, the NAD(H) binding domain in red, and NAD(H) molecules in black. For channeling to occur the subunits need to slide towards each other in the plane of the paper so that two NAD(H) sites come in a direct contact. Also hGAPDH needs to "open" by moving the catalytic domain main axis perpendicular to the plane of the complex interface. The hGAPDH structure shown suggests that the interface between catalytic and NAD(H) binding domain appears loose enough to support such opening. Once the hGAPDH structure is open the NAD(H) binding sites of two subunits can come in direct contact. The image was generated using Insight II program (Biosym, San Diego, CA).

open slightly within its R,Q plane so that one of the LDH monomers can fit in the gulf between the two GAPDH subunits. The LDH monomer could enter in the opened GAPDH structure so that GAPDH R,Q plane is parallel to the phLDH Q,P plane and the two NAD(H) binding sites come in direct contact as previously suggested (Srivastava et al., 1985). The definition of the P, Q, and R axes can be found in (Holbrook et al., 1975) for LDH and in (Rossman et al., 1975) for GAPDH. Srivastava and co-authors (Srivastava et al., 1985) might have had similar idea when they wrote in the abstract "The facile passage of the coenzyme through the first enzyme site requires an open protein conformation, characteristic of the apo-enzyme rather than the holoenzyme structure." Unfortunately Srivastava and co-authors did not describe the "open protein conformation." Actually developing the GAPDH open conformation on the basis of the available crystal structure is a significant challenge. Taking the best possible guess, the GAPDH can open by conformational change between loosely connected catalytic and NAD(H) binding domain as previously suggested for the apo-holo enzyme transition (Fig. 4.6, (Leslie & Wonacott, 1984; Skarzynski & Wonacott, 1988)). Once the LDH-GAPDH channeling complex is constructed with the two NAD(H) binding sites in direct contact, the experimentally observed properties of interaction between the mammalian enzymes can be analyzed. The driving force for the complex formation can be a significantly complementary electric field and hydrophobic interaction (Fig. 4.4, area 1, Fig. 4.5 A-C). The GAPDH tetramer is formed by interaction between the four catalytic domains (Fig. 4.1). The subunit interface contains a strong positive electric field located at helix C (Harris & Waters, 1976) and the S loop (Fig. 4.4 area 1, (Skarzynski &

Wonacott, 1988)). If the LDH and GAPDH NAD(H) binding sites come in direct contact, the positive electric field of the GAPDH catalytic domain will directly oppose the negative electric fiied in the LDH catalytic domain (Fig. 4.4 area 1, which are also known as helixes H, 1G, 2G, (Holbrook et al., 1975). In addition to the complementary electric field in the catalytic domain, LDH and GAPDH also share complementary electric fields around the NAD(H) binding sites as previously suggested (Srivastava et al., 1985). Furthermore two NAD(H) sites share considerable hydrophobicity (Fig. 4.5). Finally the NAD(H) modulation of the interaction affinity between the LDH and GAPDH can be explained by NAD(H) control of GAPDH opening as originally suggested during the apo-holo enzyme transition (Skarzynski & Wonacott, 1988).

### 4.3.2 Channeling complex between human βHAD and porcine heart mMDH

Apart from the GAPDH family, the only other B type dehydrogenase with known crystal structure is human mitochondrial βHAD (pdb code 2HDH, resolution 2.2 Å, R=0.198, (Barycki *et al.*, 1999)). NADH channeling with βHAD has only been tested with mitochondrial NADH:ubiquinine Q oxidoreductase (Fukushima et al., 1989; Ushiroyama *et al.*, 1992). There is no crystal structure of the NADH:ubiquinine Q oxidoreductase. However, the crystal structures of numerous other A type dehydrogenases are known. The most physiologically pertinent βHAD partner is pig mitochondrial MDH (pdb code 1MLD, 1.9 Å, R=0.211 (Gleason *et al.*, 1994)). A potential channeling complex between the human mitochondrial βHAD and pig mMDH is shown in Figures 4.7 and 4.8. Similar to phLDH:hGAPDH complex, the βHAD:mMDH complex forms a channeling cavity by juxtaposing the two NAD(H) binding sites (Figures

4.8 and 4.9). The docking interfaces show recognizable surface electric field complementarity (Fig. 4.10), which can guide the docking process. The surface potentials could be too weak to hold a strong complex, but strong enough to put the molecules in the preferential orientation in the dense molecular packing present *in vivo*. In diluted protein solutions *in vitro*, the complementary surface potentials can direct molecules to collide in the preferred orientation or colliding molecules to re-align themselves into the preferred orientations. Once the channeling complex is formed, NAD(H) could be channeled by diffusion within the confines of the channeling cavity. The transfer could be driven by the hydrophobic nature of the vacant binding site. It has been suggested (Srivastava et al., 1985; Visser & van Hoek, 1979) that NAD(H) is "hesitiant' to leave the protein binding site for aqueous medium due to hydrophobicity of the two rings. Our analysis of the enzyme surface in a number of dehydrogenases showed unusual hydrophobicity around NAD(H) binding sites (Fig. 4.6). The A-B type channeling preference could be explained by complementary conformations as suggested in the previous work (Srivastava et al., 1985). It is unfortunate that our enzyme buffering and protein association experiments did not include βHAD and mMDH as the channeling pair. The βHAD crystal structure and the feasibility for this analysis came at the very end of these studies (Barycki et al., 1999).

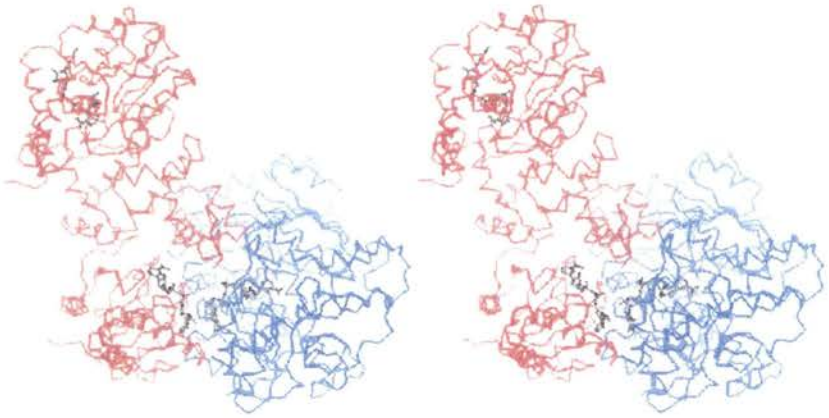

**Figure 4.7 The stereo image of the channeling complex between human βHAD and porcine mMDH.**

The βHDH dimer (2HDH, **(Barycki et al., 1999)**) backbone is shown in red, mMDH dimer (1MLD, **(Gleason et al., 1994)**) backbone is shown in blue and the NAD molecules are shown in black. The two proteins dock orthogonal to their main symmetry axis. The βHAD structure was crystallized as holo enzyme, the mMDH structure was crystallized as apo enzyme. The NAD molecule shown in mMDH structure was taken from the crystal structure of porcine heart cMDH (pdb code 4MDH, (Birktoft *et al.*, 1989)) and "implanted" into mMDH structure after superimposing enzyme backbones. The image was generated using the Insight II program (Biosym, San Diego, CA).

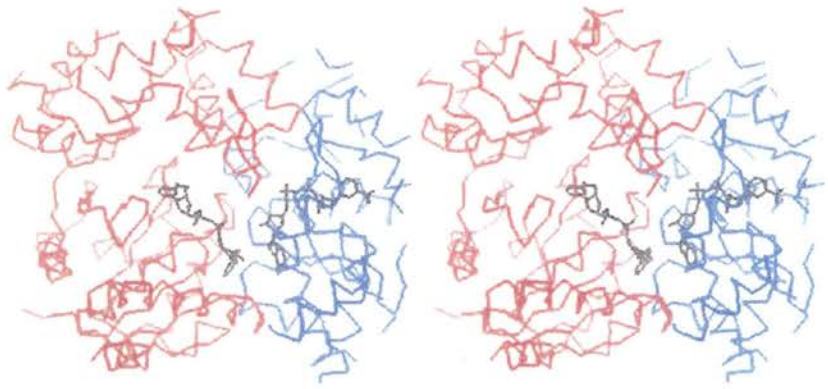

**Figure 4.8 Stereo image of the docking interface between human βHAD and porcine mMDH.**

This is a close up of figure 4.7 created to show the interface between the docking surfaces and the "channeling cavity". The "channeling cavity" is defined as the empty space at the two protein interface enclosed by the two NAD(H) sites. The βHDH (pdb code 2HDH, **(Barycki et al., 1999)**) backbone is shown in red the mMDH (pdb code 1MLD, **(Gleason et al., 1994)**) backbone in blue, and the NAD molecules in black. The βHAD structure was crystallized as the holo enzyme and the mMDH structure as the apo enzyme. The NAD molecule shown in the mMDH structure was taken from the crystal structure of cMDH (pdb code 4MDH, (Birktoft et al., 1989)) and "implanted" into the mMDH structure after superimposing the backbones of two enzymes. The βHAD-mMDH putatative channeling complex is formed by intimate contact between the two proteins. The NAD(H) molecule can be channeled by diffusion within the confines of the channeling cavity. The channeling cavity is partially open to the surrounding aqueous media, however the opening appears too small for NAD(H) escape and leaky channeling. The figure was created using Insight II program (Biosym, San Diego, CA).

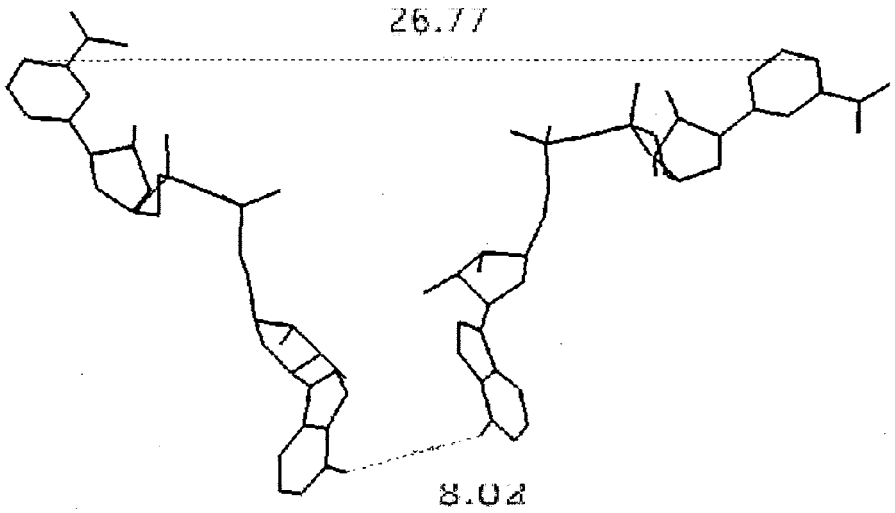


**Figure 4.9 The channeled NAD molecules within the human βHAD porcine mMDH complex.**

The figure is a close up of the figure 4.8, with only channeling NAD molecules shown. The left molecule is NAD bound to the A type dehydrogenase (mMDH) and the right molecule is NAD bound to the B type dehydrogenase (βHAD ). The two are roughly related by a two fold symmetry axis as originally suggested (Srivastava et al., 1985). The dashed lines show distances between the two most distal (nicodinamide C4) and the closer (adenine N6) parts of two NAD molecules. The figure was created using Insight II program (Biosym, San Diego, CA).

**Figure 4.10 (A-B) The electric potential on the mMDH (A) and βHAD (B) docking surfaces.**

The figures show orthogonal views of the docking surfaces of mMDH (A) and βHAD (B). The figures are generated by "cutting" Fig. 4.8 orthogonal to the plane of the paper in the middle of the channeling cavity and then rotating the docking surfaces 90 degrees towards the reader. The NAD molecules are shown in green, the protein atoms are shown as CPK spheres. The red and blue colors represent surface areas with negative and positive potentials, respectively. The color intensities are proportional to the surface potential and span from -2.0 $k_BT/e$ to 2.0 $k_BT/e$, where $k_B$ is Boltzmann constant $k_B$= 1.38 $10^{-23}$ $JK^{-1}$, T is absolute temperature taken to be 298 K, and $e$ is the charge on an electron (1.6 $10^{-19}$ C). The surface potentials are calculated using program GRASP (Honig & Nicholls, 1995). The calculation showed that the docking surfaces are covered with a relatively weak electric field. The numbers indicate interfacing surface parts, e.g. the area marked with 1 on the mMDH surface contacts the area marked with 1 on the βHAD surface. To help in orientation the letter A labels the adenine part of the NAD molecules.

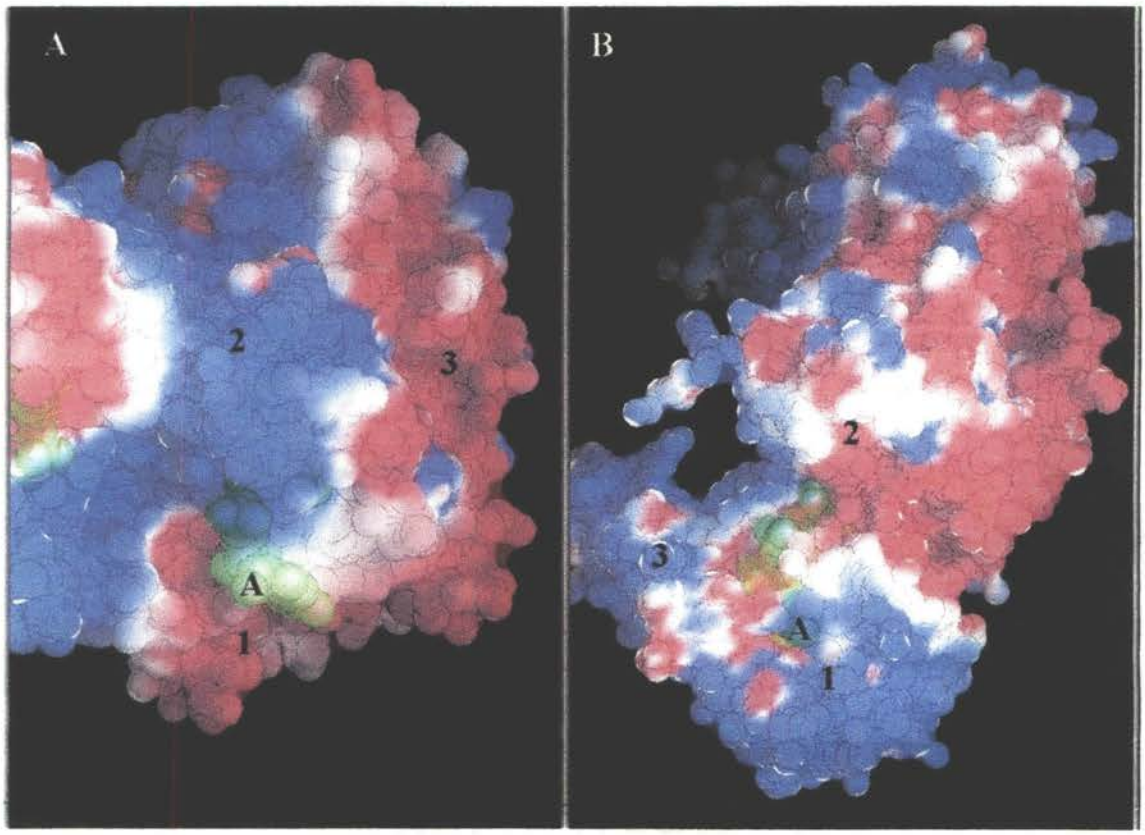
A
2
3
A
1
B
2
3
A
1

## 4.4 Discussion and Conclusions

Using molecular modeling to dock two proteins is a challenging problem at the cutting edge of the molecular modeling science. Sections 4.3.1 and 4.3.2 describe studies aimed at docking two pairs of A and B type dehydrogenases in potential channeling complexes. Each complex was constructed under guidelines (section 4.2) developed in accordance with the experimental observations described in chapters 2 and 3. The three channeling complexes described (two for the phLDH:GAPDH and one for the mMDH:βHAD complexes) represent the closest possible match with the given guidelines. The goal of the molecular modeling studies was to use NAD(H) dehydrogenase molecular structures to better understand the channeling features. Although the proposed models have some weakness, the following conclusions apply:

1. In all three channeling complexes suggested, the two protein NAD(H) binding sites come in direct contact (Spivey & Merz, 1989). NAD(H) is channeled between the two sites by diffusion limited within the confines of the channeling interface. Direct interface of the two NAD(H) binding sites supports the ping-pong channeling mechanism described in chapter 5. If the channeling complex is formed by direct interaction of the active sites, it is possible that after the NADH transfer the Ea active site is buried inside the complex interface and inaccessible to its oxidized substrate. For catalysis to proceed the channeling complex needs to disassemble to permit access of the oxidized substrate to the Ea-NADH complex. This mechanism is a "ping-pong" sequence of substrate and product addition and release steps since the first product, Ed, must be

released before the second substrate (the co-substrate of Ea) adds. As we shall see in chapter 5, this mechanism is critical to explaining the kinetic and equilibrium association properties of the channeling dehydrogenases.

2. No strong driving forces for formation of the channeling complexes can be identified. Instead this complex appears to be a preferred and transient quinary structure rather than a stable complex. The alternative LDH-GAPDH channeling complex suggested, is favored by a strong electric field interaction as described in section 4.3.1. However the favorable energy of the electrostatic interaction may be offset by need for energetically expensive conformational changes.
3. Analyses of NAD(H) dehydrogenases with available apo and holo crystal structures showed only minute structural differences. None of the differences are large enough to significantly disturb proposed channeling complexes. The presented molecular modeling studies did not give explanation for NAD(H) modulation of interaction affinity between channeling components.

The remaining interesting question is whether it is possible to generalize some of the observations from the analysis of the complexes studied in this thesis. The GAPDH family has unusually conserved backbone fold and amino acid sequence among the enzymes from different phylogenic origins, indicating that the structures are highly conserved (Harris & Waters, 1976). Also my analysis of GAPDH from 10 different species showed that all enzymes retain positive electric field at S loop and helix C surface. Similar (although less sharply defined) structure conservation is present in the LDH family (Holbrook et al., 1975). The analysis of the surface electric potentials of LDH

from sources with different phylogenic origins shows conserved negative potential on the surface part of helixes H, 1G, and 2G. Moreover the LDH protein backbone fold is very similar to the MDH backbone fold (Rossman et al., 1975). Four MDH structures I have analyzed contain negative potential on the surface of helixes 1G and 2G, and the β sheet J (Banaszak & Bradshaw, 1975) that are similar to the negative electric field at the surface of LDH helixes H, 1G, 2G. Based on the high degree of the structure conservation it is reasonable to suggest that the general features of phLDH-hGAPDH channeling complex can be found among other LDH-GAPDH pairs or even among MDH-GAPDH pairs.

## 4.5 References


Banaszak, L. J. & Bradshaw, R. A., Eds. (1975). Malate dehydrogenase. 3rd edit. Vol. XI. The Enzymes. Edited by Boyer , P. A. I-XX vols. New York: Academic Press.

Barycki, J. J., LK, O. B., Bratt, J. M., Zhang, R., Sanishvili, R., Strauss, A. W. & Banaszak, L. J. (1999). Biochemical characterization and crystal structure determination of human heart short chain L-3-hydroxyacyl-CoA dehydrogenase provide insights into catalytic mechanism. *Biochemistry* **38**, 5786-98.

Birktoft, J. J., Rhodes, G. & Banaszak, L. J. (1989). Refined crystal structure of cytoplasmic malate dehydrogenase at 2.5-A resolution. *Biochemistry* **28**, 6065-81.

Connolly, M. L. (1983). Solvent-accessible surfaces of proteins and nucleic acids. *Science* **221**, 709-13.

Elcock, A. H. & McCammon, J. A. (1996). Evidence for electrostatic channeling in a fusion protein of malate dehydrogenase and citrate synthase. *Biochemistry* **35**, 12652-8.

Fukushima, T., Decker, R. V., Anderson, W. M. & Spivey, H. O. (1989). Substrate channeling of NADH and binding of dehydrogenases to complex I. *J Biol Chem* **264**, 16483-8.

Gleason, W. B., Fu, Z., Birktoft, J. & Banaszak, L. (1994). Refined crystal structure of mitochondrial malate dehydrogenase from porcine heart and the consensus structure for dicarboxylic acid oxidoreductases. *Biochemistry* **33**, 2078-88.

Grau, U. M., Trommer, W. E. & Rossmann, M. G. (1981). Structure of the active ternary complex of pig heart lactate dehydrogenase with S-lac-NAD at 2.7 A resolution. *J Mol Biol* **151**, 289-307.

Harris, J. I. & Waters, M., Eds. (1976). Glyceraldehyde-3-phosphate dehydrogenase. 3rd edit. Vol. XIII. The Enzymes. Edited by Boyer , P. D. I-XX vols. New York: Academic Press.

Holbrook, J. J., Liljas, S., Steindel, S. J. & Rossman, M. G., Eds. (1975). Lactate Dehydrogenase. 3rd edit. Vol. XI. The Enzymes. Edited by Boyer, P. A. XX vols. New York: Academic Press.

Honig, B. & Nicholls, A. (1995). Classical Electrostatics in Biology and Chemisty. *Science* **268**, 1144-1149.

Kellogg, G. E., Semus, S. F. & Abraham, D. J. (1991). HINT: a new method of empirical hydrophobic field calculation for CoMFA. *J Comput Aided Mol Des* **5**, 545-52.

Leslie, A. G. & Wonacott, A. J. (1984). Structural evidence for ligand-induced sequential conformational changes in glyceraldehyde 3-phosphate dehydrogenase. *J Mol Biol* **178**, 743-72.

Mercer, W. D., Winn, S. I. & Watson, H. C. (1976). Twinning in crystals of human skeletal muscle D-glyceraldehyde-3- phosphate dehydrogenase. *J Mol Biol* **104**, 277-83.

Rossman, M. G., Liljas, A., Branden, C.-I. & Banaszak, L. J. (1975). Evolutionary and Structural Relationships among Dehydrogenase. In *The Enzymes* 3rd edit. (Boyer, P. D., ed.), Vol. XI, pp. 61-102. Academic Press, New York.

Skarzynski, T. & Wonacott, A. J. (1988). Coenzyme-induced conformational changes in glyceraldehyde-3-phosphate dehydrogenase from Bacillus stearothermophilus. *J Mol Biol* **203**, 1097-118.

Spivey, H. O. & Merz, J. M. (1989). Metabolic Compartmentation. *BioEssays* **10**, 127-130.

Srivastava, D. K. & Bernhard, S. A. (1984). Direct transfer of reduced nicotinamide adenine dinucleotide from glyceraldehyde-3-phosphate dehydrogenase to liver alcohol dehydrogenase. *Biochemistry* **23**, 4538-45.

Srivastava, D. K., Bernhard, S. A., Langridge, R. & McClarin, J. A. (1985). Molecular basis for the transfer of nicotinamide adenine dinucleotide among dehydrogenases. *Biochemistry* **24**, 629-35.

Ushiroyama, T., Fukushima, T., Styre, J. D. & Spivey, H. O. (1992). Substrate Channeling of NADH in Mitochondrial Redox Processes. In *From Metabolite, to Metabolism, to Metabolon* (Stadtman, E. R. & Chock, P. B., eds.), Curr. Top. Cell. Regul. **33**, 291-307. Academic Press, New York.

Visser, A. J. & van Hoek, A. (1979). The measurement of subnanosecond fluorescence decay of flavins using time-correlated photon counting and a mode-locked Ar ion laser. *J Biochem Biophys Methods* **1**, 195-208.

# CHAPTER 5 Model Mechanism for Channeling

## 5.1 Review

The preceding three chapters describe analysis of channeling between NAD(H) dependent dehydrogenases by enzyme kinetics, protein association and molecular modeling studies. Chapter 2 presents NADH channeling tests using the enzyme buffering method. The channeling reaction in the enzyme buffering tests shows apo-Ed inhibition, and an apparent maximum for the R value. The channeling can be observed between enzymes with diverse phylogenic origin, as long as the channeling enzyme pair is of opposite chiral specificity (You, 1985). Chapter 3 describes tests of potential interactions between the NAD(H) dehydrogenases. No enzyme associations with Kd < 100 μM were detected with channeling dehydrogenases under conditions (buffer, etc.) of the channeling tests. Interactions were observed only between mammalian LDH and GAPDH and only in the PEG co-precipitation and agarose gel shift experiments. The LDH-GAPDH interaction is modulated by NAD(H), and perhaps by ionic strength. Molecular modeling studies described in chapter 4 used crystal structures of various NAD(H) dehydrogenases to develop potential channeling models at the molecular structure level. The surface electric potentials and hydropathic properties were analyzed for a number of the NAD(H) dehydrogenases. These studies showed that A and B type dehydrogenases share complementary surface potentials around the NAD(H) binding sites. In this chapter the observations from the previous three sections are combined in an attempt to develop a channeling reaction mechanism.

## 5.2 Background and Theoretical Principles

*Background.* Enzyme buffering data on NADH channeling between donor and acceptor dehydrogenases, Ed and Ea, respectively, exhibit saturation kinetics of Ea with respect to the concentration of Ed-NADH. This means that all of Ea is converted to other catalytic enzyme forms and implies a substantial bi-enzyme complex of Ed-NADH-Ea. Yong and co-authors (Yong *et al.*, 1993) did report a provocative study indicating a tight equilibrium association of the LDH-αGDH enzymes at Ed/NADH ratios of about 0.5. However, our experiments on this system (Lehoux, et al. 2000, in preparation) do not support this conclusion. Furthermore, our extensive attempts to experimentally demonstrate an association between Ea and Ed in the absence of the full catalytic reaction (absence of cosubstrate) failed for other NADH channeling enzyme pairs. Therefore, in the absence of the catalytic reaction, it is most likely that there is only weak association of these enzymes in the buffers used for the enzyme buffering tests. This is equivalently, but more succinctly and quantitatively, expressed by stating that the $K_m$ for the first substrate A is in the 2-10 μM range while the dissociation constant is $K_d > 100$ μM

*Theoretical Principles.* It is well known that the "distributions" ($X_i/E_t$) of enzyme forms $X_i$ during the steady-state of the catalytic reaction are different from those in the absence of the reaction. Therefore, it would appear possible to enhance the concentration of an enzyme-substrate complex in the reaction steady-state relative to that in the absence of the catalytic reaction. The concentration of the E-S complex of the simplest (single substrate) Michaelis-Menten model, however, is actually less than that at equilibrium due to the additional rate of dissociation that exists in the reaction. One can get an enhancement of enzyme-substrate complexes by inserting enzyme forms having

fast kinetic steps of formation followed by slower rates of dissociation. Quite surprisingly, however, such kinetic steps can only increase concentrations of enzyme-substrate forms modestly (e.g., five-fold) if one considers only single substrate mechanisms or ordered two substrate mechanisms with kinetic constants similar to the putative NADH channeling systems. This was demonstrated by (Keizer & Smolen, 1992) for the case of NADH channeling and is consistent with our early attempts with numerical simulations using ordered mechanisms. However, we show that this need not be the case with a ping-pong mechanism. In the absence of Ed-NADH, most of dehydrogenases follow an ordered mechanism with NADH adding first. Therefore, for NADH channeling it is likely that Ed must dissociate from the Ed-NADH-Ea complex before addition of the cosubstrate. Hence, for the channeled path, a ping-pong mechanism as shown in Figure 5.1 is more reasonable than an ordered one. Ea is released as the first product before addition of the cosubstrate. The velocity equation is first derived in the form of $v = (V_m AB+\ldots)/Den$, where Den is the denominator. But we will find it more convenient to divide numerator and denominator by AB giving the Model equation in the form,

$$v^x = \frac{V_+^{ch} + V_+^f \frac{K_a^{ch}}{K_c^f}\frac{C}{A}}{Den} \tag{5.1}$$

where

$$\begin{aligned} Den = 1 &+ \frac{K_a^{ch}}{A} + K_1\left(\frac{K_{ic}^f}{K_{ia2}^x} + \frac{K_{d1C}}{K_{ip1}^x}\right)\frac{1}{B} + K_1 K_{ic}^f \frac{1}{AB} + \frac{K_a^{ch}}{K_c^f}\frac{C}{A} + K_1\frac{C}{AB} + \frac{K_a^{ch}}{K_{ip2}^{ch}}\frac{P}{A} \\ &+ \frac{K_1 K_{ic}^f}{K_{ia2}^x K_{ip2}^x}\frac{P}{B} + \frac{K_1 K_{ic3}^x}{K_{ip1}^x}\frac{P}{AB} + \frac{K_1 K_{ic3}^x}{K_{ip1}^x K_{ip4}^{ch}}\frac{P^2}{AB} \\ &= \sum_{i=1}^{10} T_i \end{aligned} \tag{5.2}$$

**Figure 5.1. Schematic presentation of ping-pong channeling mechanism in enzyme buffering tests.**

The scheme shows free (internal rectangle) and the channeled reaction (outer pentagon) in the ping-pong channeling mechanism. For simplicity each of the catalytic cycle species was assigned single letter; **E** is Ea, **A** is Ed-NADH, **P** is Ed, **B** is the oxidized substrate for Ea, **C** is free NADH, **Q** is reduced B, **R** is NAD. In this channeling reaction Ea (E) interacts with Ed-NADH (A) to form the ternary channeling complex Ea-NADH-Ed (EA), from which Ed dissociates after the NADH transfer to give Ea-NADH. In the free reaction the Ea-NADH complex is formed by direct interaction between Ea and NADH. Once Ea-NADH is formed, the channeled and classical reactions are identical. The scheme shows that apo-Ed (P) can act as inhibitor in two ways. Apo-Ed acts as a product inhibitor interacting with Ea-NADH and pushing the catalytic cycle "backwards" to form Ea-NADH-Ed complex. Apo-Ed can also inhibit Ea by forming a dead-end Ea-Ed complex (#6). Each enzyme form in the figure is assigned a number. The numbers are used to assign the rate constants, e.g, $k_{ij}$ indicates the rate constant for conversion of species $i$ to species $j$. The square with EAB and ERQ represents the substrate reduction step in the central complex.

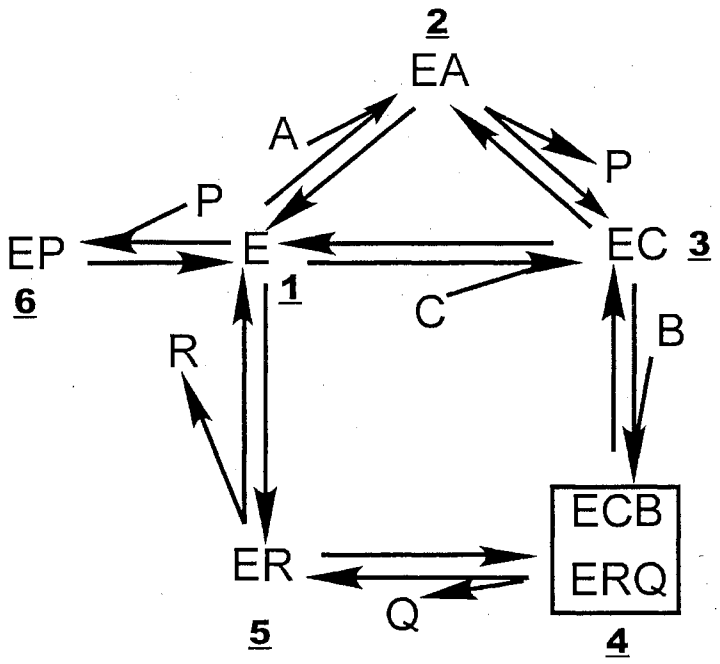
2
EA
A
P
P
EP
6
E
1
EC
3
C
B
R
ECB
ERQ
ER
5
Q
4

The substrate A is Ed-NADH, C is free NADH, B is oxidized cosubstrate, P is Ed, Q is reduced-product, R is NAD, and $K_1 \equiv K_a^{ch} K_b^f / K_c^f$ for convenience. The kinetic constants are defined in terms of rate constants in Appendix 1. The second coefficient of the 1/B term ($T_3$ of Den) comes from a PC/(AB) term in the original form of the equation. Since $PC/A = K_{d1C}$, the dissociation constant of Ed-C (C = NADH), this term becomes a function of 1/B and is combined with this coefficient in equation 5.2. The two numerator terms of equation (5.1) represent the channeled and classical ("free") reactions, respectively. Therefore the fraction of the reaction that is channeled is

$$f_{ch} = \frac{V_+^{ch}}{V_+^f} \frac{K_c^f}{K_a^{ch}} \frac{A}{C} \tag{5.3}$$

The matrices for the distribution of enzyme forms in terms of rate constants were obtained by a computer program (Fisher & Schulz, 1969; Fisher & Schulz, 1970). Transformation to enzyme kinetic constants and reformulation of denominator coefficients were derived manually as described in (Schulz, 1994). The steady-state equations for the purely channeling portion and the purely free NADH path were also derived. Wherever possible, kinetic constants of the combined model (superscript x) are expressed in terms of the simpler kinetic constants of these two component parts (superscripts ch and f for channeled and free NADH paths, respectively). This allows one to make maximal use of the known experimental constants of the classical (free NADH) path, and for many considerations to consider the simpler equations of the purely channeling path. The latter is justified in many cases since the majority of the flux goes by the channeled path in enzyme buffering experiments as demonstrated below. Implicit in the model of Figure 5.1 are additional rate constants for conformational transitions that do not affect the form of the steady-state velocity equation. Thus it is standard practice to

omit these unimolecular transitions and corresponding rate constants in the steady-state mechanism. Ignoring this fact would impose constraints of equality for the ratios k21/k12 and k23/k32 in terms of the dissociation constants of Ed-Ea and Ed-NADH-Ea that are unrealistic and would prevent fitting the model to data with the high dissociation constants that are experimentally found.

The weighted, nonlinear least-squares program used (Chandler, 1988) utilizes a Marquardt minimizer with problem dependent main and subroutine programs written in our lab to include the calculation of the fractional contribution of each term in the model equation to the velocities at each experimental point as well as various other parameters derived from the best-fit parameters. The model equation was also programmed in Microsoft® Excel to facilitate analysis of the model and the contribution of constituent terms and extrapolation of data beyond those currently available.

## 5.3 Results and Discussion

### 5.3.1 Full Model of Fig. 5.1 and Eqns 5.1 and 5.2

The data of Srivastava and Bernhard (Srivastava & Bernhard, 1985) on the LDH-αGDH system are used as a test of the model. Their halibut muscle LDH enzyme prepration of this study as Ed had a very low dissociation constant for Ed-NADH that gave a large channeling criterion and there is substantial inhibition by excess Ed. These features should provide a very good test of the channeling model. In addition, it is the dataset analyzed in previous papers using a simpler, single substrate model (Svedruzic & Spivey, in preparation). This simpler model gives a good fit, but only at the expense of a low dissociation constant (DKDEI) of the dead-end inhibitor, Ed-Ea, in contradiction with the experimental evidence against such an association.

The model of Figure 5.1 has five adjustable parameters: k12, k21, k23, k32, and DKDEI = k61/k16, the dissociation constant of the dead-end inhibitor complex. The lack of detectable equilibrium association of Ed and Ea regardless of [NADH] adds constraints of inequality since the dissociation constants DK21 = k12/k21, DK23 = k23/k32, and DKDEI must be $\geq$ 100 μM. Rate constants beyond these five are fixed by the known kinetic constants for the enzyme Ea by itself and exact thermodynamic constraints, e.g, k13 = $k^f_{cat}K^f_c$ where the superscript f refers to constants of the free NADH path. There are more model parameters than can be resolved with this dataset. However, by fixing several of the parameters, allowing only a few to vary at one time, we find a range of constants that fit the data very well. This demonstrates that the model can represent substrate channeling with a low $K_m$ for the NADH-bound substrate A, high $K_d$'s for EA and Ed-Ea, and the inhibition by excess Ed.

This model also allows us to calculate the fraction of flux $f_{ch}$ going by the channeling path under any set of conditions specified by means of Eqn (5.3). Best-fit values of the parameters, statistics of the fit and $f_{ch}$ are summarized in Table 5.1. The majority of the reaction flux goes by the channeling path when most of the NADH is bound – the condition of well designed enzyme buffering tests. This dominance of the channeled path remains over a large range of kinetic constants and is even independent of the assumed reaction mechanism since we observed the same thing with a single substrate model (Spivey and Svedruzic, in preparation). The channeled path dominates because $[NADH_b] >> [NADH_f]$, and $[NADH_b] > K_a^b$ where subscripts b and f of NADH denote enzyme bound and free NADH, respectively and $K_a^b$ is the $K_m$ for Ed-NADH. These conditions give nearly maximum rate of reaction rate of reaction through the channeled path. It is interesting to note that $V_+^{ch} \cong V_+^f$ for this mechanism. This illustrates that the previous graphical estimates of $V_+^{ch}$ (Srivastava & Bernhard, 1985) underestimate its value.

NADH channeling is more complex than model in the figure 5.1. For example, dehydrogenases are homo- tetramers and dimers whose extent of saturation with NADH varies with each concentration of $Ed_t$ (with the constant $E_t/NADH_t$ method). Thus there are micro- species of Ea and hence Ea-Ed complexes with different amounts of NADH bound that are not represented in the Figure 5.1. It does not appear practical to include these complexities in the model. Consequently the best-fit constants can only be considered an approximation of the kinetic and association constants of the channeling enzymes. Nevertheless, the model shown in figure 5.1 does demonstrate that very

**Table 5.1. Results of model fit to data on LDH and αGDH**

Data of Srivastava and Bernhard (1985) with halibut muscle LDH as Ed and rabbit muscle αGDH as Ea are analyzed by Eqns 5.1 and 5.2. $v_{ch}/v_t$ is the fraction of total velocity channeled; $\sigma_i = 0.10\ v_{exp,i}$,the assumed standard deviation of the i-th data point, and $r_i/\sigma_i$ = residual$_i/\sigma_i$ where $r_i = v_{exp} - v_{fit}$, and $R = v_{fit}/v_{cl}^f$. Constants in square brackets were fixed during this fit. DKDEI = k61/k16, the dissociation constant of the dead-end inhibitor. Additional constants are those from the reference, e.g., dissociation constants of E1-NADH and E2-NADH = 0.21 and 0.88 μM, respectively. The above constants give DK21 = 480 μM, DK23 = 330 μM, $K_a^{ch} = 4.8\,\mu M$, $V_{\cdot}^{ch} \cong V^f = 119$ U/mg where DK-ij are dissociation constants of enzyme form i to j. Thus all of the dissociation constants are above our current detectable limits.

| $[E1_t]$ μM | $[NADH_t]$ μM | $[NADH_f]$ μM | $v_{fit}$ $U/mg_t$ | $v_{ch}/v_t$ | $\sigma_1$ U/mg | $r_i/\sigma_1$ | R |
|---|---|---|---|---|---|---|---|
| 3.54 | 1.75 | 0.17 | 26.8 | 0.85 | 3.1 | 1.30 | 3.0 |
| 5.13 | 2.54 | 0.18 | 32.6 | 0.89 | 3.2 | -0.046 | 3.7 |
| 6.66 | 3.30 | 0.18 | 36.8 | 0.91 | 3.7 | 0.10 | 4.1 |
| 8.11 | 4.02 | 0.19 | 39.9 | 0.92 | 3.8 | -0.55 | 4.4 |
| 9.79 | 4.84 | 0.19 | 42.6 | 0.94 | 4.1 | -0.32 | 4.8 |
| 42.0 | 32.6 | 0.67 | 73.8 | 0.97 | 6.3 | -1.7 | 2.4 |
| 57.0 | 32.6 | 0.28 | 62.6 | 0.990 | 5.8 | -0.77 | 5.1 |
| 85.0 | 32.6 | 0.13 | 45.7 | 0.993 | 4.0 | -1.4 | 8.0 |
| 113. | 32.6 | 0.085 | 33.8 | 0.996 | 3.6 | 0.51 | 9.0 |
| 141. | 32.6 | 0.063 | 25.6 | 0.997 | 3.0 | 1.4 | 9.2 |

Best-fit and fixed constants#.

| $10^{-6}k12$, $M^{-1}s^{-1}$ | k21, $s^{-1}$ | k23, $s^{-1}$ | $10^{-6}k32$, $M^{-1}s^{-1}$ | DKDEI |
|---|---|---|---|---|
| 21 ± 3 | [10,000] | [50,000] | 150 ± 30 | [100] |

Statistics of fit (Chandler, 1972):

Chis-square, $X^2 = 9.6$; Expected $X^2 = 8 \pm 4$ with 8 degrees of freedom; Maximum variance inflation factor = 3.8; parameter correlation coefficient, $\rho 14 = 0.86$; Signs confidence level = 0.754, and Runs confidence level = 0.405.

reasonable kinetic models can account for NADH channeling in spite of undetectable equilibrium associations between the enzymes.

### 5.3.2 Simpler Models with Low Km and High Kd

It is important to elucidate the necessary and/or sufficient conditions for the kinetic properties of model in figure 5.1 to be expressed. For this purpose, we utilize the simplest bi-bi ping-pong mechanism, first without the dead-end complex E-P and then with it. The scheme is shown in Figure 5.2 for the latter. Consider first the simplest case where the dead-end complex EP is absent, B is saturating, and P is not present. Then the $K_a$ is also the apparent-$K_a$ (app-$K_a$) and is given by equation (5.4) (Cornish-Bowden, 1995).

$$K_a = \frac{k41(k21 + k23)}{k12(k23 + k41)} = \frac{k41(K_d + k23/k12)}{(k23 + k41)} \qquad (5.4)$$

where $K_d$ = k21/k12 is the dissociation constant for EA. Therefore, the necessary conditions for $K_a << K_d$ are k23 >> than both k21 and k41. These are rather special conditions that might not be expected without evolutionary adaptation of the enzyme. Under these conditions, $K_a \approx$ k41/k12 which we desire to keep in the range of 2- 10 μM. This latter condition is easily achieved by normal rate constants. Simulations of Eqn. 5.4 show that a $K_a$ of 2.4 μM is achieved with a $K_d$ = 100, k12 = $25x10^6$ $M^{-1}s^{-1}$, k21 = 10,000 $s^{-1}$, k23 = 50,000 $s^{-1}$, and $k_{cat}$ = 75 $s^{-1}$, constants identical to those found for Eqns. 5.1 and 5.2 fitted to the NADH channeling data (Table 5.1). It is noteworthy that k23 is only 5–times larger than k21, i.e., the condition of k23 >> k21 is not as stringent as might be expected without numerical simulation. Again virtually any value of $K_d$ for E-A can be accommodated with a $K_m$ for A of about 5 μM. The reason is that for any increase in the dissociation rate constant k21 of E-A, a comparable increase in the forward rate constant k23 can capture the substrate A with equal ability. In other words, any reactant A can be

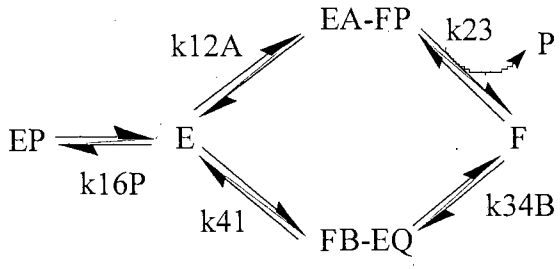


**Figure 5.2. Ping-pong mechanisms used to reveal conditions needed to give low $K_a$ with high $K_d$.**

captured by reactant B and converted to product if this rate of conversion is faster than the rate of back dissociation A-B. This simple mechanism provides the low $K_a$ found with many enzymes with protein substrates (Rudolph & Stubbe, 1995), but it doesn't consider two other features of the enzyme buffering data. These are the necessary presence of P (free Ed) in all data and the less than saturating concentrations of the cosubstrate B. For example, the αGDH enzyme has a $K_b$ of about 150 μM and enzyme buffering measurements were made with 500 μM B. Adding these features to the ping-pong mechanism of Figure 5.2, however, did not significantly decrease its ability to give low $K_a$'s with high $K_d$'s. This is consistent with the fact that model 2 can fit the NADH channeling data, even accommodating the possible dead-end inhibition from Ed-Ea. A sequential ordered, two substrate mechanism, however, is much more limited. With non-saturating [B], its apparent $K_m$ for the A substrate is given by

$$\text{app-}K_a = \frac{K_{ia}K_b + K_aB}{K_b + B} \tag{5.5}$$

where $K_{ia}$ = the dissociation constant of E-A and B is the concentration of the second substrate. With high dissociation constant $K_d = K_{ia}$ and the usual $K_b$ values, the first term in the numerator dominates and keeps app-$K_a$ from being much lower than $K_d$. For example with the best-fit values of the data from Table 1 assuming the minimum $K_d$ of 100 μM, the app-$K_a$ (27 μM) is only 3.8-fold lower than the $K_d$. It would require very much higher [B] values to improve this situation significantly. Such high concentrations often cause substrate inhibition. With higher $K_d$ values, it would be still more difficult to achieve a low app-$K_a$. Equation (5.5) also demonstrates that when $K_{ia}$ and $K_b$ are large as with these dehydrogenase systems, the usual rule of thumb for "saturating" concentrations of B, namely $[B]/K_b \approx 10$ is very inadequate. With the constants just used, it would require a [B] = 40 mM, i.e., 80-fold larger than $K_b$ to give an app-$K_a$ within 90%

of $K_a$. The ping-pong mechanism is not so limited as we have seen. Another advantage of the ping-pong mechanism is the substrate B is competitive with respect to the product P. Thus product inhibition is significantly less in the ping-pong mechanism than expected for an ordered one.

### 5.3.3 Similar Enzyme Reactions with Low Km and High Kd

Substrate channeling requires at least a transient Ed-Ea interchanging the common substrate. Well known channeling complexes like pyruvate dehydrogenase, fatty acid synthease and α-ketoglutarate dehydrogenase involve stable complexes. Many of the analysis in the past presumed that for the channeling to take place a considerable equilibrium association has to be present between the NADH dehydrogenases (Brooks & Storey, 1991; Keizer & Smolen, 1992; Wu *et al.*, 1992). It is not widely known that several enzyme reactions other than NADH channeling occur with low Km for the first substrate yet no association of the enzyme and substrate can be detected in the absence of the catalytic reaction. For example, effective channeling of phosphoribosylamine between glutamine phosphoribosylpyrophosphate amidotransferase and glycinamide ribonucleotide synthetase has been reported (Rudolph & Stubbe, 1995). However the same study indicates no detectable equilibrium interaction between the channeling enzyme pair. The authors explained their results by suggesting channeling with a short lived transient complex, but offered no specific mechanism. The next three examples are of enzymes with protein substrates as reviewed by Rudolph and Stubbe (Rudolph & Stubbe, 1995) where specific references may be found. There can be no doubt about these associations during catalysis since they involve efficient electron transfer or redox reactions between tightly bound $FADH_2$ or Cys. Yet no enzyme-substrate complexes are

detectable in the absence of the catalytic reaction. The first of these examples is cytochrome c and cytochrome c peroxidase. The enzymes can channel electrons with greater than 99% efficiency, yet no detectable interaction is observed between the proteins. Interestingly the two protein interaction can be observed at low ionic strength, but not at higher more physiological ionic strength where electron transfer rates are actually faster. Thus there can be no doubt about the adequacy of the methods for detecting enzyme-substrate complexes. Also *E. coli* ribonucleotide reductase and thioredoxin do not form detectable complex, yet strong kinetic evidence indicates that the two proteins functionally interact. The third example is p-aminobenzoate synthase complex (PABA). Kinetic measurements show evidence of interaction between phosphoribosylamine amidotransferase and glycinamide ribonucleotide synthetase in concentration as low as 10 nM. However protein association experiments gave no evidence of interaction when components were present in micromolar levels.

At this time it is not known whether short lived transient complexes proposed by us and others are specific feature of a dynamic biological processes present *in vivo*, or an artifact produced by the *in vitro* experimental conditions. Protein association studies *in vitro* are usually performed in dilute protein solutions. These conditions are far different from the conditions *in vivo* where channeling has evolved. Multiple experimental and theoretical examples showed that the high molecular crowding present *in vivo* enhances molecular interaction relative to the standard *in vitro* experiments (Zimmermann & Minton, 1993). The mitochondrial MDH and citrate synthase is good example of such situation. Citrate synthase and mMDH show no detectable interaction in the equilibrium association studies (Srere *et al.*, 1978). However specific interaction can be observed in

the presence of PEG (Halper & Srere, 1977; Merz *et al.*, 1987), or agarose gel (Ashmarina *et al.*, 1994). Both the aqueous solution of PEG and the agarose gel matrix are believed to mimic some of the properties characteristic for the molecular crowding effects present *in vivo* (Zimmermann & Minton, 1993). The channeling observed within the PEG induced complex of citrate synthase and mMDH proves the complex functional integrity (Datta *et al.*, 1985). Channeling was also observed within citrate synthase and mMDH fusion protein (Lindbladh *et al.*, 1994). The channeling mechanism has been suggested using molecular modeling studies (Elcock *et al.*, 1997).

However, although associations may be more extensive in vivo, analysis of the model of Figure 5.1 demonstrates that kinetic capture can occur with low Km values in the absence of strong interactions.

### 5.3.4 Limiting Form of the Channeling Criterion R of the Enzyme Buffering Test

We limit our consideration to the enzyme buffering method that uses constant $[NADH]_t$ and varying [Ed] since this method gives larger R values as verified by both experiments and the model equations. Table 2.1 (chapter 2) showed that for a number of dehydrogenase pairs R values are very close to 1. Figures 2.4, 2.5 and 2.6 showed that increasing the concentration of apo-Ed, which decreases $[NADH]_f$, causes R to approach a maximum value. Reasons for such a maximum are not immediately obvious. R is defined as the ratio of $v_{exp}$ and $v_{cal}$. Since $v_{cal}$ is proportional to the $[NADH]_f$ and $[NADH]_f \rightarrow 0$ with inreasing [apo-Ed], $v_{cal}$ might be expected to go to zero and hence R increase without limit. This would be desirable since it would greatly increase the power of the enzyme buffering method for testing NADH channeling. However, experiments

(chapter 2) have shown that R appears to reach a maximum with respect to increasing [apo-Ed]. This limiting value of R results from the inhibition of $v_{exp}$ by apo-Ed. This behavior is predicted by the mechanism of equation 5.1. This limiting form of R as $[NADH]_f \rightarrow 0$ becomes (App. A2)

$$R \rightarrow \frac{V_+^{ch}}{V_+^f}\frac{K_c^f}{K_{d1c}}\frac{1}{[(LC_1/P) + LC_2 + LC_3 * P]} \quad \text{where}$$

$$LC_1 = A + CT_2 + CT_3 * A/B + CT_4/B \qquad (5.6)$$

$$LC_2 = CT_7 + CT_8 * A/B + CT_9/B$$

$$LC_3 = CT_{10}/B$$

The limiting coefficients $LC_i$ are defined in terms of the coefficients $CT_i$ of the denominator terms $T_i$ of equation (5.2). A (=[Ed-NADH]) and B (= [cosubstrate]) are constant within experimental error in this method. P (=[apo-Ed]) is, therefore, the only variable in equations (5.6). Starting with a low ratio of $Ed_t/NADH_t$, e.g. 2, the $LC_1$ term of the equations (5.6) dominates keeping R low. As P increases, the $LC_2$ and then $LC_3$ terms become dominant. The $LC_3$ term exists only if there is significant dead-end inhibitor complex, Ed-Ea. In the absence of the $LC_3$ term, R would increase to an asymptotic limit value. However, with a significant dead-end inhibitor complex, R would reach a maximum and subsequently decrease with increasing P. We don't see such a decrease in R so it is tempting to discount formation of the dead-end inhibitor. However, computer simulations of equation (5.6) using best-fit parameters indicate that the LC3 is quite significant and keeps R from reaching as high a value as it would otherwise.

Computer simulations of equation (5.2) show that with commonly encountered values of these constants, R is equal to 1 within experimental error yet the fraction

channeled is > 95% (Svedruzic & Spivey, in preparation). Thus, the most important conclusion from equation (5.6) is that R is limited to a maximum value by ratios of kinetic and equilibrium constants that are unrelated to the magnitude of NADH channeling. In summary, when the kinetic and equilibrium constants are favorable, the enzyme buffering method allows a very rigorous test by means of the R criterion. However, often these constants are not favorable in which cases the enzyme buffering method becomes insensitive to channeling.

## 5.4 Conclusions

The previous sections of this chapter have analyzed the properties of the ping-pong channeling mechanism. The mechanism is consistent with the kinetic data as well as the lack of enzyme association in the absence of the catalytic reaction. That is, the mechanism is compatible with a low Km for the substrate Ed-NADH in spite of very much higher equilibrium dissociation constant for this Ed-NADH. The mechanism also provides some new insights into the enzyme buffering experiments. For example, the analysis shows how to optimize the enzyme buffering experiments to obtain the maximum R possible. This R value is shown to depend on the ratio of kinetic and equilibrium constants that constrain R to values independent of the fraction of the reaction that is channeled. This fact limits the usefulness of the enzyme buffering test in many cases where these constants are not favorable to permit an R value significantly larger than 1.

The proposed ping-pong mechanism can be used in the future to analyze experiments with other enzymes that behave similarly with respect to having low Km in spite of high Kd values (Rudolph & Stubbe, 1995).

## 5.5 APPENDICES: Derivation of Equations in Chapter 5.

A.1. Steady State Equation for the Ping-pong Channeling Mechanism in the Enzyme Buffering Tests

For simplicity and compatibility with the FORTRAN program, most of the following kinetic constants are written without the super- and subscripting shown in equation (5.2), but should be easily identified.

$$VMX = VMCH = \frac{k23k45k51\,Et}{k23(k45+k51)+k45k51} = \frac{k23k^{f}_{cat}\,Et}{k23+k^{f}_{cat}}$$

$$Kax = \frac{CfB}{CfAB} = \frac{k45k51(k21+k23)}{k12(k23k45+k23k51+k45k51)} = \frac{k^{f}_{cat}(k21+k23)}{k12(k23+k^{f}_{cat})} = Kach$$

$$Kia2x = \frac{Cnst}{CfA} = \frac{k31(k23+k21)}{k12(k23+k31)}$$

$$Kib1x = \frac{CfC}{CfBC} = \frac{k51(k43+k45)}{k34(k45+k51)} = Kbf$$

$$Kic1x = \frac{CfB}{CfBC} = \frac{k45k51}{k13(k45+k51)} = Kcf$$

$$K^{x}_{ic2} = \frac{Cnst}{CfC} = \frac{CfQ}{CfCQ} = \frac{k31}{k13} = Kicf$$

Kic3x =

$$\frac{CfP}{CfCP} = \frac{k21k32k61+k16k31(k21+k23)}{k13k32k61} = \frac{k21k32*DKDEI*+k31(k21+k23)}{k13k32*DKDEI};$$

where DKDEI (dissociation constant for dead-end inhibitor complex, Ed-Ea) is k61/k16.

$$Kip1x = \frac{CfC}{CfCP} = \frac{CfCQ}{CfCPQ} = \frac{k21+k23}{k32}$$

$$Kip2x = \frac{CfA}{CfAP} = \frac{CfAQ}{CfAPQ} = \frac{(k23+k31)}{k32}$$

$$Kip3x = \frac{CfB}{CfBP} = \frac{k61}{k16} \equiv DKDEI = Kip2ch$$

$$Kip4x = \frac{CfP}{CfPP} = \frac{k21k32k61 + k16k31(k21 + k23)}{k16k21k32} = \frac{k21k32 * DKDEI + k31(k21 + k23)}{k21k32}$$
$$= K^x_{ic3} k13 * DKDEI/k21$$

See note under Kic3x.

$$k^f_{cat} = \frac{k45k51}{k45 + k51}; \quad V^f_x = k^f_{cat} Et$$

$k13 = \frac{V^f_m}{K^f_c Et}$ from the definition of $Kc^f$.

## Reformulation: Coefficients to Kinetic Constants

NOTE: These terms are defined with coefficients of the v equation in the form: v = V*AB/Den, in contrast to the terms of equation (5.2). Therefore, divide the following terms by AB to obtain the terms of equation (5.2). In the following, "CfAB," etc., represent the coefficient of the AB or corresponding term in the velocity equation. Ti are the 10 terms of the denominator of equation (5.2) after multiplying the latter by AB.

$$T1 \equiv \frac{CfAB}{CfAB} AB = AB$$

$$T2 \equiv \frac{CfB}{CfAB} B = K^{ch}_a B$$

$$T3 \equiv \frac{CfA}{Cnst}\frac{Cnst}{CfC}\frac{CfC}{CfBC}\frac{CfBC}{CfB}\frac{CfB}{CfAB} A = \frac{1}{K^x_{ia2}} K^f_{ic} K^f_b \frac{1}{K^f_c} K^{ch}_a A = \frac{K_1 K^f_{ic}}{K^x_{ia2}} A$$

$$T4 \equiv \frac{Cnst}{CfC}\frac{CfC}{CfBC}\frac{CfBC}{CfB}\frac{CfB}{CfAB} = K^f_{ic} K^f_b \frac{1}{K^f_c} K^{ch}_a = K_1 K^f_{ic}, \text{ where } K_1 \equiv \frac{K^{ch}_a K^f_b}{K^f_c}$$

$$T5 \equiv \frac{CfBC}{CfB}\frac{CfB}{CfAB} BC = \frac{1}{K^f_c} K^{ch}_a BC$$

$$T6 \equiv \frac{CfC}{CfBC}\frac{CfBC}{CfB}\frac{CfB}{CfAB} C = K^f_b \frac{1}{K^f_c} K^{ch}_a C = K_1 C$$

$$T7 \equiv \frac{CfBP}{CfB}\frac{CfB}{CfAB}BP = \frac{1}{K_{ip2}^{ch}}K_a^{ch}\,BP$$

$$T8 \equiv \frac{CfAP}{CfA}\frac{CfA}{Cnst}\frac{Cnst}{CfC}\frac{CfC}{CfBC}\frac{CfBC}{CfB}\frac{CfB}{CfAB}AP = \frac{1}{K_{ip2}^{x}}\frac{1}{K_{ia2}^{x}}K_{ic}^{f}K_b^{f}\frac{1}{K_c^{f}}K_a^{ch}\,AP = \frac{K_1K_{ic}^{f}}{K_{ip2}^{x}K_{ia2}^{x}}AP$$

$$T9 \equiv \frac{CfP}{CfCP}\frac{CfCP}{CfC}\frac{CfC}{CfBC}\frac{CfBC}{CfB}\frac{CfB}{CfAB}P = K_{ic3}^{x}\frac{1}{K_{ip1}^{x}}K_b^{f}\frac{1}{K_c^{f}}K_a^{ch}\,P = \frac{K_1K_{ic3}^{x}}{K_{ip1}^{x}}P$$

$$T9' \equiv \frac{CfCP}{CfC}\frac{CfC}{CfBC}\frac{CfBC}{CfB}\frac{CfB}{CfAB}CP = \frac{1}{K_{ip1}^{x}}K_b^{f}\frac{1}{K_c^{f}}K_a^{ch}\,CP = \frac{K_1}{K_{ip1}^{x}}CP = \frac{K_1K_{d1C}}{K_{ip1}^{x}}A \text{ where}$$

$K_{d1C}$ is dissociation constant of Ed-C (Ed-NADH). Thus T9' is combined with T3 in velocity equation.

$$T10 \equiv$$

$$\frac{CfPP}{CfP}\frac{CfP}{CfCP}\frac{CfCP}{CfC}\frac{CfC}{CfBC}\frac{CfBC}{CfB}\frac{CfB}{CfAB}P^2 = \frac{1}{K_{ip4}^{x}}K_{ic3}^{x}\frac{1}{K_{ip1}^{x}}K_b^{f}\frac{1}{K_c^{f}}K_a^{ch}P^2 = \frac{K_1K_{ic3}^{x}}{K_{ip1}^{x}K_{ip4}^{x}}P^2$$

## A.2. Asymptotic Maximum for R in the Enzyme Buffering Tests

Enzyme buffering tests are analyzed with the channeling criterion

$$R \equiv \frac{v_{exp}}{v_o^{f}} \qquad (A5.1)$$

for $[Ed]_t$ in excess of $[NADH]_t$.

As [Edt] is further increased at constant $[NADH]_t$, all concentration terms in the v equation remain essentially constant except for C (= $[NADH]_f$), which continually decreases. Thus the terms in the model equation containing C become negligible relative to the other terms. Computer simulations using best-fit constants demonstrate that these terms containing C (T5 & T6) do indeed become negligible quickly. Thus, for

calculating limiting forms of R, we ignore the terms containing C. In the following derivation, it is convenient to use the following form of the model equation

$$v = \frac{V_+^{ch} + k_{13}[E2_t]K_a^{ch}C/A}{Den} \tag{A5.2}$$

to calculate the $v_{exp}$. Thus, since the 2nd term in the numerator is negligible relative to the first term, all substrate and product P terms are in the denominator Den. In this form we designate

$$\begin{aligned} Den = \sum_{i=1}^{10} T_i = 1 + CT2\frac{1}{A} + CT3\frac{1}{B} + CT4\frac{1}{AB} + CT5\frac{C}{A} + CT6\frac{C}{AB} \\ + CT7\frac{P}{A} + CT8\frac{P}{B} + CT9\frac{P}{AB} + CT10\frac{P^2}{AB} \end{aligned} \tag{A5.3}$$

The identity of all coefficient terms $CT_i$ are specified in equation (5.2). Thus for the limiting form of R we use equation (A5.3) without the terms T5 and T6 to calculate $v_{exp}$ of equation (A5.1). For the denominator of equation (A5.1), $v^f_o$, we use

$$v_o^f = \frac{V_+^f}{Den^f} \tag{A5.4}$$

where

$$Den^f = 1 + \frac{K_c^f}{C} \rightarrow \frac{K_c^f}{C} \quad \text{as C goes 0} \tag{A5.5}$$

The B terms are implicit in the definition of $V_+^f$ since $V_+^f$ is the apparent V for the concentration of B used. Thus the liminting form of R becomes

$$R \rightarrow \frac{V_+^{ch}}{V_+^f}\frac{Den^f}{Den^b} = \frac{V_+^{ch}}{V_+^f}\frac{K_c^f}{C}\frac{1}{Den^b} \tag{A5.6}$$

However, not all of the concentrations in equation (A5.6) are independent since PC/A = $K_{d1c}$ (dissociation constant of Ed-NADH). Therefore, extracting P/A from $Den^b$ and

combining it with C gives the constant $K_{dlc}$. This transforms equation (A5.6) into equation (5.6) of the text, reproduced as

$$R \rightarrow \frac{V_+^{ch}}{V_+^f} \frac{K_c^f}{K_{dlc}} \frac{1}{[(LC_1/P) + LC_2 + LC_3 * P]} \quad \text{where}$$

$$LC_1 = A + CT_2 + CT_3 * A/B + CT_4/B \qquad \text{(A5.7)}$$

$$LC_2 = CT_7 + CT_8 * A/B + CT_9/B$$

$$LC_3 = CT_{10}/B$$

## 5.6 References


Ashmarina, L. I., Pshezhetsky, A. V., Spivey, H. O. & Potier, M. (1994). Demonstration of Enzyme Associations by Countermigration Electrophoresis in Agarose Gel. *Anal. Biochem.* **219**, 349-355.

Brooks, S. P. J. & Storey, K. B. (1991). Re-evaluation of the Glycerol-3-phosphate Dehydrogenase/L-lactate Dehydrogenase Enzyme System. *Biochem. J.* **278**, 875-881.

Chandler, J. P. (1988). STEPT. Program QCPE 307. Quantum Chemistry Program Exchange, Indiana University, Bloomington, IN 47401.

Chandler, J. P., Hill, D. E. & Spivey, H. O. (1972). A Program for Efficient Integration of Rate Equations and Least-Squares Fitting of Chemical Reaction Data. *Comput. Biomed. Res.* **5**, 515-534.

Cornish-Bowden, A. (1995). *Fundamentals of Enzyme Kinetics*, Portland Press Ltd., London.

Datta, A., Merz, J. M. & Spivey, H. O. (1985). Substrate Channeling of Oxaloacetate in Solid-state Complexes of Malate Dehydrogenase and Citrate Synthase. *J. Biol. Chem.* **260**, 15008-15012.

Elcock, A. H., Huber, G. A. & McCammon, J. A. (1997). Electrostatic Channeling of Substrates between Active Sites: Comparison of Simulation and Experiment. *Biochemistry* **36**, 16049-16058.

Fisher, D. D. & Schulz, A. R. (1969). Connection Matrix Representation of Enzyme Reaction Sequences. *Math. Biosci.* **4**, 189-200.

Fisher, D. D. & Schulz, A. R. (1970). Computer-based Derivation and Reformulation of Enzyme Reaction Models. *Biomed. Comp.* **1**, 221-235.

Halper, L. A. & Srere, P. A. (1977). Interaction between Citrate Synthase and Mitochondrial Malate Dehydrogenase in the Presence of Polyethylene Glycol. *Arch. Biochem. Biophys.* **184**, 529-534.

Keizer, J. & Smolen, P. (1992). Mechanisms of Metabolite Transfer between Enzymes: Diffusional versus Direct Transfer. In *From Metabolite, to Metabolism, to Metabolon* (Stadtman, E. R. & Chock, P. B., eds.), Curr. Top. Cell. Regul., **33**, pp. 391-405. Academic Press, New York.

Lindbladh, C., Rault, M., Hagglund, C., Small, W. C., Mosbach, K., Bulow, L., Evans, C. & Srere, P. A. (1994). Preparation and kinetic characterization of a fusion protein of yeast mitochondrial citrate synthase and malate dehydrogenase. *Biochemistry* **33**, 11692-11698.

Marquardt, D. W. & Snee, R. D. (1975). Ridge Regression in Practice. *Amer. Statistician* **29**, 3-20.

Merz, J. M., Webster, T. A., Appleman, J. R., Manley, E. R., Yu, H.-A., Datta, A., Ackerson, B. J. & Spivey, H. O. (1987). Polyethylene Glycol-Induced Heteroassociation of Malate Dehydrogenase and Citrate Synthase. *Arch. Biochem. Biophys.* **258**, 132-142.

Rudolph, J. & Stubbe, J. (1995). Investigation of the Mechanism of Phosphoribosylamine Transfer from Glutamine Phosphoribosylpyrophosphate Amidotransferase to Glycinamide Ribonucleotide Synthetase. *Biochemistry* **34**, 2241-2250.

Schulz, A. R. (1994). *Enzyme Kinetics*, Cambridge Univerisity Press, New York.

Srere, P. A., Halper, L. A. & Finkelstein, M. B. (1978). Interaction of Citrate Synthase and Malate Dehydrogenase. In *Microenvironments and Metabolic Compartmentation* (Srere, P. A. & Estabrook, R. W., eds.), pp. 421-422. Academic Press, New York.

Srivastava, D. K. & Bernhard, S. A. (1985). The Mechanism of Transfer of NADH Among Dehydrogenases. *Biochemistry* **24**, 623-628.

Wu, X., Gutfreund, H. & Chock, P. B. (1992). Kinetic Method for Differentiating Mechanisms for Ligand Exchange Reactions: Application to Test for Substrate Channeling in Glycolysis. *Biochemistry* **31**, 2123-2128.

Yong, H., Thomas, G. A. & Peticolas, W. L. (1993). Metabolite-Modulated Complex Formation between α-Glycerophosphate Dehydrogenase and Lactate Dehydrogenase. *Biochemistry* **32**, 11124-11131.

You, K. S. (1985). Stereospecificity for nicotinamide nucleotides in enzymatic and chemical hydride transfer reactions. *CRC Crit Rev Biochem* **17**, 313-451.

Zimmermann, S. B. & Minton, A. P. (1993). Macromolecular crowding: biochemical, biophysical, and physiological consequences. *Ann. Rev. Biophys. Biomol. Struct.* **22**, 27-65.

# VITA

Zeljko M. Svedruzic

Candidate for the Degree of

Doctor of Philosophy

Thesis: NADH CHANNELING BETWEEN DEHYDROGENASES: ENZYME KINETICS, PROTEIN INTERACTION AND MOLECULAR MODELING STUDIES

Major Field: Biochemistry and Molecular Biology

Biographical:

Personal Data: Born on March 16th 1969, Osijek Croatia.

Education: 1993 - April 1998, Ph.D. student at Department of Biochemistry and Molecular Biology at Oklahoma State University, Stillwater Oklahoma. Fall 1988 -June 1992 student of Biochemistry, Molecular Biology and Physics at the Faculty of Natural Sciences and Mathematics, University of Zagreb Croatia. Degree completed June 1998. Graduated from high school 1987 majoring in telecommunication electronics. Completed the requirements for the Doctor of Philosophy degree at Oklahoma State University in December, 2000.

Experience: August 1993 - April 1998, Graduate research assistant at Department of Biochemistry and Molecular Biology at Oklahoma State University, Stillwater Oklahoma. September 1992- June 1993 diploma thesis student at Max-Planck Institute for Biochemistry, Munich, Germany.

Professional Membership: American Chemical Society.